

Control of Arabidopsis vein-network formation by cell proliferation

by

Osama Odat

Zh

A thesis submitted in partial fulfillment of the requirements for the degree of

Doctor of Philosophy

in

Plant Biology

Department of Biological Sciences
University of Alberta

© Osama Odat, 2015

ABSTRACT

In most multicellular organisms, signals and nutrients are transported throughout the body by a vascular system. For normal development and optimal function, no area of the body should thus be devoid of vessels. Therefore, the growth of tissues and their vascularization must be tightly coordinated, and understanding the molecular basis of this coordination is a key question in biology. In animals, signals from proliferating nonvascular tissues promote their vascularization; in turn, vessels signal back to surrounding nonvascular tissues to control their growth and development. By contrast, in plant organs, vascular and nonvascular tissues differentiate from the same precursor cells; yet it is possible that the logic that integrates the growth of tissues and their vascularization in plants is no different from that in animals. Here, I investigated this possibility for *Arabidopsis* leaves, in which internal, ground cells proliferate and differentiate into either mesophyll or veins. I combined: (i) molecular genetic interference with core regulators of cell cycle progression and cell differentiation; (ii) cellular imaging of cell fate markers; and (iii) analysis of vein network topology. And I used this combined approach to show that cell proliferation inhibits progression of ground cells to mesophyll fate, thus permitting their recruitment into veins, and that cessation of cell proliferation permits progression of ground cells to mesophyll fate, thus preventing their recruitment into veins. Though this logic resembles that of tissue patterning in animal appendages, it is different from that which integrates tissue growth and vascularization in animal organs. What molecular mechanisms control the integration of tissue growth and vascularization in plant organs? By combining (i) molecular genetic interference with core regulators of cell cycle progression and signaling pathways, (ii) topological analysis of vein networks, and (iii) imaging of cell proliferation markers, I show that leaf growth and vascularization are integrated by the activity of two pathways that

antagonistically control cell proliferation and vein network formation: transcriptional input provided by the CINCINNATA-related TCP (for TEOSINTE BRANCHED1/CYCLOIDEA/PROLIFERATING CELL FACTOR) proteins inhibits these processes; transduction of the signaling molecule auxin mediated by the MONOPTEROS transcription factor promotes them. My results thus suggest a molecular mechanism that controls the unique logic by which timing of cessation of cell proliferation integrates tissue growth and vascularization in plants.

PREFACE

Chapter 3 has been published as O Odat, J Gardiner, MG Sawchuk, C Verna, TJ Donner and E Scarpella, “Characterization of an allelic series in the *MONOPTEROS* gene of *Arabidopsis*,” *genesis*, volume 52, issue 2, 127-133. All authors shared the responsibilities for conceiving and designing the experiments, analyzing the data and writing the manuscript. J Gardiner and I—the co-first authors—collectively performed 55% of the experiments while MG Sawchuk, C Verna and TJ Donner performed 20%, 15% and 10% of the experiments, respectively. E Scarpella was the supervisory author and was involved with concept formation and manuscript composition.

All the authors and publishers have given their permission for the inclusion of this publication in my thesis.

ACKNOWLEDGMENTS

I would never have been able to finish my dissertation without the guidance, help and support from many people.

For kindly providing plasmids, seeds and reagents, I would like to thank the Arabidopsis Biological Resource Center (ABRC), the RIKEN BioResource Center, Thomas Berleth, Ken-ichiro Hayashi, Philip Head, Thomas Jack, James Murray, Megan Sawchuk, Masaaki Umeda, Detlef Weigel and Dolf Weijers.

For providing technical advice, I would like to thank Renze Heidstra, Dolf Weijers and Viola Willemsen.

For critically reading parts of my thesis, I would like to thank both Carla Verna and Jason Gardiner.

I would like to thank the members of my supervisory committee, Dr. Michael Deyholos and Dr. Uwe Hacke for the support and advice they kindly provided during my Ph.D studies.

I would like to thank my fellow labmates for the fun environment they created and for the stimulating discussions that we shared, which made the lab a good place for work. Thank you to Teresa Ceserani, Tyler Donner, Jason Gardiner, Linh Nguyen Manh, Megan Sawchuk, Ira Sherr and Carla Verna.

I would like to give a special thanks to my family—my parents, my wife and my kids and my sisters and brothers—for supporting me spiritually and being patient throughout my Ph.D studies and my life in general.

Finally, I would like to express my sincere gratitude to my supervisor Dr. Enrico Scarpella for accepting me to be part of his lab and for the continuous support during my PhD studies. I am very grateful for his immense knowledge, motivation and patience; I appreciate his guidance throughout these years, which helped me in my research and in the writing of this thesis. I feel very privileged to have had Dr. Scarpella as a supervisor and mentor for my Ph.D.

TABLE OF CONTENTS

CHAPTER 1: GENERAL INTRODUCTION	1
1.1 Introduction	1
1.2 Leaf vein patterns	1
1.3 Leaf vein development	2
1.4 Auxin transport and vascular strand formation	3
1.5 Auxin signalling and leaf vascular development	5
1.6 Leaf cell proliferation and leaf vascular development	7
1.7 Scope and outline of the thesis	8
CHAPTER 2: CONTROL OF LEAF TISSUE PATTERN BY GROUND CELL PROLIFERATION	11
2.1 Introduction	11
2.2 Results and Discussion	12
2.2.1 Specification to mesophyll and vascular fates in Arabidopsis leaves	12
2.2.2 Ground cell proliferation and vein network formation	16
2.2.3 Ground cell proliferation and mesophyll fate specification	20
2.2.4 Leaf cell differentiation and vein network formation	20
2.2.5 Control of leaf tissue pattern by ground cell proliferation	27
2.3 Materials and methods	28
2.3.1 Plants	28
2.3.2 Imaging	34
2.3.3 Vein network analysis	34

CHAPTER 3: CHARACTERIZATION OF AN ALLELIC SERIES IN THE <i>MONOPTEROS</i> GENE OF ARABIDOPSIS	37
3.1 Introduction	37
3.2 Results and Discussion	38
3.3 Materials and methods	48
3.3.1 Plants	48
3.3.2 Vectorette PCR	48
3.3.3 RT-PCR	48
3.3.4 Imaging	48
CHAPTER 4. CONTROL OF LEAF VASCULARIZATION BY CELL PROLIFERATION	54
4.1 Introduction	54
4.2 Results and Discussion	56
4.2.1 <i>MONOPTEROS</i> functions in Arabidopsis vein-network topology	56
4.2.2 Leaf cell proliferation and vein network topology	57
4.2.3 Leaf cell proliferation and <i>MP</i> -dependent vein network topology	57
4.2.4 <i>CIN-TCP</i> -dependent repression of leaf cell proliferation and <i>MP</i> - dependent vein network topology	60
4.2.5 <i>MP</i> - and <i>CIN-TCP</i> -dependent expression of cell cycle regulators	64
4.2.6 Integration of tissue growth and vascularization by cell proliferation	66
4.3 Materials and methods	68
4.3.1 Plants	68
4.3.2 Imaging	68
4.3.3 Vein network analysis	73

CHAPTER 5. CHARACTERIZATION OF GENETIC SUPPRESSORS OF THE <i>monopteros</i> PHENOTYPE	74
5.1 Introduction	74
5.2 Results and Discussion	75
5.3 Materials and methods	88
CHAPTER 6: DISCUSSION	89
6.1 Conclusion summary	89
6.2 A model of vein formation by auxin-dependent cell proliferation ...	90
6.3 Unresolved questions and future approaches	94
LITERATURE CITED	96

LIST OF TABLES

CHAPTER 2

Table 2.1. Origin and nature of lines	29
Table 2.2. Oligonucleotide sequences	32
Table 2.3. Imaging parameters	35

CHAPTER 3

Table 3.1. Origin of lines	49
Table 3.2. Genotyping strategies	50
Table 3.3. Oligonucleotide sequences	51

CHAPTER 4

Table 4.1. Origin and nature of lines	69
Table 4.2. Genotyping strategies	70
Table 4.3. Oligonucleotide sequences	71
Table 4.4. Marker-line-specific conditions of β -glucuronidase (GUS) detection	72

CHAPTER 5

Table 5.1. Fertility of M2 lines	78
Table 5.2. Penetrance of <i>mp</i> suppression in M2 lines	81
Table 5.3. Phenotype of F1 progeny of crosses between M2 lines and <i>MP/mp</i>	84
Table 5.4. Phenotype of F1 progeny of crosses between M2 lines	85
Table 5.5. Phenotype of F3 progeny of <i>MP/mp</i> F2 plants lacking <i>MP::MP:GR</i> derived from cross between M2 line 25-3-2 and <i>MP/mp</i>	87

LIST OF FIGURES

CHAPTER 2

Figure 2.1. Ground cell proliferation and specification to mesophyll and vascular fates	13
Figure 2.2. Ground cell proliferation and vein network formation	18
Figure 2.3. Ground cell proliferation and mesophyll fate specification	21
Figure 2.4. Leaf cell differentiation and vein network formation	24
Figure 2.1. <i>mTCP10</i> vs. <i>TCP10</i>	26

CHAPTER 3

Figure 3.1. Mutations in the <i>MP</i> gene	39
Figure 3.2. Seedling axis defects of <i>mp</i> alleles	42
Figure 3.3. Cotyledon pattern defects of <i>mp</i> alleles	43
Figure 3.4. Vein pattern defects of <i>mp</i> alleles	45
Figure 3.5. Putative transcription-factor binding sites in the 295-bp region of the <i>MP</i> promoter from nucleotide -972 to nucleotide -678	46

CHAPTER 4

Figure 4.1. <i>MP</i> -dependent auxin signaling, cell proliferation and vein network formation in Arabidopsis leaves	58
Figure 4.2. TIR1/AFB-mediated, <i>MP</i> -dependent auxin signaling, <i>CIN-TCP</i> -dependent inhibition of cell proliferation and vein network formation	62
Figure 4.3. <i>MP</i> -dependent auxin signaling, <i>CIN-TCP</i> -dependent inhibition of cell proliferation and expression of cell cycle regulators	65
Figure 4.4. Summary and interpretation	67

CHAPTER 5

Figure 5.1. Overview of characterization of putative genetic suppressors of the <i>mp</i> phenotype	76
--	----

CHAPTER 6

Figure 6.1. A model of vein formation by auxin-dependent cell proliferation	91
--	----

LIST OF ABBREVIATIONS AND NOTATIONS

AD	Activation Domain
<i>AMP1</i>	<i>ALTERED MERISTEM PROGRAM1</i>
<i>ANT</i>	<i>AINTEGUMENTA</i>
ARF	AUXIN RESPONSE FACTOR
<i>ATHB8</i>	<i>ARABIDOPSIS THALIANA HOMEBOX 8</i>
AUX/IAA	AUXIN/INDOLE-3-ACETIC ACID
AuxREs	Auxin Response Elements
CDK	Cyclin-Dependent Kinases
CIN	CINCINNATA
CTD	Carboxyl-terminal domain
CYC	CYCLIN
<i>CYCA</i>	<i>CYCLIN A</i>
DP	DIMERIZATION PARTNER
E2F	EARLY 2 FACTOR
EP	End Points
GRAS	GIBBERELIC ACID INSENSITIVE, REPRESSOR OF <i>gibberellic acid1-3/</i> , and SCARECROW
GUS	β -glucuronidase
<i>HD-ZIP III</i>	Class III <i>HOMEODOMAIN-LEUCINE ZIPPER</i>
HSP90	HEAT-SHOCK PROTEIN90
IAA	Indole-3-acetic acid
ICK	INTERACTORS OF CDC2 KINASE
KRP	KIP-RELATED PROTEINS
<i>LHCB2.3</i>	<i>LIGHT HARVESTING COMPLEX B2.3</i>
<i>miR319a</i>	<i>microRNA319a</i>
MP	MONOPTEROS
nCFP	Nuclear Cyan Fluorescent Protein
nYFP	Nuclear Yellow Fluorescent Protein
PIN1	PIN-FORMED1

RBR	RETINOBLASTOMA-RELATED
<i>RPS5A</i>	<i>RIBOSOMAL PROTEIN S5A</i>
SCF	Skp1(S-phase kinase-associated protein 1)/Cullin1/F-box protein
<i>SHR</i>	<i>SHORT-ROOT</i>
TCP	TEOSINTE BRANCHED1/CYCLOIDEA/PROLIFERATING CELL FACTOR
TIR1/AFB	TRANSPORT INHIBITOR RESISTANT1/AUXIN SIGNALLING F-BOX PROTEIN
TPs	Touch Points
<i>UBQ10</i>	<i>UBIQUITIN 10</i>
VP16	VIRION POLYPEPTIDE 16
XPs	Exit Points

Gene and protein notation

MP	Wild-type protein
mp	Mutant protein
<i>MP</i>	Wild-type gene
<i>mp</i>	Mutant gene

Gene fusion notation

Doubled colons (::) are used to indicate transcriptional fusions

Single colons (:) are used to indicate translational fusions

CHAPTER 1: GENERAL INTRODUCTION

1.1 Introduction

In most multicellular organisms, signals and nutrients are transported throughout the body by a vascular system. In plants, such vascular system is composed of a network of continuous vascular strands that connect different areas of an organ and different organs of a plant (Esau, 1965).

Mature vascular strands are cylinders composed of two vascular tissues: xylem—toward the inside in cylindrical organs on the upper side in flat organs—and phloem—toward the outside in cylindrical organs on the lower side in flat organs. Xylem is composed of tracheary elements, parenchyma cells and fibers (Esau, 1965), and mainly transports water and minerals from the roots, which absorb them from the soil, to the leaves, where water will evaporate through transpiration (Taiz and Zeiger, 2006). Phloem is composed of sieve elements, parenchyma cells, fibers and sclereids (Esau, 1965), and mainly transport the products of photosynthesis from source tissues, such as leaves, to sink tissues, such as roots (Taiz and Zeiger, 2006).

During plant growth by lengthening—primary growth—xylem and phloem differentiate from within bundles of files of narrow, elongated vascular-precursor procambial cells (Esau, 1965). In plants and organs that undergo growth by thickening—secondary growth—a layer of procambial cells remains in each vascular strands between the xylem and phloem formed during primary growth. During secondary growth, this layer of procambial cells resumes cell division to give rise to the vascular cambium, from which secondary xylem and phloem will differentiate.

1.2 Leaf vein patterns

In dicot leaves, vascular strands—or veins—are arranged in a hierarchical branching pattern with one or more centrally located midveins that extend the length of the leaf and are continuous with the vascular strands of the stem (Nelson and Dengler, 1997). Lateral veins branch from the

midvein and extend laterally into the leaf lamina toward the leaf margin, where they can end freely or where they can curve and connect back to the midvein or to more apically located lateral veins to form closed loops. Minor veins branch from midvein and loops, and connect to other veins, or end freely in the leaf lamina.

In monocot leaves, veins are arranged in a grid-like pattern in which major veins extend parallel to one another along the length of the leaf, and minor veins connect transversely major veins (Nelson and Dengler, 1997).

1.3 Leaf vein development

In the leaf, veins form *de novo* from within the population of isodiametric, polygonal cells—the ground cells—that make up the inner tissue at early stages of leaf development (Foster, 1952; Pray, 1955). The sequence of events that lead to vein formation has been investigated in detail in *Arabidopsis thaliana*. In this species, expression and localization of the plasma-membrane-localized transporter of the plant signalling molecule auxin PIN-FORMED1 (PIN1) suggests two different vein ontogenies (Scarpella et al., 2006; Wenzel et al., 2007).

(1) Each midvein and lateral vein is initiated in association with an epidermal “convergence point”: a point in the epidermis of the leaf margin in which PIN1 localization to the plasma membrane is directed toward a single epidermal cell. Each epidermal convergence point is associated with a broad domain of PIN1 expression in the inner tissue that connects the epidermal convergence point with a pre-existing vein; within such broad domain of PIN1 expression, PIN1 is localized isotropically to the plasma membrane. Over time, each broad domain of PIN1 expression narrows to a site of vein formation, in which PIN1 is localized to the side of the plasma membrane away from the convergence point and toward the pre-existing vein.

(2) Minor veins form from PIN1 expression domains with no association with epidermal convergence points and that branch from pre-existing veins. Initially, all minor veins end freely in the leaf inner tissue, and PIN1 is localized to the side of the plasma membrane toward the pre-existing veins. However, over time, some minor veins can become connected to pre-existing veins at both sides; at the ends of these “connected” veins, PIN1 is localized to the side of the

plasma membrane toward the pre-existing veins, and the two, opposite PIN1 polarities are joined by a “bipolar” cell: a cell with PIN1 localized to two opposite sides of the plasma membrane.

PIN1 expression behaviour during loop formation shows that each loop is formed by a minor vein branching from a lateral vein (Scarpella et al., 2006; Wenzel et al., 2007). Initially the minor vein ends freely in the leaf inner tissue, but over time it connects to the midvein or to more apically located lateral veins. As in all other connected veins, at the ends of each loop, PIN1 is localized to the side of the plasma membrane toward the pre-existing veins it connects to, and the two, opposite PIN1 polarities are joined by a bipolar cell.

Domains of PIN1 expression in the inner tissue are initially broad and overlap with broad domains of expression of the auxin-response transcription factor MONOPTEROS (MP) (Donner et al., 2009; Wenzel et al., 2007). As broad domains of PIN1 expression, broad domains of MP expression narrow over time until they become restricted to sites of vein formation.

Within broad expression domains of PIN1 and MP, ground cells destined to become procambial cells start expressing the class III *HOMEODOMAIN-LEUCINE ZIPPER (HD-ZIP III)* gene *ARABIDOPSIS THALIANA HOMEBOX8 (ATHB8)*, the GRAS (after GIBBERELIC ACID INSENSITIVE, REPRESSOR OF *gibberellic acid1-3*, and SCARECROW) transcription factor gene *SHORT-ROOT (SHR)*, and the enhancer-trap J1721 (Baima et al., 1995; Donner et al., 2009; Gardiner et al., 2011; Kang and Dengler, 2004; Sawchuk et al., 2007; Scarpella et al., 2004). Unlike expression of PIN1 and MP, however, expression of *ATHB8*, *SHR* and J1721 is initiated in narrow domains.

Finally, cells expressing *ATHB8*, *SHR* and J1721 will elongate simultaneously along the length of a vein to differentiate into procambial cells, an event which is marked by the onset of expression of the enhancer-trap lines ET1335 and Q0990 (Sawchuk et al., 2007; Scarpella et al., 2004).

1.4 Auxin transport and vascular strand formation

Many signals can promote vascular cell differentiation (Aloni, 1987; Cano-Delgado et al., 2010; Fukuda, 2004; Vera-Sirera et al., 2010), but among such signals auxin remains unique because it

is the only substance that not only promotes the differentiation of vascular cells but aligns this differentiation along continuous lines to form vascular strands (Berleth, 2000; Sachs, 1981).

Evidence of the effect of auxin on the formation of vascular strands was first derived from the results of experiments in which auxin had been applied locally to mature tissues. In these tissues, auxin application induces the differentiation of single files of cells into continuous vascular strands that extend basally from the site of auxin application toward the pre-existing vasculature. As such, auxin-induced vascular differentiation response is characterized by unique properties.

(1) The response is localized to the site of auxin application.

(2) The response is polar, as it is directed toward pre-existing vasculature that is located basally to the site of auxin application.

(3) The response is continuous, as it produces uninterrupted vascular cell files.

(4) The response is constrained laterally, as vascular differentiation is restricted to strips of cells rather than clouds of cells surrounding the site of auxin application.

(5) The response requires polarly transported auxins, and it is obstructed by polar auxin transport inhibitors, suggesting that the underlying mechanism recruits the machinery that polarly transports auxin.

Auxin is in fact produced in immature shoot organs and transported toward the roots through vascular strands (Michniewicz et al., 2007; Normanly, 2010; Zhao, 2010). This apical-basal polarity of auxin transport is thought to derive from the polar localization of auxin efflux proteins to the basal plasma membrane of auxin-transporting cells (Raven, 1975; Rubery and Sheldrake, 1974). As a weak acid, in fact, indole-3-acetic acid (IAA)—the most abundant auxin in plants—is protonated at the acidic pH of the extracellular space. This apolar form of IAA can freely diffuse into the cell. However, at the neutral intracellular pH, IAA is negatively charged and can only leave the cell through specialized efflux proteins.

These observations form the basis of the “auxin canalization hypothesis” (Sachs, 1981, 1991). The hypothesis postulates that a positive feedback exist between auxin transport through a cell and the cell’s auxin conductivity. The hypothesis predicts that the applied auxin initially moves by diffusion with no preferred orientation, and that auxin efflux proteins are randomly distributed. By efficiently transporting auxin along the apical–basal auxin-transport polarity of

the tissue, the pre-existing vasculature would act as an auxin sink and orient auxin movement in neighbouring cells, polarizing the localization of auxin efflux proteins in these cells. The initiation of polar auxin transport in these cells would be gradually enhanced by positive feedback between auxin transport and efflux protein localization. By draining auxin in an increasingly more efficient and polar way, these cells would in turn induce polar auxin transport and polarization of efflux protein localization in the cells above them, and inhibit the same processes in their lateral neighbours. Iteration of these events would result in preferential transport of auxin through limited cell files, which would eventually differentiate into vascular strands.

The localization of the plasma-membrane-localized auxin efflux protein of *Arabidopsis* PIN1 marks the presumed auxin-efflux side of the cell (Petrasek and Friml, 2009). Therefore, the polarity of auxin transport can be inferred from the localization of PIN1 proteins at the plasma membrane. Consistent with predictions of the canalization hypothesis, local application of auxin to pea tissues induces broad domains of PIN1 expression between the site of auxin application and a pre-existing vascular strand. Over time, broad domains of PIN1 expression, in which PIN1 is localized isotropically to the plasma membrane, narrow to define sites of auxin-induced vascular-strand formation, in which PIN1 is localized to the side of the plasma membrane away from the source of auxin and toward the pre-existing vascular strand.

Consistent with a role for auxin transport in vein development, vein patterns are abnormal in leaves of *pin1* mutants and of plants grown on auxin transport inhibitors (Mattsson et al., 1999; Sieburth, 1999).

1.5 Auxin signalling and leaf vascular development

The auxin signal is transduced by multiple pathways (Leyser, 2010); best understood is that which ends with the transcriptional activation or repression of auxin-responsive genes by transcription factors of the AUXIN RESPONSE FACTOR (ARF) family (Chapman and Estelle, 2009).

At low concentrations of auxin in the cell, proteins of the AUXIN/INDOLE-3-ACETIC ACID (AUX/IAA) family bind to ARF transcription factors, preventing them from inducing transcription of their target genes (Mockaitis and Estelle, 2008). At higher concentrations of auxin in the cell, auxin is bound by auxin receptors of the TRANSPORT INHIBITOR RESISTANT1/AUXIN SIGNALLING F-BOX PROTEIN (TIR1/AFB) family. TIR1/AFB receptors are the F-box-protein subunit of the SCF^{TIR1/AFB} (Skp1-Cul1-F-box protein) E3 ubiquitin ligase complex. Auxin binding to the receptor facilitates the interaction between the receptor itself and proteins of the AUXIN/INDOLE-3-ACETIC ACID (AUX/IAA) family, which are poly-ubiquitinated by the SCF^{TIR1/AFB} and thus targeted for degradation by the 26S proteasome. Degradation of AUX/IAA protein releases ARF transcription factors from inhibition, thus allowing them to induce transcription of their target genes through ARF binding to Auxin Response Elements (AuxREs) located in the promoter of their target genes. This model is probably an over-simplification because it only explains the function of the minority of ARF transcription factors. In fact, only five of the 22 ARF proteins in Arabidopsis (ARF5/MP, ARF6, ARF7/NPH4, ARF8 and ARF19) have been shown to be able to activate transcription of target genes, while the remaining 17 have been shown, at least in protoplast, to act as repressors of transcription (Guilfoyle and Hagen, 2007).

That auxin signalling is required for vascular differentiation is suggested by two pieces of evidence.

(1) Veins form along domains of expression of ARF target genes—such as expression of *ATHB8*, which is directly controlled by ARF5/MP—and of activity of synthetic promoters composed of multimers of AuxREs (Donner et al., 2009; Mattsson et al., 2003).

(2) Vascular differentiation is reduced in leaves of mutants in auxin signalling components (Alonso-Peral et al., 2006; Candela et al., 1999; Esteve-Bruna et al., 2013; Hardtke and Berleth, 1998; Przemeck et al., 1996; Strader et al., 2008)

1.6 Leaf cell proliferation and leaf vascular development

The product of animal embryogenesis is a miniature version of the adult animal (Wolpert et al., 2015). During post-embryonic development, this miniature version will grow to reach the size of the adult animal, and no new organs will be formed during this growth. By contrast, plants continue to form new organs throughout their life. This is possible because plant cells retain the ability to proliferate and differentiate. During normal development, this property is limited to cells that are spatially segregated. For example, cells at the shoot tip proliferate to self-regenerate and to give rise to daughter cells that proliferate and differentiate to form leaves and flowers, and vascular cells in the root proliferate and differentiate to form lateral roots. However, all plant cells can artificially be induced to resume cell proliferation and differentiation, such that a whole new plant can be formed from a single somatic cell.

Despite these unique properties, as in animals, progression through the cell cycle in plants is promoted by complexes between members of the EARLY 2 FACTOR (E2F) and the DIMERIZATION PARTNER (DP) families of transcriptional regulators [(reviewed in (Dewitte and Murray, 2003; Gutierrez, 2009; Inze and De Veylder, 2006)]. The activity of E2F/DP complexes is inhibited by binding of the non-phosphorylated form of the RETINOBLASTOMA-RELATED (RBR) protein. Phosphorylation of RBR by complexes between cyclin-dependent kinases (CDKs) and their regulatory proteins, the cyclins, leads to RBR degradation and thus to activation of E2F/DP complexes. The formation of CDK/cyclin complexes is stimulated by growth promoting signals (eg. auxin and sucrose), and the activity of CDK/cyclin complexes is inhibited by INTERACTORS OF CDC2 KINASE (ICKs)/KIP-RELATED PROTEINS (KRPs).

Several pieces of evidence suggest a role for cell proliferation in vein development.

(1) Leaf vascular cells proliferate longer than any other cell in the leaf (Donnelly et al., 1999; Kang and Dengler, 2002).

(2) Simultaneous loss of function of all four *CYCLIN A (CYCA)* genes of Arabidopsis—all of which are expressed during vein development—leads to reduced proliferation of leaf vascular cells (Donner and Scarpella, 2013; Vanneste et al., 2011).

(3) Overexpression of the transcription factor *AINTEGUMENTA* (*ANT*) leads to prolonged leaf expression of *CYCD3;1*, prolonged leaf cell proliferation and formation of more minor-veins in *Arabidopsis* (Kang et al., 2007; Mizukami and Fischer, 2000).

(4) Overexpression of *ICK1/KRP1* leads to premature cessation of leaf cell proliferation and formation of fewer minor veins (Kang et al., 2007).

1.7 Scope and outline of the thesis

The evidence discussed above strongly suggests a role for auxin signalling in vein network formation; by contrast, the evidence that suggests a role for leaf cell proliferation in vein network formation is indirect. Though overwhelming evidence supports a role for auxin in cell proliferation [reviewed in (Demeulenaere and Beeckman, 2014)], such evidence was derived from results of experiments in roots or tissue culture; the evidence that auxin signalling controls leaf cell proliferation is instead scarce (Hu et al., 2003; Perez-Perez et al., 2010; Schruff et al., 2005), and no evidence is currently available that suggests a role of auxin-signalling-dependent leaf cell-proliferation in vein network formation. The scope of my Ph.D. thesis was to understand whether and how cell proliferation controls vein network formation, and whether auxin-signalling-dependent vein-network formation is mediated by leaf cell proliferation.

The relative timing of cessation of cell proliferation and onset of cell differentiation controls tissue patterns of animal organs [e.g., (Lopez-Rios et al., 2012; Towers et al., 2008; Zhu et al., 2008)], but it is unclear whether it controls tissue patterns of plant organs. In Chapter 2, I address this problem for *Arabidopsis* leaves, in which internal, ground cells proliferate and differentiate into either mesophyll or veins (Kang and Dengler, 2004; Scarpella et al., 2004). By prolonging or prematurely ceasing cell proliferation, and by delaying or prematurely promoting cell differentiation, I show that cell proliferation inhibits progression of ground cells to mesophyll fate, thus permitting their recruitment into veins, and that cessation of cell proliferation permits progression of ground cells to mesophyll fate, thus preventing their recruitment into veins. Therefore, the relative timing of cessation of cell proliferation and onset of cell differentiation controls tissue patterns of plant as well as of animal organs, suggesting that the logic of organ

tissue patterning is conserved between plants and animals despite their independent evolution of multicellularity.

The best understood auxin signalling pathway relies on the function of a family of ARF transcription factors (Chapman and Estelle, 2009), but only the function of one of them—ARF5/MP—seems to be crucial for vascular differentiation (Donner et al., 2009; Hardtke et al., 2004; Przemeck et al., 1996). Thus analyses of vascular defects of *mp* mutants have advanced, and will continue to advance, our understanding of the role of auxin signalling in vascular differentiation. Unfortunately, an *mp* allelic series in the widely used Columbia wild-type background of Arabidopsis is lacking. In Chapter 3 (Odat et al., 2014), I address this limitation by extending the characterization of two known *mp* mutant alleles in the Columbia background of Arabidopsis, and by identifying and characterizing four new alleles of *mp* in the Columbia background. Among these four new *mp* mutant alleles, I find the first low-expression allele of *mp* and the strongest Columbia allele of *mp*.

In Chapter 4, I use the low-expression allele of *mp* I identified and characterized in Chapter 3 (Odat et al., 2014) to test the hypothesis that vein network defects of *mp* result from defects in leaf cell proliferation. By prolonging or prematurely ceasing leaf cell proliferation in WT or *mp* background, I show that vein network defects of *mp* result from premature cessation of leaf cell proliferation. Moreover, I show that the promoting effects of *MP* on leaf cell proliferation and vein network formation are antagonized by the functions of *CINCINNATA* (*CIN*)-related *TCP* for *TEOSINTE BRANCHEDI*/*CYCLOIDEA*/*PROLIFERATING CELL FACTOR*) (Cubas et al., 1999) genes. My results suggest a molecular mechanism underlying the logic by which timing of cessation of cell proliferation integrates tissue growth and vascularization in plants—a logic that seems to be different from that underlying integration of tissue growth and vascularization in animals [e.g., (Clever and Melton, 2003)].

My results suggest that vein network formation results, at least partially, from the interaction of two pathways that antagonistically control leaf cell proliferation: *MP*-dependent auxin signalling, which promotes leaf cell proliferation, and *CIN-TCP*-dependent transcriptional regulation, which inhibits it (Chapter 4). Likewise, other inputs of auxin in plant development result from the interaction of auxin signalling with other, nonoverlapping pathways [reviewed in (Kuppusamy et al., 2009)]. To identify new nonoverlapping pathways—as well as additional

components of the leaf cell-proliferation pathway—that interact with auxin signalling in vein network formation, I characterized in Chapter 5 putative genetic suppressors of the *mp* phenotype that had recently been identified (E. Scarpella, unpublished).

Finally, in Chapter 6, I propose and discuss a hypothesis to account for the mechanism by which the interaction between auxin signalling and cell proliferation results in vein network formation.

CHAPTER 2: CONTROL OF LEAF TISSUE PATTERN BY GROUND CELL PROLIFERATION

2.1 Introduction

The relative timing of cessation of cell proliferation and onset of cell differentiation is thought to control organ tissue patterns. In animals, this view is well supported by evidence. For example, in vertebrate limb development, premature cessation of mesenchyme proliferation and early onset of chondrogenic differentiation leads to formation of fewer digits, while prolonged mesenchyme proliferation and delayed onset of chondrogenic differentiation leads to formation of more digits (Lopez-Rios et al., 2012; Towers et al., 2008; Zhu et al., 2008).

As in animals, progression through the cell cycle in plants is promoted by complexes between members of the EARLY 2 FACTOR (E2F) and the DIMERIZATION PARTNER (DP) families of transcriptional regulators [reviewed in (Dewitte and Murray, 2003; Inze and De Veylder, 2006)]. The activity of E2F/DP complexes is inhibited by binding of the non-phosphorylated form of the RETINOBLASTOMA-RELATED (RBR) protein. Phosphorylation of RBR by complexes between cyclin-dependent kinases (CDKs) and their regulatory proteins, the cyclins, leads to RBR degradation and thus to activation of E2F/DP complexes. The activity of CDK/cyclin complexes is inhibited by INTERACTORS OF CDC2 KINASE (ICKs)/KIP-RELATED PROTEINS (KRPs).

While many core cell-cycle regulators are conserved between plants and animals (Harashima et al., 2013), key regulators of cell differentiation are not. For example, SMAD transcription factors (Benazet et al., 2012; Derynck et al., 1996; Retting et al., 2009) are absent in plants, and CIN-TCP (for CINCINNATA-related TEOSINTE BRANCHED1/CYCLOIDEA/PROLIFERATING CELL FACTOR) transcription factors (Cubas et al., 1999; Efroni et al., 2008; Koyama et al., 2010; Nath et al., 2003; Ori et al., 2007; Palatnik et al., 2003; Sarvepalli and Nath, 2011; Schommer et al., 2008) are absent in animals. Nevertheless, it is possible that the logic of cell differentiation is conserved between plants and animals. Consistent with this possibility, both SMAD4 and TCP4 induce expression of CDK

inhibitors (Gomis et al., 2006a; Gomis et al., 2006b; Schommer et al., 2014; Seoane et al., 2004). However, it remains unclear whether the relative timing of cessation of cell proliferation and onset of cell differentiation controls tissue patterns of plant organs [e.g., (Kang et al., 2007; McKown and Dengler, 2009; Scarpella et al., 2004; Wenzel et al., 2012)]. Here we address this problem for the internal tissues of *Arabidopsis thaliana* (L.) Heynh. leaves.

In *Arabidopsis* leaves, internal, ground cells proliferate and differentiate into either mesophyll or vascular tissues (Kang and Dengler, 2004; Scarpella et al., 2004). By prolonging or prematurely ceasing ground cell proliferation, and by delaying or prematurely promoting leaf cell differentiation, we show that cell proliferation inhibits progression of ground cells to mesophyll fate, thus permitting their recruitment into veins, and that cessation of cell proliferation permits progression of ground cells to mesophyll fate, thus preventing their recruitment into veins. Therefore, the relative timing of cessation of cell proliferation and onset of cell differentiation controls tissue patterns of plant as well as of animal organs.

2.2 Results and Discussion

2.2.1 Specification to mesophyll and vascular fates in *Arabidopsis* leaves

The vein network of mature first-leaves of *Arabidopsis* consists of: a central midvein; lateral veins that branch from the midvein, and that contact apically the midvein or other lateral veins to form closed loops; and minor veins that branch from midvein and loops, and that contact other veins or terminate free of contact (Candela et al., 1999; Kinsman and Pyke, 1998; Mattsson et al., 1999; Nelson and Dengler, 1997; Sieburth, 1999; Steynen and Schultz, 2003; Telfer and Poethig, 1994) (Figure 2.1Ni). In *Arabidopsis* leaf development, loops form after the midvein, and in the same area of the leaf, minor veins form after the loops (Kang and Dengler, 2004; Mattsson et al., 1999; Sawchuk et al., 2007; Scarpella et al., 2004; Sieburth, 1999) (Figure 2.1Nii). Loops and minor veins form first in the apical part of the leaf and then in progressively more basal parts of it (Kang and Dengler, 2004; Mattsson et al., 1999; Sawchuk et al., 2007; Scarpella et al., 2004; Sieburth, 1999) (Figure 2.1Nii).

Five tissue layers can be distinguished in cross sections of mature leaves of dicotyledonous

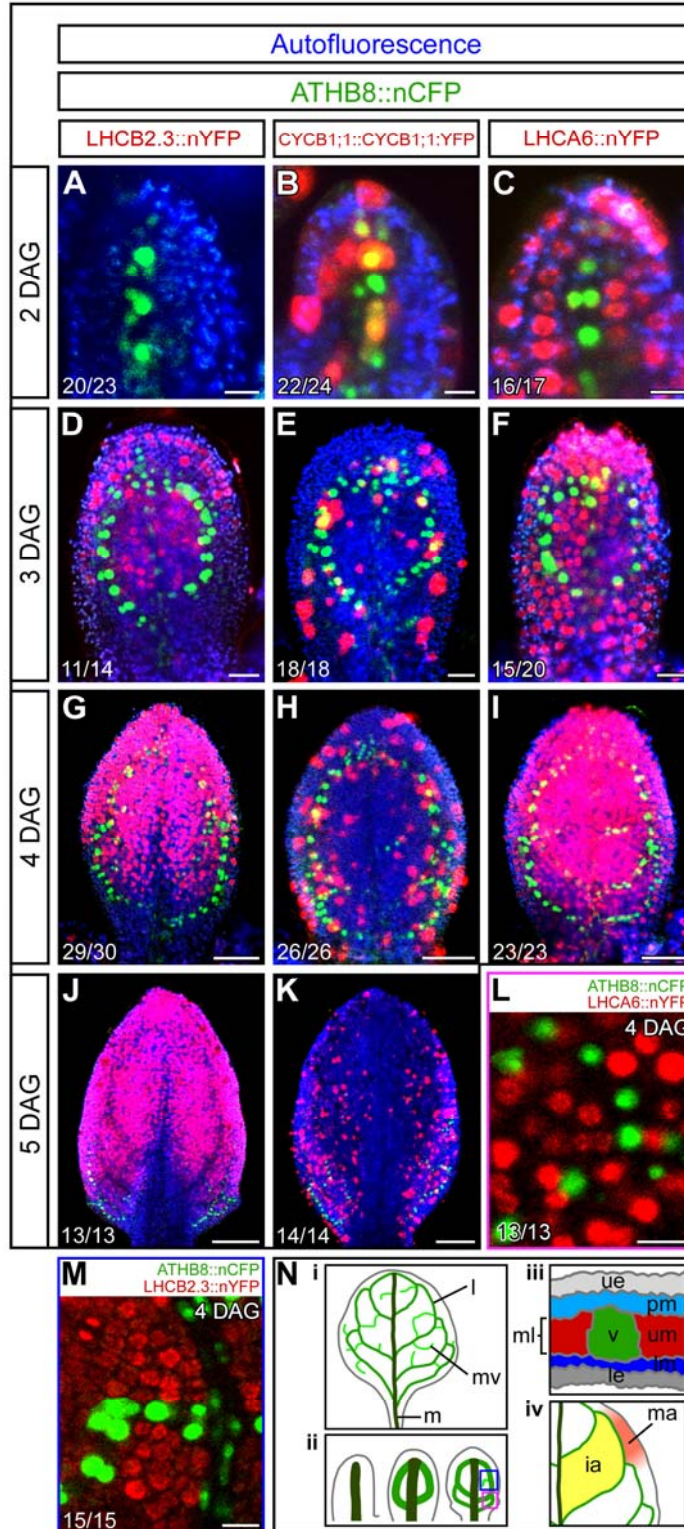


Figure 2.1. Ground cell proliferation and specification to mesophyll and vascular fates. (A-M) Confocal laser scanning microscopy of Arabidopsis first leaves respectively 2 (A-C), 3 (D-

F), 4 (G-I,L,M), and 5 (J,K) days after germination (DAG). (A-K) Blue: autofluorescence. (A-M) Green: ATHB8::nCFP expression. Red: expression of LHCB2.3::nYFP (A,D,G,J,M), CYCB1;1::CYCB1;1:YFP (B,E,H,K), or LHCA6::nYFP (C,F,I,L). (L,M) Close-ups of second (L) or first (M) loops (see Dii for close-up positions). Top right: markers. Bottom left: reproducibility index. (N) (i) The vein network of mature leaves of Arabidopsis consists of midvein (m; dark green), loops (l; green), and minor veins (mv; light green). (ii) In Arabidopsis leaf development (left to right), loops (green) form after the midvein (dark green), and in the same area of the leaf, minor veins (light green) form after the loops. Loops and minor veins form first in the apical part of the leaf, and then in progressively more basal parts of it. Boxes illustrate positions of close-ups in L (magenta) and M (blue). (iii) Five tissue layers can be distinguished in cross sections of mature leaves: upper epidermis (ue; light grey); palisade mesophyll (pm; light blue); middle layer (ml), comprising veins (v; green) and upper spongy mesophyll (um; red); lower spongy mesophyll (lm; dark blue); lower epidermis (le; dark grey). (iv) Leaf intercostal area (ia; yellow), i.e. area comprised by midvein (dark green) and loop (green), and leaf intramarginal area (ma; orange), i.e. area external to loop. Scale bars: 10 μm in A-C,L,M; 20 μm in D-F; 50 μm in G-I; 100 μm in J,K.

plants [reviewed in (Foster, 1936)] (Figure 2.1Niii): (1) upper epidermis; (2) palisade mesophyll; (3) middle layer; (4) lower spongy mesophyll; (5) lower epidermis. The middle layer comprises veins and upper spongy mesophyll (Figure 2.1Niii), both of which typically differentiate from middle-layer ground cells [reviewed in (Stewart, 1978; Tilney-Bassett, 1986)]. In *Arabidopsis*, the pattern with which ground cells are specified to vascular fate has been characterized (Kang and Dengler, 2004; Sawchuk et al., 2007; Scarpella et al., 2004), but the pattern with which ground cells are specified to mesophyll fate is unknown. In *Arabidopsis*, expression of LHC2.3::nYFP [nuclear yellow fluorescent protein (YFP) expressed by the *LIGHT HARVESTING COMPLEX B2.3 (LHC2.3)* promoter] is initiated in ground cells that have been specified to mesophyll fate (Sawchuk et al., 2008). Therefore, to characterize the pattern of specification of middle-layer ground cells to upper- spongy mesophyll or vascular fate, we simultaneously imaged expression of the mesophyll-fate-specification marker LHC2.3::nYFP (Sawchuk et al., 2008) and of the vascular-fate-specification marker ATHB8::nCFP [nuclear cyan fluorescent protein (CFP) expressed by the *ARABIDOPSIS THALIANA HOMEBOX 8 (ATHB8)* promoter] (Sawchuk et al., 2007) in first leaves of *Arabidopsis* 2, 3, 4 and 5 days after germination (DAG).

LHC2.3::nYFP expression was first detected in 3-DAG leaves, throughout the areas comprised within the midvein and first-loop domains of ATHB8::nCFP expression [i.e. the first intercostal areas (Figure 2.1Niv)] and approximately half-way down the areas external to the first-loop domains of ATHB8::nCFP expression [i.e. the first intramarginal areas (Figure 2.1Niv)] (Figure 2.1A,D). In 4-DAG leaves, LHC2.3::nYFP expression had extended to the most basal part of the second intercostal areas and approximately half-way down the second intramarginal areas (Figure 2.1G). Finally, in 5-DAG leaves LHC2.3::nYFP expression had extended to the whole leaf blade (Figure 2.1J). In agreement with previous observations (Sawchuk et al., 2008), the expression domains of LHC2.3::nYFP and those of ATHB8::nCFP were mutually exclusive (Figure 2.1M). Therefore, our results suggest an apical-basal wave of specification of middle-layer ground cells to upper-spongy mesophyll fate, and mutual exclusivity of upper-spongy mesophyll and vascular fates in leaf development.

2.2.2 Ground cell proliferation and vein network formation

Signals that induce vascular fate specification are unable to override mesophyll differentiation (Scarpella et al., 2006). By contrast, conditions that promote premature differentiation of ground cells into mesophyll prevent their specification to vascular fate (Scarpella et al., 2004); however, what controls the onset of mesophyll differentiation—and thus vein formation—is poorly understood. One possibility is that cessation of cell proliferation instructs ground cells to differentiate into mesophyll (Kang et al., 2007). Seemingly consistent with this possibility, the apical-basal wave of specification to upper-spongy mesophyll fate—as visualized by the pattern of initiation of LHCB2.3::nYFP expression in leaf development (Figure 2.1A,D,G,J)—seems to be complementary to the reported apical-basal wave of cessation of cell proliferation in the internal tissues of the leaf—as visualized by the pattern of cessation of expression of the mitotic cyclin CYCLIN B1;1 (CYCB1;1) in leaf development (Donnelly et al., 1999; Kalve et al., 2014; Kang and Dengler, 2002; Kazama et al., 2010). However, only by 5 DAG had expression of CYCB1;1::CYCB1;1:YFP (CYCB1;1:YFP fusion protein expressed by the *CYCB1;1* promoter) subsided in the middle-layer ground cells of the apical part of the leaf, whereas LHCB2.3::nYFP was expressed in those cells already since 3 DAG (Figure 2. 1A,D,H,K). Therefore, mesophyll fate specification precedes cessation of ground cell proliferation in leaf development, suggesting that cessation of cell proliferation may simply permit ground cells to progress to a fate that has already been specified. Here we tested the hypothesis that cessation of cell proliferation prevents recruitment of ground cells into veins by permitting progression to mesophyll fate.

The hypothesis predicts that premature cessation of ground cell proliferation will lead to formation of networks of fewer veins. To test this prediction, we used a variant of ICK2/KRP2 (KRP2 here after) in which the putative protein degradation signal (De Veylder et al., 2001; Torres Acosta et al., 2011) had been removed (KRP2^{Δ73-97}), and a dominant-negative variant of CDKA;1 (CDKA;1^{D146N}) (Hemerly et al., 1995); we expressed KRP2^{Δ73-97} and CDKA;1^{D146N} by the *LHCA6* promoter (Sawchuk et al., 2008), which is active in all ground cells except those that have been specified to vascular fate—as visualized by nonoverlapping expression of LHCA6::nYFP and ATHB8::nCFP in leaf development (Figure 2.1C,F,I,L) (Sawchuk et al., 2008); and we calculated the cardinality index—a measure of the number of veins in a network (Verna et al., 2015)—of vein networks of mature first-leaves of LHCA6::KRP2^{Δ73-97} and

LHCA6::CDKA;1^{D146N}, and compared it with that of vein networks of control mature first-leaves.

The cardinality index of LHCA6::KRP2^{Δ73-97} and LHCA6::CDKA;1^{D146N} was lower than that of the control (Figure 2.2A-C,I), suggesting that premature cessation of ground cell proliferation leads to formation of networks of fewer veins.

The hypothesis also predicts that delayed cessation of ground cell proliferation will lead to formation of networks of more veins. To test this prediction, we used a hyperactive variant of CYCD3;1 (CYCD3;1^{S343A}) (Menges et al., 2006), fusions between E2Fa or DPa and the activation domain (AD) of the Herpes simplex virus type 1 VIRION POLYPEPTIDE 16 (VP16) (Campbell et al., 1984) (E2Fa:VP16 and DPa:VP16, respectively), and an artificial microRNA targeting *RBR* (amiRBR); we expressed CYCD3;1^{S343A}, E2Fa:VP16, DPa:VP16 and amiRBR by the *LHCA6* promoter; and we calculated the cardinality index of vein networks of mature first-leaves of LHCA6::CYCD3;1^{S343A}, LHCA6::E2Fa:VP16, LHCA6::DPa:VP16 and LHCA6::amiRBR, and compared it with that of vein networks of control mature first-leaves.

The cardinality index of LHCA6::CYCD3;1^{S343A}, LHCA6::E2Fa:VP16, LHCA6::DPa:VP16 and LHCA6::amiRBR was higher than that of the control (Figure 2.2A,E-I), suggesting that delayed cessation of ground cell proliferation leads to formation of networks of more veins.

Premature onset of mesophyll differentiation interferes with progression of vein formation, thus leading to formation of leaves in which lateral veins occasionally fail to contact apically other veins (Scarpella et al., 2004). If premature cessation of ground cell proliferation permitted premature progression to mesophyll fate, premature cessation of ground cell proliferation should also lead to formation of leaves in which lateral veins occasionally fail to contact apically other veins—i.e. leaves with open loops. We tested this prediction by calculating the percentage of mature first-leaves of LHCA6::KRP2^{Δ73-97} and LHCA6::CDKA;1^{D146N} with open loops, and compared it with the percentage of control mature first-leaves with open loops.

Whereas no control mature first-leaf had open loops, ~15% of mature first-leaves of LHCA6::KRP2^{Δ73-97} and LHCA6::CDKA;1^{D146N} had open loops (Figure 2.2D).

In conclusion, our results are consistent with the hypothesis that cessation of cell proliferation prevents recruitment of ground cells into veins by permitting progression to mesophyll fate.

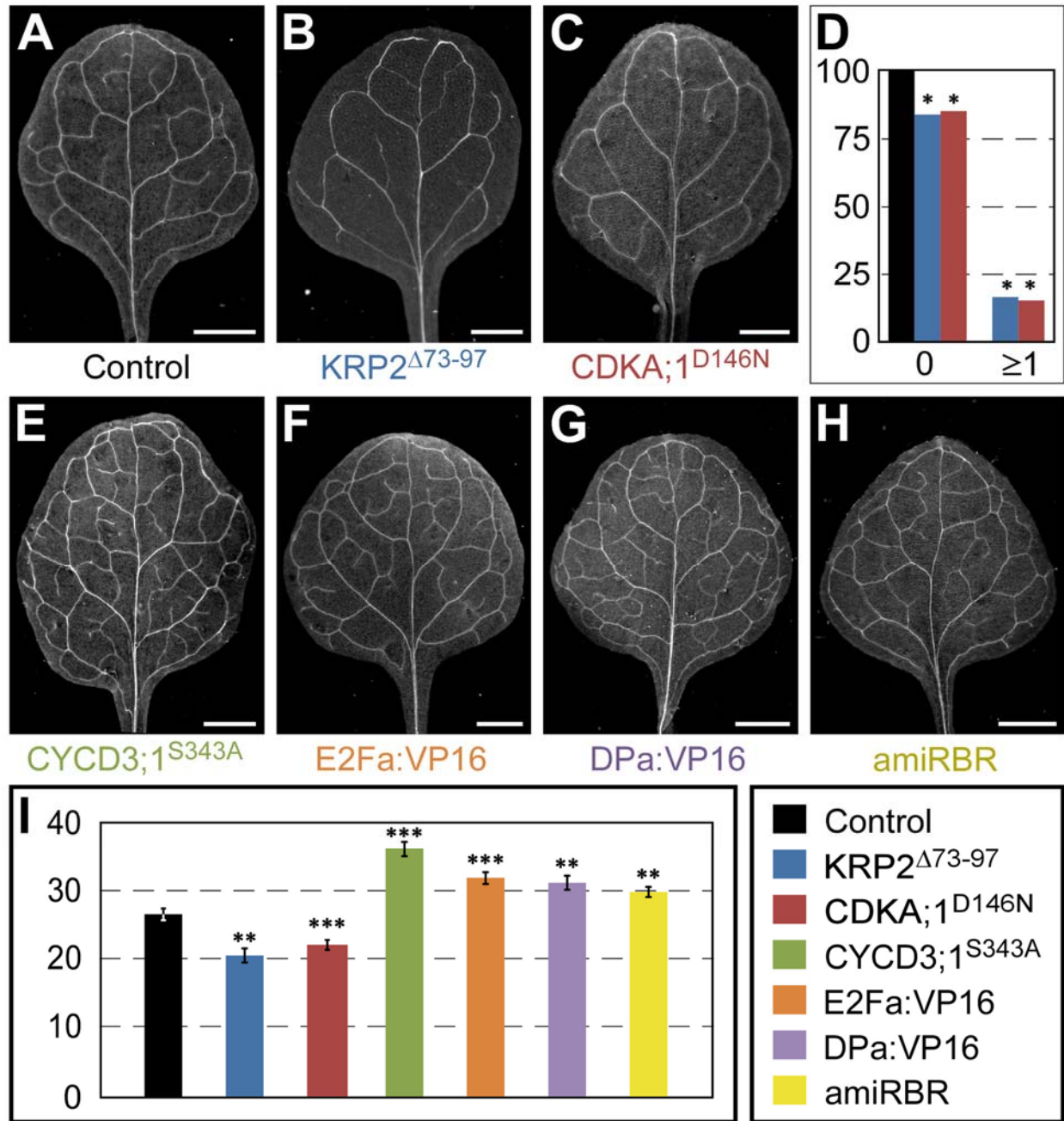


Figure 2.2. Ground cell proliferation and vein network formation. (A-C,E-H) Dark-field illumination of mature first leaves of control plants (A), or of plants expressing LHCA6::KRP2 Δ 73-97 (B), LHCA6::CDKA;1^{D146N} (C), LHCA6::CYCD3;1^{S343A} (E), LHCA6::E2Fa:VP16 (F), LHCA6::DPa:VP16 (G) or LHCA6::amiRBR (H). (D) Percentage of mature first leaves with 0 or \geq 1 open loops. Difference between LHCA6::KRP2 Δ 73-97 and control, and between LHCA6::CDKA;1^{D146N} and control was significant at $P < 0.05$ (*) by Kruskal-Wallis and Mann-Whitney test with Bonferroni correction. Sample population sizes: control, 35; LHCA6::KRP2 Δ 73-97, 37; LHCA6::CDKA;1^{D146N}, 59. (I) Cardinality index of mature first leaves

expressed as mean \pm SEM. Difference between LHCA6::KRP2 Δ ⁷³⁻⁹⁷ and control, between LHCA6::CDKA;1^{D146N} and control, between LHCA6::CYCD3;1^{S343A} and control, between LHCA6::E2Fa:VP16 and control, between LHCA6::DPa:VP16 and control, and between LHCA6::amiRBR and control was significant at $P < 0.01$ (**) or $P < 0.001$ (***) by F-test and t -test with Bonferroni correction. Sample population sizes: control, 35; LHCA6::KRP2 Δ ⁷³⁻⁹⁷, 37; LHCA6::CDKA;1^{D146N}, 59; LHCA6::CYCD3;1^{S343A}, 35; LHCA6::E2Fa:VP16, 38; LHCA6::DPa:VP16, 34; LHCA6::amiRBR, 48. Scale bars: 1 mm in A,E-H; 0.5 mm in B,C.

2.2.3 Ground cell proliferation and mesophyll fate specification

To test whether premature cessation of ground cell proliferation permitted premature progression to mesophyll fate, we compared LHCB2.3::nYFP expression in first-leaf development of LHCA6::KRP2^{Δ73-97} and WT.

Though in very few nuclei (one to three), LHCB2.3::nYFP was already expressed in LHCA6::KRP2^{Δ73-97} leaf primordia 2 DAG—a stage at which WT leaf primordia failed to express LHCB2.3::nYFP (Figure 2.3A,E). Furthermore, at comparable stages of leaf development, LHCB2.3::nYFP expression had extended to more-basal positions in LHCA6::KRP2^{Δ73-97} than in WT (Figure 2.3B,C,F,G,I). We observed a similar shift in the front of LHCB2.3::nYFP expression to more-basal positions in LHCA6::CDKA;1^{D146N} first leaves (Figure 2.3H). Therefore, our results suggest that premature cessation of ground cell proliferation permits premature progression to mesophyll fate.

We next tested whether delayed cessation of ground cell proliferation delayed progression to mesophyll fate by comparing LHCB2.3::nYFP expression in first-leaf development of LHCA6::CYCD3;1^{S343A} and WT.

LHCB2.3::nYFP was expressed in only very few nuclei (one to three) of LHCA6::CYCD3;1^{S343A} leaves 3 DAG—a stage at which, in WT, LHCB2.3::nYFP was already expressed in the apical half of the leaf (Figure 2.3B,J). Furthermore, at comparable stages of leaf development, LHCB2.3::nYFP expression had extended to less-basal positions in LHCA6::CYCD3;1^{S343A} than in WT (Figure 2.3C,D,I,K,L). We observed a similar shift in the front of LHCB2.3::nYFP expression to less-basal positions in first leaves of LHCA6::E2Fa:VP16, LHCA6::DPa:VP16 and LHCA6::amiRBR (Figure 2.3M-O). Therefore, our results suggest that delayed cessation of ground cell proliferation delays progression to mesophyll fate.

2.2.4 Leaf cell differentiation and vein network formation

Delayed cessation of ground cell proliferation delays progress to mesophyll fate and leads to formation of networks of more veins (Figures 2.2, 2.3). We asked whether a similar effect on vein network formation were induced by delayed onset of leaf cell differentiation. To address this question, we used *microRNA319a* (*miR319a*), which targets five of the eight members of the

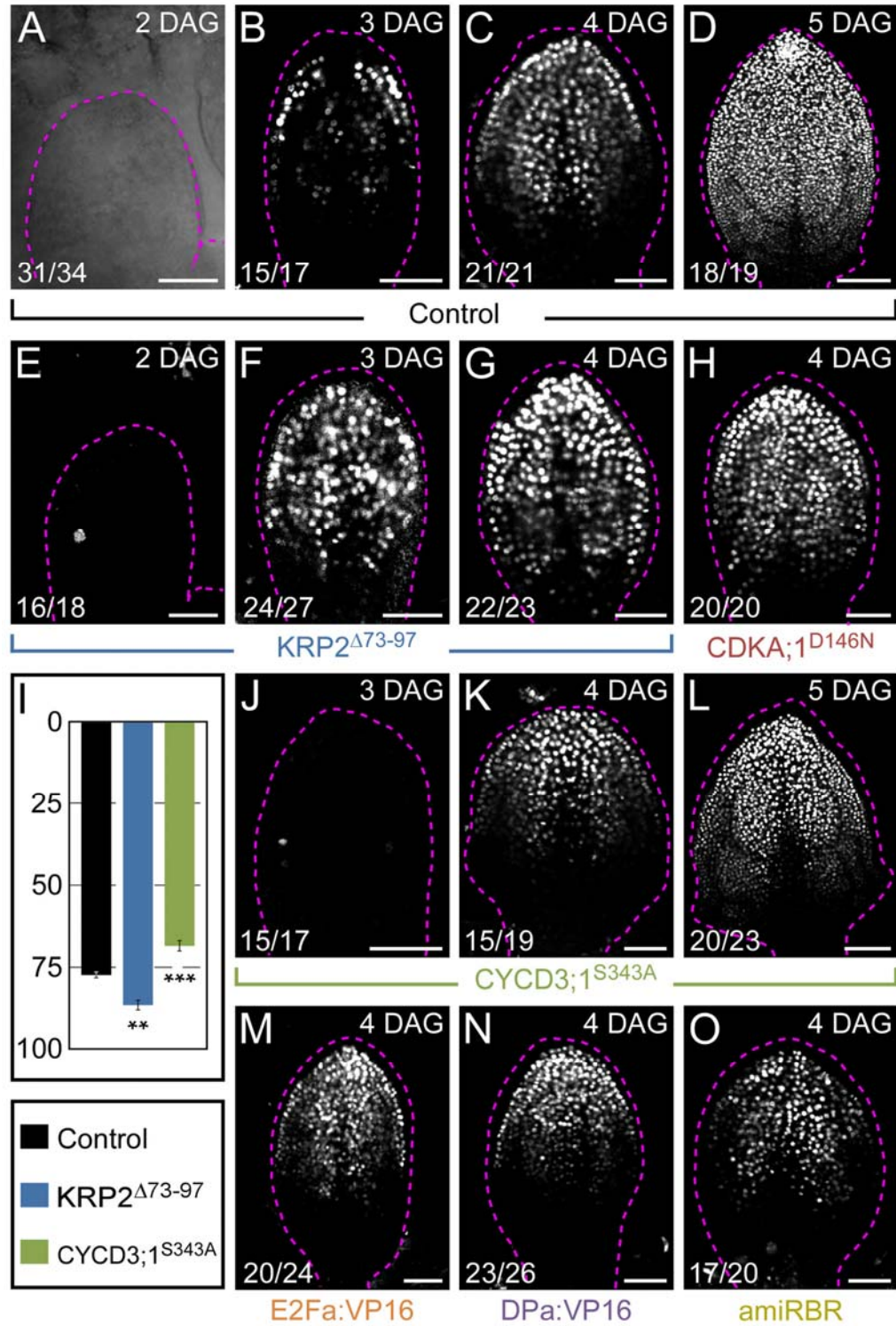


Figure 2.3. Ground cell proliferation and mesophyll fate specification. (A-H, J-O) Confocal laser scanning microscopy with (A) or without (B-H, J-O) transmitted light. White:

LHCB2.3::nYFP expression in first leaves of WT plants (A-D) or of plants expressing LHCA6::KRP2 Δ^{73-97} (E-G), LHCA6::CDKA;1 D146N (H), LHCA6::CYCD3;1 S343A (J-L), LHCA6::E2Fa:VP16 (M), LHCA6::DPa:VP16 (N) or LHCA6::amiRBR (O). Top right: leaf age in days after germination (DAG). Bottom left: reproducibility index. Dashed magenta line delineates leaf primordium outline. (I) Position of basal front of LHCB2.3::nYFP expression in 4-DAG first leaves (see Materials and methods for details), expressed as percentage of leaf blade length (0: leaf apex; 100: leaf base) \pm SEM. Difference between LHCA6::KRP2 Δ^{73-97} and control, and between LHCA6::CYCD3;1 S343A and control was significant at $P < 0.01$ (**) or $P < 0.001$ (***) by F-test and t -test with Bonferroni correction. Sample population sizes: control, 11; LHCA6::KRP2 Δ^{73-97} , 10; LHCA6::CYCD3;1 S343A , 10. Scale bars: 20 μ m in A,E; 50 μ m in B,C,F-H,J,K,M-O; 100 μ m in D,L.

CIN-TCP family of positive regulators of cell differentiation (Cubas et al., 1999; Efroni et al., 2008; Koyama et al., 2010; Nath et al., 2003; Ori et al., 2007; Palatnik et al., 2003; Sarvepalli and Nath, 2011; Schommer et al., 2008)—all five of which are expressed in the leaf, as visualized by expression of TCP::TCP:YFPs (TCP:YFP fusion proteins expressed by the respective *TCP* promoters) (Figure 2.4A-E); we overexpressed *miR319a* by the *UBIQUITIN 10* (*UBQ10*) promoter (Norris et al., 1993); and we calculated the cardinality index of vein networks of UBQ10::miR319a mature first-leaves, and compared it with that of vein networks of WT mature first-leaves.

The cardinality index of UBQ10::miR319a was higher than that of WT (Figure 2.4F,G,L), suggesting that delayed onset of leaf cell differentiation leads to formation of networks of more veins.

Premature cessation of ground cell proliferation leads to premature progress to mesophyll fate, formation of networks of fewer veins, and formation of leaves with open loops (Figures 2.2, 2.3). We asked whether a similar effect on vein network formation were induced by premature onset of leaf cell differentiation. To address this question, we used a fusion between the VP16 activation domain and an *miR319*-resistant variant of *TCP10* (*mTCP10*) (Figure 2.5); we overexpressed mTCP10:VP16 by the *UBQ10* promoter; we calculated the cardinality index of vein networks of UBQ10::mTCP10:VP16 mature first-leaves, and compared it with that of vein networks of WT mature first-leaves; and we calculated the percentage of UBQ10::mTCP10:VP16 mature first-leaves with open loops, and compared it with the percentage of WT mature first-leaves with open loops.

The cardinality index of UBQ10::mTCP10:VP16 was lower than that of WT (Figure 2.4F,H,L), suggesting that premature onset of leaf cell differentiation leads to formation of networks of fewer veins. Furthermore, nearly 85% of UBQ10::mTCP10:VP16 mature first-leaves had open loops, whereas only 2.5% of WT mature first-leaves had open loops (Figure 2.4M). Therefore, our results suggest that the effects on vein network formation of premature onset of leaf cell differentiation mimic those of premature cessation of ground cell proliferation, and the effects on vein network formation of delayed cessation of ground cell proliferation are mimicked by delayed onset of leaf cell differentiation.

We finally asked whether the effects of delayed onset of leaf cell differentiation on vein

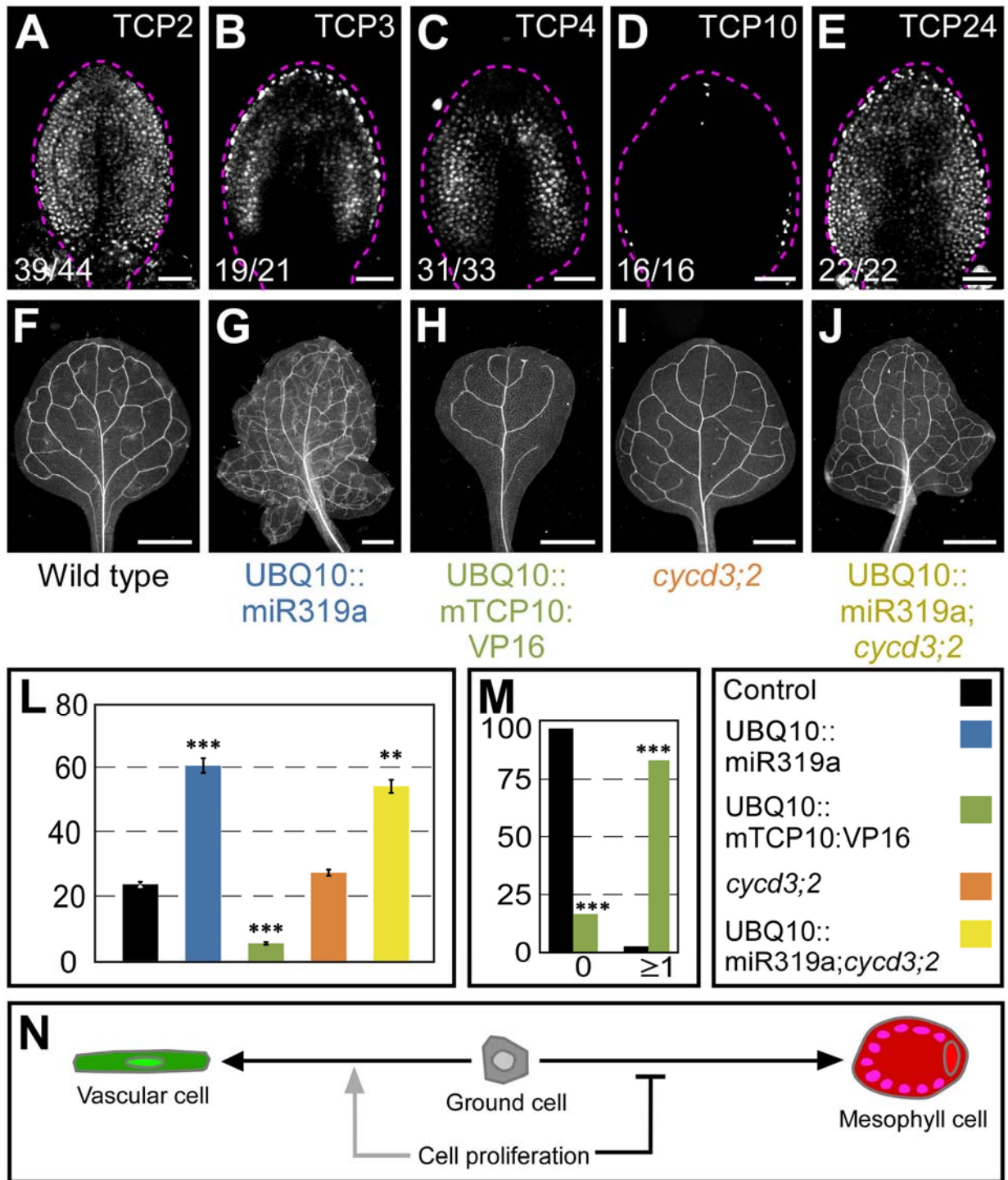


Figure 2.4. Leaf cell differentiation and vein network formation. (A-E) Confocal laser scanning microscopy. White: Expression of TCP2::TCP2:YFP (TCP2:YFP fusion protein expressed by the TCP2 promoter) (A), TCP3::TCP3:YFP (B), TCP4::TCP4:YFP (C), TCP10::TCP10:YFP (D) or TCP24::TCP24:YFP (E) in first leaves 4 days after germination.

Bottom left: reproducibility index. Dashed magenta line delineates leaf primordium outline. (F-J) Dark-field illumination of mature first leaves of WT (F) or *cyd3;2* (I) plants, or of plants expressing UBQ10::miR319a or UBQ10::mTCP10:VP16 in the WT background (G and H, respectively), or UBQ10::miR319a in the *cyd3;2* background (J). (L) Cardinality index of mature first leaves expressed as mean \pm SEM. Difference between UBQ10::miR319a and WT, between UBQ10::mTCP10:VP16 and WT, and between UBQ10::miR319a;*cyd3;2* and UBQ10::miR319a was significant at $P < 0.01$ (**) or $P < 0.001$ (***) by F-test and *t*-test with Bonferroni correction. (M) Percentage of mature first leaves with 0 or ≥ 1 open loops. Difference between UBQ10::mTCP10:VP16 and WT was significant at $P < 0.001$ (***) by Kruskal-Wallis and Mann-Whitney test with Bonferroni correction. Sample population sizes: WT, 40; UBQ10::miR319a, 23; UBQ10::mTCP10:VP16, 30; *cyd3;2*, 24; UBQ10::miR319a;*cyd3;2*, 30. (N) Summary and interpretation. During leaf development, ground cells progress to either mesophyll or vascular tissue fate (black arrows). Cell proliferation inhibits progression of ground cells to mesophyll fate (black blunt-ended line), thus permitting their recruitment into veins; conversely, cessation of cell proliferation permits progression of ground cells to mesophyll fate, thus preventing their recruitment into veins. This account by no means excludes that cell proliferation might also directly promote progression of ground cells to vascular fate (grey arrow). Scale bars: 50 μ m in A-E; 1 mm in F,H-J; 0.5 mm in G.

network formation were mediated, at least partly, by delayed cessation of leaf cell proliferation. Were this so, the effects of delayed leaf cell differentiation on vein network formation should be, at least partially, suppressed by mutation in a positive regulator of leaf cell proliferation. To test this prediction, we determined whether mutation in *CYCD3;2* (Dewitte et al., 2007; Swaminathan et al., 2000) lowered the cardinality index of vein networks of UBQ10::miR319a mature first-leaves.

The cardinality index of *cycd3;2* was no different from that of WT (Figure 2.4F,I,L), but the cardinality index of UBQ10::miR319a;*cycd3;2* was lower than that of UBQ10::miR319a (Figure 2.4G,J,L). Therefore, our results suggest that the effects of delayed onset of leaf cell differentiation on vein network formation are mediated, at least partly, by delayed cessation of leaf cell proliferation, an account that is consistent with the inhibitory function on cell proliferation of recently identified targets of TCP4 (Schommer et al., 2014).

2.2.5 Control of leaf tissue pattern by ground cell proliferation

It has long been known that during leaf development ground cells progress to either one of two tissue fates: mesophyll or vascular (Flot, 1905); but what controls this decision is still poorly understood. Our results suggest that cell proliferation inhibits progression of ground cells to mesophyll fate, thus permitting their recruitment into veins, and that cessation of cell proliferation permits progression of ground cells to mesophyll fate, thus preventing their recruitment into veins (Figure 2.4N). This account is consistent with the inability of ground cells that have progressed to mesophyll fate to respond to vein-formation-inducing signals (Scarpella et al., 2006), and with the responsiveness of minor vein formation to changes in leaf cell proliferation (Kang et al., 2007).

One alternative account of our results is that cell proliferation permits files of ground cells to progress to vascular fate, and that files of ground cells that have progressed to vascular fate non-cell-autonomously inhibit progression of surrounding ground cells to mesophyll fate. However, this less-parsimonious account is inconsistent with the unresponsiveness of the timing of vascular fate specification to changes in leaf cell proliferation (Kang et al., 2007), and with the inability of vein-formation-inducing signals to override progression of ground cells to mesophyll fate (Scarpella et al., 2006).

Available evidence suggests that within both plant and animal tissues the timing of cessation of cell proliferation controls progression to cell fate. For example, in mouse, premature cessation of cell proliferation in neural progenitors leads to formation of neural tubes in which early-specified cell types differentiate at the expense of late-specified ones (Hatakeyama et al., 2004). Likewise, in Arabidopsis roots, premature cessation of cell proliferation in vascular precursors leads to the formation of vascular cylinders in which the early-specified xylem cell-types differentiate at the expense of the late-specified phloem cell-types (Mahonen et al., 2000). Further, in Arabidopsis sepals, premature cessation of epidermal cell proliferation permits progression to giant-cell fate at the expense of small-cell fate, and prolonged cell proliferation permits progression to small-cell fate at the expense of giant-cell fate (Roeder et al., 2012). Our results suggest that the timing of cessation of cell proliferation controls not only progression to cell fate within tissues but progression to tissue fate within organs. This is not unprecedented in animals [e.g., (Lopez-Rios et al., 2012; Towers et al., 2008; Zhu et al., 2008)], but it is to some extent unexpected that plants, which have evolved multicellularity independently of animals [reviewed in (Grosberg and Strathmann, 2007)], may have converged to a similar strategy. In leaves, this strategy could account for the close correlation between leaf growth and vein formation that prevents functional mistakes—for example, areas of the leaf without vein supply (Sachs, 1989). Future work will show how common this strategy is in the control of tissue patterns of other plant-organs.

2.3 Materials and methods

2.3.1 Plants

Origin and nature of lines, and oligonucleotide sequences are in Table 2.1 and 2.2, respectively. Seeds were sterilized and germinated, seedlings and plants were grown (seedlings: $\sim 60 \mu\text{mol m}^{-2} \text{s}^{-1}$; plants: $80 \mu\text{mol m}^{-2} \text{s}^{-1}$), and plants were transformed as described in (Sawchuk et al., 2008).

Table 2.1. Origin and nature of lines

Line	Origin/Nature
LHCB2.3::nYFP	(Sawchuk et al., 2008)
ATHB8::nCFP	(Sawchuk et al., 2007)
CYCB1;1::CYCB1;1:YFP	Translational fusion of <i>CYCB1;1</i> (AT4G37490; -1068 to +712; primers: ‘CycB1;1 Eco Forw’ and ‘CycB1;1 Bam Rev’) to EYFP-N1 (Clontech)
LHCA6::nYFP	(Sawchuk et al., 2008)
LHCA6::KRP2 ^{Δ73-97}	Transcriptional fusion of <i>LHCA6</i> (AT1G19150; -391 to -1; primers: ‘A6 HindIII FORW’ and ‘Sali A6 rev’) to <i>KRP2</i> (AT3G50630) cDNA (GenBank accession no.: AK176528; RIKEN resource no.: pda14901 (Seki et al., 1998; Seki et al., 2002); +1 to +213 and +292 to +630; primers: ‘KRP2-3 BamHI’ and ‘KRP2-4 EcoRV’; ‘KRP2-1 EcoRV’ and ‘KRP2-2 KpnI’)
LHCA6::CDKA;1 ^{D146N}	Transcriptional fusion of <i>LHCA6</i> (AT1G19150; -391 to -1; primers: ‘A6 HindIII FORW’ and ‘Sali A6 rev’) to <i>CDKA;1</i> (AT3G48750) cDNA (GenBank accession no.: AY090353; RIKEN resource no.: pda07963 (Seki et al., 1998; Seki et al., 2002); +1 to +885; primers: ‘CDKA DN Forw’ and ‘CDKA DN rev’; ‘CDKA-Sali forw’ and ‘CDKA Sali rev’)
LHCA6::CYCD3;1 ^{S343A}	Transcriptional fusion of <i>LHCA6</i> (AT1G19150; -391 to -1; primers: ‘A6 HindIII FORW’ and ‘Sali A6 rev’) to <i>CYCD3;1</i> (AT4G34160) cDNA (GenBank accession no.: AK221712; RIKEN resource no.: pda15584 (Seki et al., 1998; Seki et al., 2002); +1 to +1131; primers: ‘NEW CYCD SA FORW’ and ‘CYCD SA Rev’; ‘CYCD-Sali forw’ and ‘CYCD-BamHI rev’)
LHCA6::E2Fa:VP16	Transcriptional fusion of <i>LHCA6</i> (AT1G19150; -391 to -1; primers: ‘A6 HindIII FORW’ and ‘Sali A6 rev’) to translational fusion of <i>E2Fa</i> (AT2G36010) cDNA (GenBank accession no.: BT026376; ABRC clone no.: U85762; +1 to +1542; primers: ‘BamHI-E2Fa Forw’ and ‘XhoI-E2Fa rev’) to VP16 activation domain (GenBank accession: HM585511; a kind gift of D. Weijers; +1 to +237; primers: ‘XhoI-VP16 forw’ and ‘KpnI-VP16 rev’)

LHCA6::DPa:VP16	Transcriptional fusion of <i>LHCA6</i> (AT1G19150; -391 to -1; primers: 'A6 HindIII FORW' and 'SalI A6 rev') to translational fusion of <i>DPa</i> (AT5G02470) cDNA (GenBank accession no.: AK117135; RIKEN resource no.: pda10164; +1 to + 876 (Seki et al., 1998; Seki et al., 2002); primers: 'SalI-DPa Forw' and 'XhoI-DPa rev') to VP16 activation domain (GeneBank accession: HM585511; a kind gift of D. Weijers; +1 to +237; primers: 'XhoI-VP16 forw' and 'KpnI-VP16 rev')
LHCA6::amiRBR	Transcriptional fusion of <i>LHCA6</i> (AT1G19150; -391 to -1; primers: 'A6 HindIII FORW' and 'SalI A6 rev') to an artificial microRNA (Ossowski et al., 2008; Schwab et al., 2006) targeting <i>RBR</i> (AT3G12280; primers: 'pRS300 A' and 'IV miRBR*a'; 'II miRBR-a' and 'III miRBR*s'; 'I miRBR-s' and 'pRS300 B')
TCP2::TCP2:YFP	Translational fusion of <i>TCP2</i> (AT4G18390; -3105 to +1095; primers: 'TCP2 pro SalI Forw' and 'TCP2 BamHI Rev') to EYFP (primers: 'YFP BamHI linker Forw' and 'YFP KpnI Rev')
TCP3::TCP3:YFP	Translational fusion of <i>TCP3</i> (AT1G53230; -3119 to +1173; primers: 'TCP3 pro SalI Forw' and 'TCP3 SalI rev') to EYFP (primers: 'YFP BamHI linker Forw' and 'YFP KpnI Rev')
TCP4::TCP4:YFP	Translational fusion of <i>TCP4</i> (AT3G15030; -3032 to +1260; primers: 'TCP4 pro XhoI Forw' and 'TCP4 BamHI Rev') to EYFP (primers: 'YFP BamHI linker Forw' and 'YFP KpnI Rev')
TCP10::TCP10:YFP	Translational fusion of <i>TCP10</i> (AT2G31070; -1150 to +1086; primers: 'TCP10 prom Forw (XhoI)' and 'TCP10 rev (BamHI)') to EYFP (-10 to + 725 relative to the transcription start site; primers: 'YFP BamHI linker Forw' and 'YFP KpnI Rev')
TCP24::TCP24:YFP	Translational fusion of <i>TCP24</i> (AT1G30210; -3111 to +972; primers: 'TCP24 pro SalI Forw' and 'TCP24 BamHI rev') to EYFP (primers: 'YFP BamHI linker Forw' and 'YFP KpnI Rev')

UBQ10::miR319a	Transcriptional fusion of <i>UBQ10</i> (AT4G05320; -1516 to -1; primers: 'UBQ10 HindIII Forw' and 'UBQ10 SmaI Rev') to <i>miR319a</i> (AT4G23713; -55 to +335 relative to the transcription start site; primers: 'gJaw KpnI forw' and 'gJAW BamHI rev')
UBQ10::mTCP10:VP16	Transcriptional fusion of <i>UBQ10</i> (AT4G05320; -1516 to -1; primers: 'UBQ10 HindIII Forw' and 'UBQ10 SmaI Rev') to translational fusion of <i>mTCP10</i> (GeneArt AG; Figure 2.5; primers: 'TCP10-XhoI Forw' and 'TCP10-EcoRI Rev, and 'mTCP10 end Forw' and 'mTCP10 end Rev') to VP16 activation domain (GeneBank accession: HM585511; a kind gift of D. Weijers; +1 to +237; primers: 'XhoI-VP16 forw' and 'KpnI-VP16 rev')
<i>cycd3;2</i>	(Dewitte et al., 2007; Swaminathan et al., 2000)

Unless otherwise indicated, all coordinates are relative to the start codon. The Arabidopsis full-length cDNA clones of *KRP2*, *CDKA;1*, *CYCD3;1* and *DPa* were developed by the plant genome project of RIKEN Genomic Sciences Center.

Table 2.2. Oligonucleotide sequences

Name	Sequence (5' to 3')
CycB1;1 Eco Forw	TACGAATTCGGGAACCATAGCTACACCACACC
CycB1;1 Bam Rev	ATAGGATCCTTCTCTCGAGCAGCAACTAAAC
A6 HindIII FORW	ACTAAGCTTCGTTCCGGAGTAAGAG
Sall A6 rev	GATGTCGACCTTTGATTCGTGGGGAGATG
KRP2-3 BamHI	TAAGGATCCATGGCGGCGGTTAGGAGAAG
KRP2-4 EcoRV	GAGGATATCTCGCCGTCGTACTATAACAAC
KRP2-1 EcoRV	CAGGATATCAAATCGAAACGGAGAATCG
KRP2-2 KpnI	ACTGGTACCTCATGGATTCAATTTAACCCACTC
CDKA DN Forw	ACTGAAGCTTGCTAATTTTGGACTGGC
CDKA DN rev	GAGTTTGTGCGGCGATCAATCAAC
CDKA-Sall forw	CTGGTTCGACATGGATCAGTACGAGAAAG
CDKA Sall rev	ATAGTCGACCTAAGGCATGCCTCCAAG
New CYCD SA Forw	CGTCGTCGTCGGCCCCGCAGCAACAAC
CYCD SA Rev	TTGGTGGGTTCACGAACTCGCTGACC
CYCD-Sall forw	ATAGTCGACATGGCGATTTCGGAAGGAGG
CYCD-BamHI rev	GTCGGATCCTTATGGAGTGGCTACGATTG
BamHI-E2Fa Forw	ATAGGATCCATGTCCGGTGTTCGTACGATC
XhoI-E2Fa rev	TATCTCGAGTCTCGGGGTTGAGTCAACAGC
XhoI-VP16 forw	ATACTCGAGGCCCGCCCGACCGATGTCAG
KpnI-VP16 rev	CGTGGTACCCTACCCACCGTACTCGTCAATTC
Sall-DPa Forw	TCAGTCGACATGAGTATGGAGATGGAGTTG
XhoI-DPa rev	ATTCTCGAGGCGAGTATCAATGGATCCCG
pRS300 A	CTGCAAGGCGATTAAGTTGGGTAAC
IV miRBR*a	GAAACTCTGAATTACCTTGTTATCTACATATATATTCCT
II miRBR-a	GATAGCAAGGTAATTGAGAGTTATCAAAGAGAATCAATGA
III miRBR*s	GATAACAAGGTAATTCAGAGTTTTTCACAGGTCGTGATATG
I miRBR-s	GATAACTCTCAATTACCTTGCTATCTCTTTTTGTATTCC
pRS300 B	GCGGATAACAATTTACACACAGGAAACAG
TCP2 pro Sall Forw	CTTGTCGACGACCAAGAAGCAGACACGTGC
TCP2 BamHI Rev	GCGGGATCCTCGTTCTTGCCTTTACCCTTATG

YFP BamHI linker Forw	ATAGGATCCAGGTGTGAGCAAGGGCGAGGAGC
YFP KpnI Rev	ATAGGTACCCTAGATAGATCTCTTGTACAGCTC
TCP3 pro Sall Forw	GTTGTTCGACGGAGGACTTGCATAGGTAGAG
TCP3 Sall rev	CATGTTCGACCTATGGCGAGAATCTGATGAAGC
TCP4 pro XhoI Forw	ACTCTCGAGGTGGTCATCGGGTCGATTGG
TCP4 BamHI Rev	TGAGGATCCACATGGCGAGAAATAGAGGAAG
TCP10 prom Forw (XhoI)	CGACTCGAGATTGTTTTGATGCATGCCAG
TCP10 rev (BamHI)	GCGGGATCCTCGAGGTGTGAGTTTGGAGGAG
TCP24 pro Sall Forw	CGTGTCGACTGAATCTACTTATTGGAGCAAG
TCP24 BamHI rev	TACGGATCCTCTCTCCTTTCCTTTGCCTTGTC
UBQ10 HindIII Forw	CTCAAGCTTTCCCATGTTTCTCGTCTGTC
UBQ10 SmaI Rev	CGACCCGGGCTGTTAATCAGAAAACTCAG
gJaw KpnI forw	GTCGGTACCTGTTTCATACACTTAATACTCGC
gJAW BamHI rev	GACGGATCCTCTTCTTCACCTATCCATGGC
TCP10-XhoI Forw	ACACTCGAGATGGGACTTAAAGGATATAGC
TCP10-EcoRI Rev	GTAGAATTCGAGGTGTGAGTTTGGAGGAGAAG
mTCP10 end Forw	CAGGATGACAACAACATGGTCTCAAG
mTCP10 end Rev	TGCAGGAATTCGAGGTGTGAGTTTG

2.3.2 Imaging

Developing leaves were mounted and imaged as in (Sawchuk et al., 2013), except that emission was collected from ~5- μ m-thick optical slices. Marker-line-specific imaging parameters are in Table 2.3. Position of basal front of LHCb2.3::nYFP expression was equated to basal-most point of leaf blade length where fluorescence signal in 8-bit, grayscale images acquired at identical settings exceeded by more than 3 standard deviations average local background (estimated from a ~1,500-pixel area containing fluorescent features of no interest), and was measured with the Plot Profile plugin of ImageJ (National Institutes of Health). Mature leaves were fixed in 3:1 ethanol:acetic acid, rehydrated in 70% ethanol and water, cleared briefly (few seconds to few minutes) in 0.4 M sodium hydroxide, washed in water and mounted in 1:3:8 water:glycerol:chloral hydrate (Sigma-Aldrich Corp., St. Louis, MO). Mounted leaves were imaged as in (Odat et al., 2014). (Chapter 3) Image brightness and contrast were adjusted by linear stretching of the histogram with ImageJ (National Institutes of Health). Images were cropped with Photoshop (Adobe Systems Inc., San Jose, CA) and assembled into figures with Canvas (ACD Systems International Inc., Victoria, BC).

2.3.3 Vein network analysis

Vein networks were analyzed as in (Verna et al., 2015). Briefly, number of “touch points” (TPs; TP defined as point where a vein end contacts another vein), “end points” (EPs; EP defined as point where an “open” vein—a vein that contacts another vein only at one end—terminates free of contact with another vein), and “exit points” (XPs; XP defined as point where a vein exits leaf blade and enters leaf petiole) in dark-field images of cleared mature leaves was calculated with the Cell Counter plugin of ImageJ (National Institutes of Health). Because a vein network can be understood as an undirected graph in which TPs, EPs and XPs are vertices and veins are edges, and because each vein is incident to two TP, a TP and an XP, a TP and an EP, or an XP and an EP, the cardinality index—a measure of the size (i.e. the number of edges) of a graph—is a proxy for the number of veins and is calculated as: $[(TPs+XPs-EPs)/2]+EPs$, or: $(TPs+XPs+EPs)/2$.

Table 2.3. Imaging parameters

A								
Line	Laser	Wavelength (nm)	Main dichroic beam splitter	First secondary dichroic beam splitter	Second secondary dichroic beam splitter	Emission filter (detector)		
LHCB2.3::EYFP	Ar	514	HFT 405/514/594	NFT 595	NFT 515	BP 520-555 IR (PMT3)		
TCP2::TCP2:EYFP	Ar	514	HFT 405/514/594	NFT 595	NFT 515	BP 520-555 IR (PMT3)		
TCP3::TCP3:EYFP	Ar	514	HFT 405/514/594	NFT 595	NFT 515	BP 520-555 IR (PMT3)		
TCP4::TCP4:EYFP	Ar	514	HFT 405/514/594	NFT 595	NFT 515	BP 520-555 IR (PMT3)		
TCP10::TCP10:EYFP	Ar	514	HFT 405/514/594	NFT 595	NFT 515	BP 520-555 IR (PMT3)		
TCP24::TCP24:EYFP	Ar	514	HFT 405/514/594	NFT 595	NFT 515	BP 520-555 IR (PMT3)		
B								
Multi-marker lines	Single-marker lines		Laser	Wavelength (nm)	Main dichroic beam splitter	First secondary dichroic beam splitter	Second secondary dichroic beam splitter	Emission filter (detector)
ATHB8::nCFP; LHCB2.3::nYFP	ATHB8::nCFP		Ar	458	HFT 458/514	NFT 595	NFT 545	BP 475-525 (PMT2)

	LHCB2.3::nYFP	Ar	514	HFT 458/514	NFT 595	NFT 515	BP 520- 555 IR (PMT3)
	Chlorophyll	Ar	458	HFT 458/514	NFT 595		604-700 (META)
ATHB8::nCFP; CYCB1;1::CYCB1,1:YFP	ATHB8::nCFP	Ar	458	HFT 458/514	NFT 595	NFT 545	BP 475- 525 (PMT2)
	CYCB1;1::CYCB1,1:YFP	Ar	514	HFT 458/514	NFT 595	NFT 515	BP 520- 555 IR (PMT3)
	Chlorophyll	Ar	458	HFT 458/514	NFT 595		604-700 (META)
ATHB8::nCFP; LHCA6::nYFP	ATHB8::nCFP	Ar	458	HFT 458/514	NFT 595	NFT 545	BP 475- 525 (PMT2)
	LHCA6::nYFP	Ar	514	HFT 458/514	NFT 595	NFT 515	BP 520- 555 IR (PMT3)
	Chlorophyll	Ar	458	HFT 458/514	NFT 595		604-700 (META)

CHAPTER 3: CHARACTERIZATION OF AN ALLELIC SERIES IN THE *MONOPTEROS* GENE OF *ARABIDOPSIS*

3.1 Introduction

Auxin is a central regulator of plant development: during embryogenesis, it controls patterning of the embryo parts; during post-embryonic development, it controls the patterned formation of lateral shoot organs and lateral roots, and of their tissues (De Smet and Jurgens, 2007). The auxin signal is transduced by multiple pathways (Leyser, 2010); best understood is that which ends with the transcriptional activation or repression of auxin-responsive genes by transcription factors of the AUXIN RESPONSE FACTOR (ARF) family (Chapman and Estelle, 2009).

Of the 22 *ARF* genes in *Arabidopsis thaliana* (Guilfoyle and Hagen, 2007), *MONOPTEROS* (*MP*)/*ARF5* is the only one whose mutation results in conspicuous patterning defects in embryos and seedlings (Okushima et al., 2005). In *mp* embryos and seedlings, hypocotyl and root are typically replaced by a conical structure with no apparent cellular organization (“basal peg”), but weak mutant alleles occasionally form a short hypocotyl (Berleth and Jurgens, 1993) or both hypocotyl and root (Cole et al., 2009; Donner et al., 2009; Schlereth et al., 2010). In *mp*, the two cotyledons may be separate—as in wild-type (WT)—they may be fused to varying extents, or a single cotyledon may be formed (Berleth and Jurgens, 1993). Invariably, however, the vein network of *mp* cotyledons is simplified (Berleth and Jurgens, 1993). The severity of these defects has been shown to be inversely proportional to the amount of residual *MP* function and has thus been conventionally used as criterion to define allele strength (Berleth and Jurgens, 1993; Cole et al., 2009; Donner et al., 2009; Hardtke and Berleth, 1998; Schlereth et al., 2010).

Most *mp* alleles are in the Landsberg *erecta* background (Berleth and Jurgens, 1993), and only seven, recessive *mp* alleles have been reported in the widely used Columbia (Col) background: two extensively characterized (*mp*^{G33} and *mp*^{S319}/*arf5-2*) and five only partially characterized (*mp*^{G12}, *mp*^{G25}, *mp*^{BS1354}, *arf5-1* and *mp*^{B4149}) (Cole et al., 2009; Donner et al., 2009; Hardtke and Berleth, 1998; Okushima et al., 2005; Przemeck et al., 1996; Schlereth et al., 2010; Weijers et al., 2005a). One of these five *mp* alleles (*mp*^{G25}) appears to be extinct and thus unavailable for

analysis. We show that two of the four remaining, partially characterized *mp* alleles reported to be in the Columbia background (*mp*^{BS1354} and *mp*^{B4149}) are in fact not in this background. We extend characterization of the remaining two Columbia alleles of *mp* (*mp*^{G12} and *arf5-1*), and we identify and characterize four new alleles of *mp* in the Columbia background (*mp-11*, *mp-12*, *mp-13* and *mp-14*), among which the first low-expression allele of *mp* (*mp-11*) and the strongest Columbia allele of *mp* (*mp-13*). These genetic resources provide the research community with new experimental opportunities for insight into the function of *MP*-dependent auxin signalling in plant development.

3.2 Results and Discussion

We were unable to induce germination of seed stocks of *mp*^{G25}; it is therefore possible that this allele has to be considered extinct and thus unavailable for further analysis. Because WT-looking siblings of *mp*^{BS1354} and *mp*^{B4149} appeared different from Col plants, we characterized their background and found that *mp*^{BS1354} is in a Col/Wassilewskija mixed background (Figure 3.1B) and *mp*^{B4149} is in the Utrecht background (Figure 3.1C). We thus excluded these two alleles from further analysis.

The inviability of *mp*^{G25} seed stocks and the non-Col backgrounds of *mp*^{BS1354} and *mp*^{B4149} left only *mp*^{G12} and *arf5-1* as partially characterized *mp* alleles in the Col background. We thus surveyed available resources and identified seven additional, putative alleles of *mp* in the Col background: lines WiscDsLox489-492C10, SAIL_1265_F06, SALK_144183, SALK_149553, WiscDsLoxHs148_11H, WiscDsLoxHs148_12G and SALK_001058.

None of the 30 plants that grew from the seed stock of line SALK_144183 (predicted to have an insertion in the first intron of *MP*) or of the 60 plants that grew from the seed stock of line WiscDsLoxHs148_12G (predicted to have an insertion in the 10th exon of *MP*) had *mp*-like defects. Furthermore, we were unable to confirm the presence of insertion in *MP* in any of those plants. Finally, none of the progeny of those plants (~50 seedlings/plant) had *mp*-like defects. It is thus possible that lines SALK_144183 and WiscDsLoxHs148_12G are incorrectly annotated or that seeds that have inherited those insertions are extremely infrequent in the currently

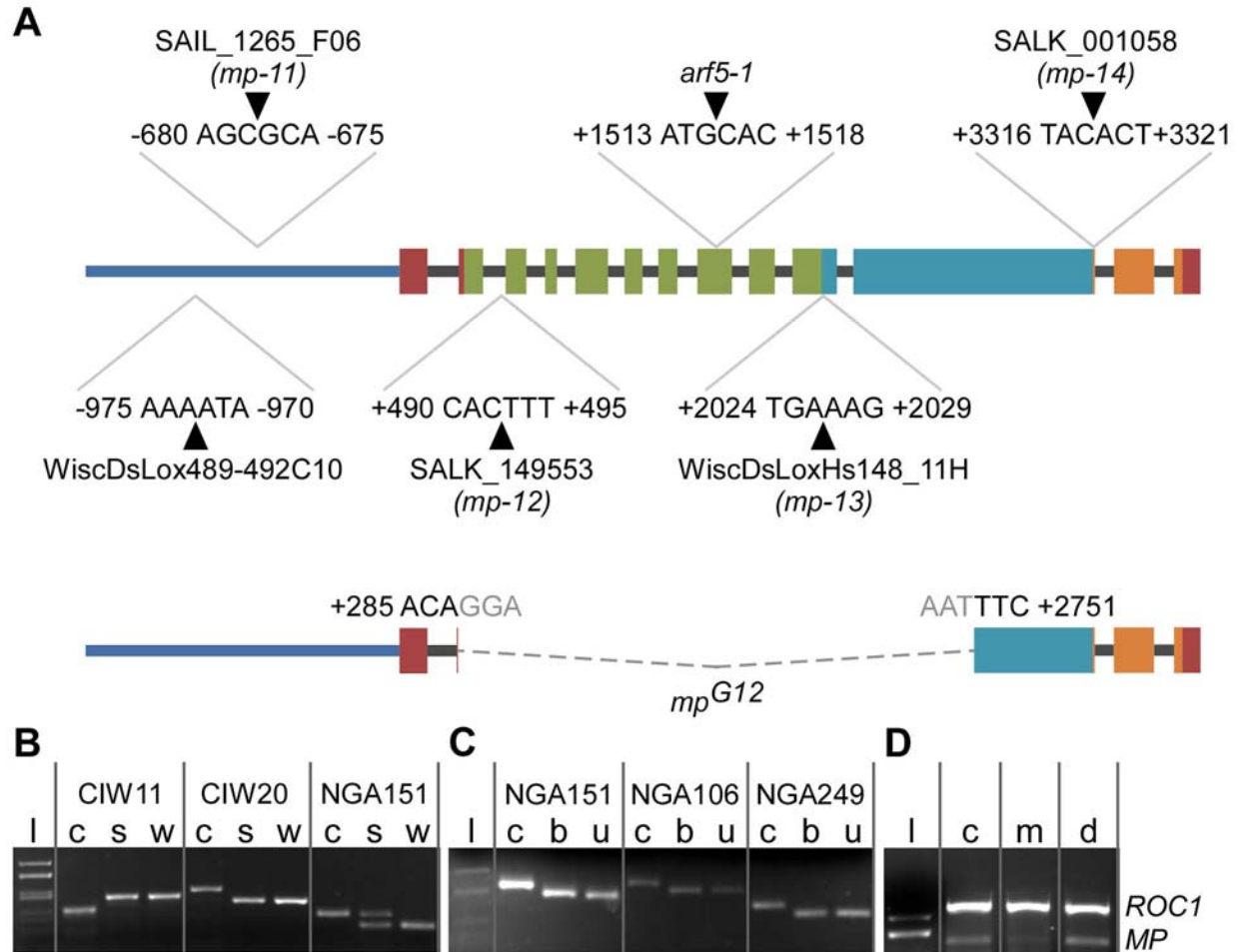


Figure 3.1. Mutations in the *MP* gene. (A) Schematic diagram of the *MP* gene indicating position of insertions (black triangles) in *mp* mutants (top) or nature of molecular lesion in *mp^{G12}* (bottom). Coordinates are in nucleotides relative to the first nucleotide of the start codon. Lines depict promoter (blue, -1500 to -1) or introns (grey). Boxes depict translated exons: brown, sequences with unclear function (+1 to +309 and +3744 to +3827); green, sequence encoding the DNA-binding domain (Ulmasov et al., 1999a) (+310 to +2018); teal, sequence encoding the activation domain (Tiwari et al., 2003) (+2019 to +3312); orange, sequence encoding the carboxyl-terminal dimerization domain (Guilfoyle and Hagen, 2012) (+3313 to +3743). Dashed line depicts region of *MP* deleted in *mp^{G12}* and replaced with a sequence identical to sequences on all chromosomes (grey font, 5'-end of deletion) or with a sequence identical to gene AT1G16400 (grey font, 3'-end of deletion). See text for details. (B) Analysis of SSCP markers CIW11, CIW20, and NGA151 in Columbia (c), *mp^{BS1354}* (s), and Wassilewskija (w). I, molecular weight marker (*Hae*III-digested pBluescript II). (C) Analysis of SSCP markers NGA151, NGA106, and NGA249 in Columbia (c), *mp^{B4149}* (b), and Utrecht (u). I, molecular weight marker (*Hae*III-digested pBluescript II). (D) RT-PCR analysis of *MP* expression in 4-day-old seedlings of Columbia (c), SAIL_1265_F06/*mp-11* (m), and WiscDsLox489-492C10 (d). The nearly evenly expressed *ROC1* (Lippuner et al., 1994) was used as control. I, molecular weight marker (*Hae*III-digested pBluescript II).

available stocks.

We found a T-DNA insertion after nucleotide -973 of *MP*—nucleotide coordinates are relative to the first nucleotide of the start codon—in line WiscDsLox489-492C10 (Figure 3.1A), but seedlings homozygous for such insertion had no defects or reduction in *MP* transcript (Figure 3.1D). We thus excluded line WiscDsLox489-492C10 from further analysis.

Here we extend the characterization of the Col alleles *mp^{G12}* and *arf5-1*, and we characterize four new alleles of *mp* in the Col background, including the first low-expression allele and the strongest Col allele.

We first determined the precise location of insertion in lines SAIL_1265_F06, SALK_149553, WiscDsLoxHs148_11H, and SALK_001058, and in *arf5-1*. We found a T-DNA insertion after nucleotide -678 of *MP* in line SAIL_1265_F06 (Figure 3.1A); seedlings homozygous for such insertion had lower levels of *MP* transcript (Figure 3.1D). Line SALK_149553 has a T-DNA insertion in the second intron of *MP* (Figure 3.1A). *arf5-1* has a T-DNA insertion in the eighth exon of *MP*, which encodes part of the DNA-binding domain (DBD) (Ulmasov et al., 1999b) (Figure 3.1A). Line WiscDsLoxHs148_11H has a T-DNA insertion in the 10th exon of *MP*, at the beginning of the sequence encoding the activation domain (AD) (Tiwari et al., 2003; Ulmasov et al., 1999a) (Figure 3.1A). And line SALK_001058 has a T-DNA insertion in the 11th exon of *MP*, at the beginning of the sequence encoding for the carboxyl-terminal domain (CTD), which mediates interaction with ARF proteins or with repressors of the AUX/IAA family (Guilfoyle and Hagen, 2012) (Figure 3.1A). Next, we determined by PCR the nature of the *MP* lesion in *mp^{G12}* and found that in this allele part of the *MP* gene was missing. By Vectorette PCR, we found that the missing sequence extended from nucleotide +288 to nucleotide +2748 (Figure 3.1A). We isolated 435 bp of the sequence that preceded nucleotide +2748 of *MP* in *mp^{G12}* and found it to be identical to the sequence from nucleotide +2076 to nucleotide +1641 of gene AT1G16400. We also isolated 34 bp of the sequence that followed nucleotide +288 of *MP* in *mp^{G12}* and found it to be identical to a sequence present on all five chromosomes. Our results are thus consistent with those of RFLP mapping, suggesting that the *mp^{G12}* allele is the result of a large chromosomal defect (Hardtke and Berleth, 1998).

We next analyzed the axis of seedlings homozygous for *mp^{G12}* or *arf5-1*, or for insertions SAIL_1265_F06, SALK_149553, WiscDsLoxHs148_11H, or SALK_001058. WT seedlings can be formalized as a top-to-bottom sequence of pattern elements: shoot meristem, cotyledons, and seedling axis—composed of hypocotyl and root (Capron et al., 2009) (Figure 3.2A). In ~20-25% of the progeny of self-fertilized plants heterozygous for *mp^{G12}* ($n=667$) or *arf5-1* ($n=626$), or for insertions SAIL_1265_F06 ($n=823$), SALK_149553 ($n=669$), or WiscDsLoxHs148_11H ($n=735$), hypocotyl and root were replaced by a basal peg lacking the central vein typical of WT hypocotyl and root (Figure 3.2A,B,D,E,G). Approximately 22% ($n=784$) of the progeny of self-fertilized plants heterozygous for insertion SALK_001058 were rootless; the hypocotyl was missing from most rootless seedlings, but a short hypocotyl with its central vein was formed in small proportion (<1%) of them (Figure 3.2C,F). The proportion of rootless seedlings in the progeny of self-fertilized plants heterozygous for *mp^{G12}* or *arf5-1*, or for insertions SAIL_1265_F06, SALK_149553, WiscDsLoxHs148_11H, or SALK_001058, was not significantly different from that expected for a recessive phenotype associated with mutation in a single nuclear gene as tested by Chi-squared test. We renamed SAIL_1265_F06, SALK_149553, WiscDsLoxHs148_11H, and SALK_001058 as *mp-11*, *mp-12*, *mp-13*, and *mp-14*, respectively.

Next, we analyzed cotyledon patterns of seedlings homozygous for *mp^{G12}*, *arf5-1*, *mp-11*, *mp-12*, *mp-13*, or *mp-14*. WT seedlings had two separate cotyledons (Figure 3.3E). Nearly 75% of *mp-11* seedlings had two separate cotyledons, and all *mp-11* seedlings had at least one cotyledon (Figure 3.3E). Approximately 50% of *mp^{G12}* seedlings had two separate cotyledons, and all *mp^{G12}* seedlings had at least one cotyledon (Figure 3.3E). The spectrum of cotyledon pattern phenotypes of *arf5-1* seedlings was similar to that of *mp-12* seedlings: ~35-45% of seedlings had two separate cotyledons, and ~5% of seedlings had no cotyledons (Figure 3.3E). And the spectrum of cotyledon pattern phenotypes of *mp-13* seedlings was similar to that of *mp-14* seedlings: ~15-20% of seedlings had two separate cotyledons, and ~5% of seedlings had no cotyledons (Figure 3.3E).

Finally, we analyzed cotyledon vein patterns of seedlings homozygous for *mp^{G12}*, *arf5-1*, *mp-11*, *mp-12*, *mp-13*, or *mp-14*. Four days after germination, nearly 75% of WT cotyledons had a central midvein and at least four vein loops (phenotype class I); ~25% had a simpler vein pattern,

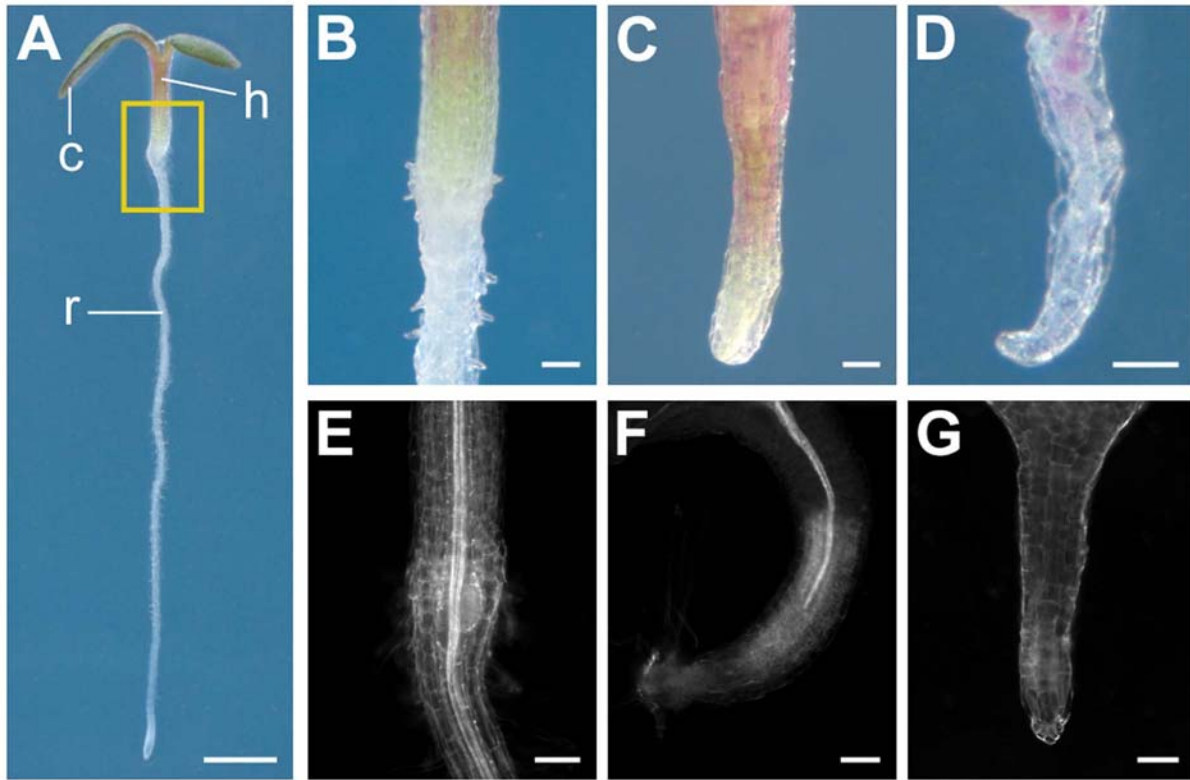


Figure 3.2. Seedling axis defects of *mp* alleles. (A-G) Dark-field illumination of seedlings 3 days after germination. (A,B,E) WT. c, cotyledon; h, hypocotyl; r, root. (C,D,F,G) *mp*. (A-D) Live. (E-G) Cleared; mature veins appear bright due to their refraction properties. (B,E) Hypocotyl-root transition zone. Detail of an area as boxed in (A). (C,F) Hypocotyl-basal peg transition zone. (D,G) Basal peg. Scale bars: 1 mm in A; 0.1 mm in B-G.

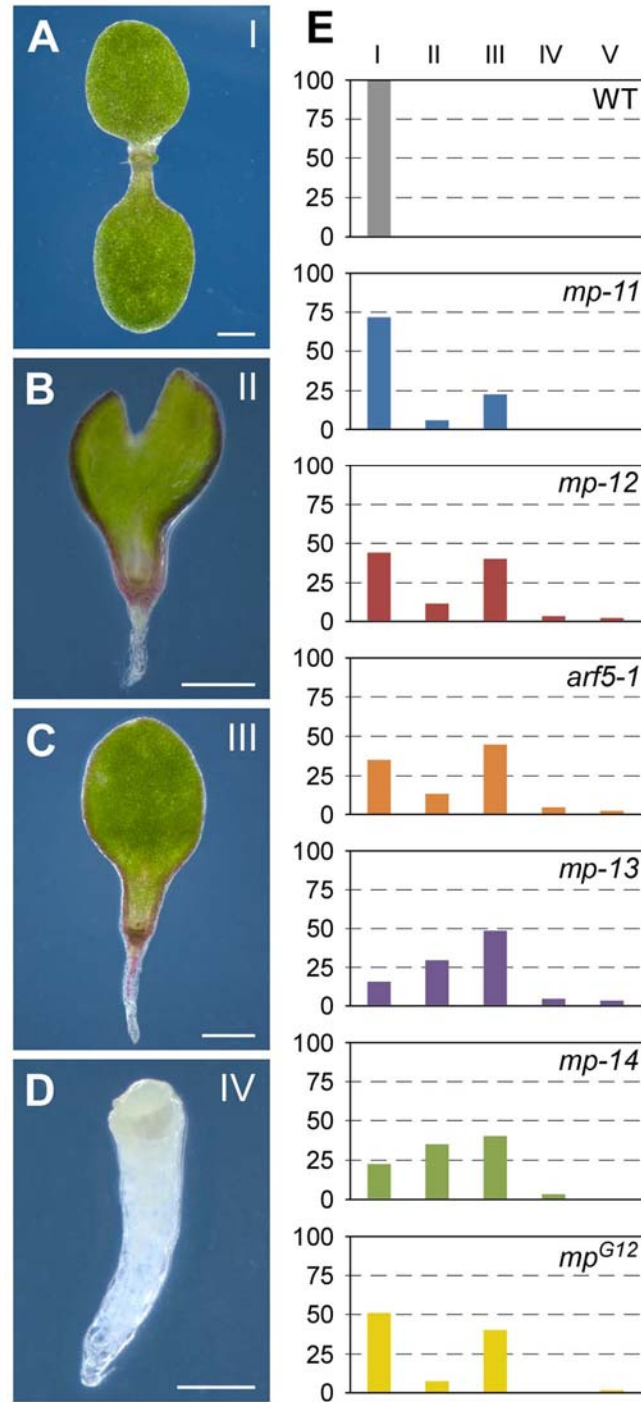


Figure 3.3. Cotyledon pattern defects of *mp* alleles. (A-D) Dark-field illumination of seedlings 4 days after germination illustrating phenotype classes: Class I, two separate cotyledons (A); Class II, fused cotyledons (B); Class III, single cotyledon (C); Class IV, no cotyledons (D). Other, infrequent cotyledon-pattern defects were grouped in Class V (not shown). (E) Percentage of seedlings in phenotype classes. Sample population sizes: WT, 191; *mp-11*, 168; *mp-12*, 188; *arf5-1*, 164; *mp-13*, 179; *mp-14*, 172; *mp^{G12}*, 207. Scale bars: 0.5 mm in A-C; 0.25 mm in D.

with a central midvein and up to three loops (class II) (Figure 3.4A,B,F). Nearly 35% of *mp-11* cotyledons belonged to class I, ~45% belonged to class II, ~5% had no loops (class III), ~10% had a vein pattern in which the midvein bifurcated near the cotyledon tip (class IV), and nearly 5% had no veins (class V) (Figure 3.4C-F). Most (~55%) of *mp-14* cotyledons belonged to class II, and the remaining ~45% were nearly equally distributed among classes III-V (Figure 3.4F). The spectrum of vein pattern phenotypes of *mp-12* cotyledons was similar to that of *arf5-1* cotyledons and of *mp^{G12}* cotyledons: ~5-10% belonged to class II, ~65-70% to class III, and 25-35% to class V (Figure 3.4F). Approximately 45% of *mp-13* cotyledons belonged to class III, and ~50% belonged to class V (Figure 3.4F).

Our results suggest that *mp-11* is the weakest of the Col alleles characterized here and the first low-expression allele of *mp*. Insertion after nucleotide -973 of *MP* in line WiscDsLox489-492C10 results in WT-looking individuals with normal levels of *MP* transcript. By contrast, insertion after nucleotide -678 of *MP* in *mp-11* results in ~30% reduction in levels of *MP* transcript and defects in hypocotyl and root formation, cotyledon separation and vein patterning. This suggests that the 295-bp region of the *MP* promoter from nucleotide -972 to nucleotide -678—which contains putative binding sites for several transcription-factor families (Figure 3.5)—might be required for *MP* function in these processes. Though it will be interesting to determine whether any of the putative regulatory elements in this promoter region are required for functional *MP* expression, the low-expression allele *mp-11* could already be used to test the hypothesis that *MP* expression dynamics are dependent on *MP* levels (Lau et al., 2011).

Our results also suggest that *mp-13* is the strongest Col allele available. *mp-13* has an insertion at the beginning of the sequence that encodes MP's AD. It is difficult to explain how such mutation could result in stronger defects than those of *mp^{G12}*, in which the entire sequence encoding MP's DBD is missing. However, part of the sequence encoding MP's AD and the entire sequence encoding MP's CTD are present in *mp^{G12}*, and a similar *ARF* fragment has been shown to be sufficient to enhance auxin-responsive gene expression (Ulmasov et al., 1999a). Should the *mp^{G12}* allele be transcribed and translated, the resulting gene product might thus account for the weaker defects of *mp^{G12}* relative to those of *mp-13*. Alternatively, should the *mp-13* allele be transcribed and translated, the resulting protein—presumably lacking AD and CTD—might still be able to occupy MP binding sites in target promoters. Binding of such

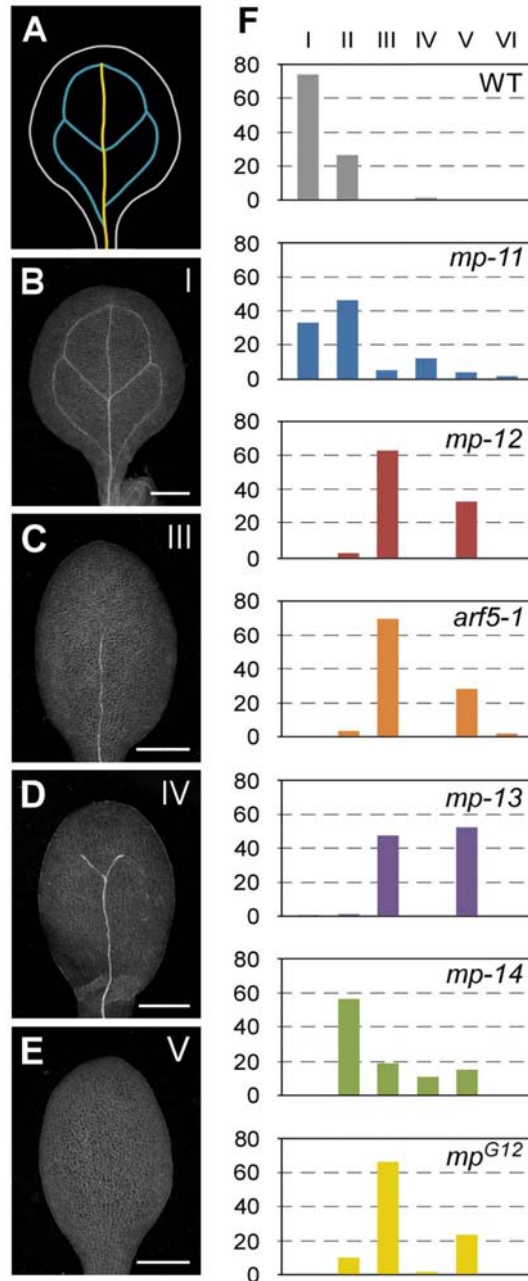


Figure 3.4. Vein pattern defects of *mp* alleles. (A,B) Vein pattern of WT mature cotyledon. In (A), yellow, midvein; blue, vein loops. (B-E) Dark-field illumination of cleared cotyledons 4 days after germination illustrating phenotype classes: Class I, unbranched midvein and four or more loops (B); Class III, solitary, unbranched midvein (C); Class IV, bifurcated midvein (D); Class V, no veins (E). Class II is defined by unbranched midvein and up to three loops (not shown). Other, infrequent vein-pattern defects were grouped in Class VI (not shown). (F) Percentage of cotyledons in phenotype classes. Samples population sizes: WT, 191; *mp-11*, 168; *mp-12*, 188; *arf5-1*, 164; *mp-13*, 179; *mp-14*, 172; *mp^{G12}*, 207. Scale bars: 0.5 mm in B-E.

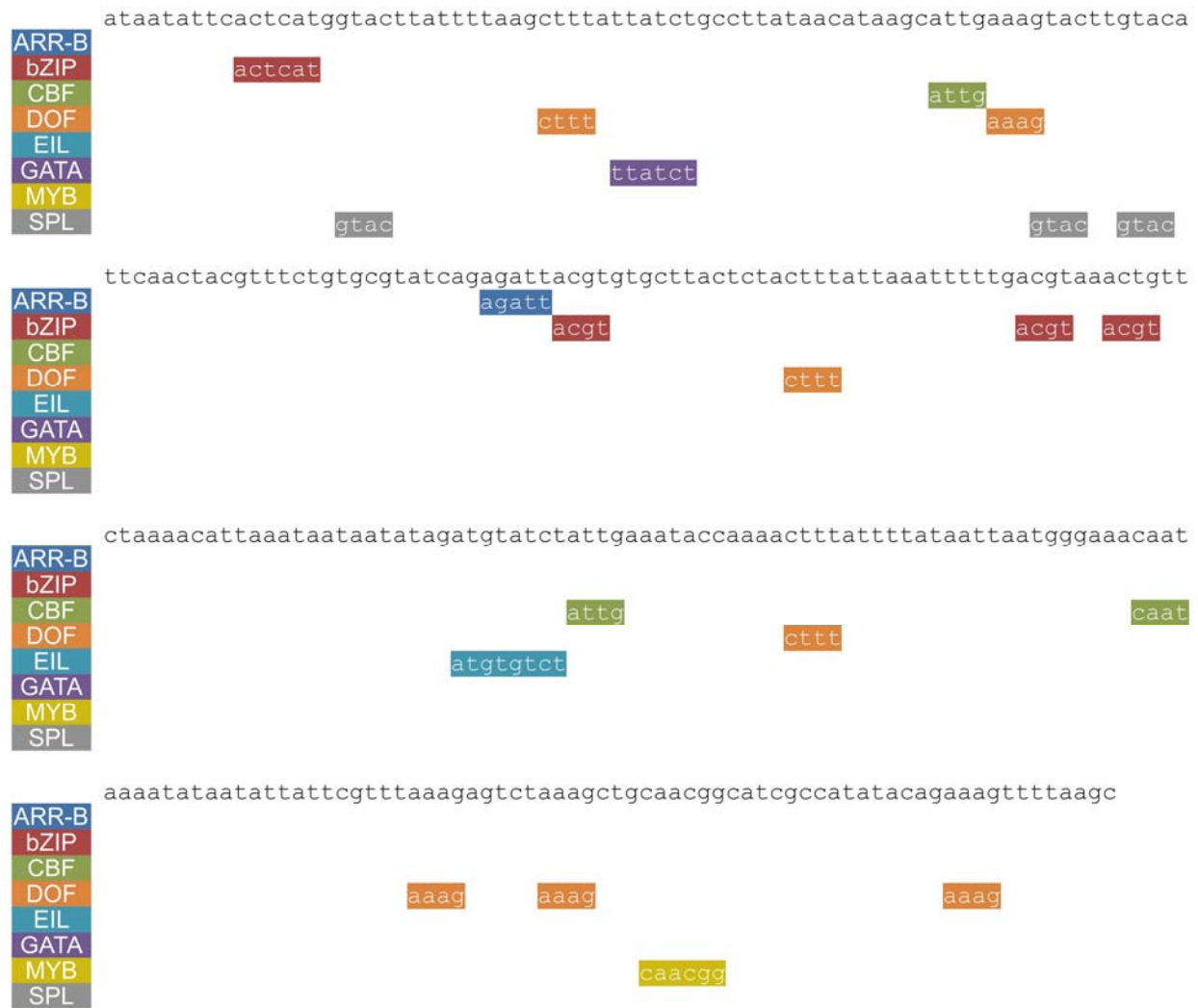


Figure 3.5. Putative transcription-factor binding sites in the 295-bp region of the *MP* promoter from nucleotide -972 to nucleotide -678. Putative binding sites for transcription factors of the ARR-B (Hosoda et al., 2002), bZIP (Jakoby et al., 2002; Satoh et al., 2004), CBF (Bezhani et al., 2001), DOF (Yanagisawa, 2002), EIL (Kosugi and Ohashi, 2000), GATA (Reyes et al., 2004), MYB (Prouse and Campbell, 2012), and SPL (Birkenbihl et al., 2005) families are below sequence. Putative transcription-factor binding sites were identified as in (Donner and Scarpella, 2012). Presence of intact core sequence for each bioinformatically identified transcription-factor binding site was manually confirmed.

truncated protein might prevent binding of ARF proteins whose function is redundant to that of MP [e.g., (Hardtke et al., 2004)] and might thus account for the stronger defects of *mp-13* relative to those of *mp^{G12}*. However, these and other possibilities remain to be tested experimentally.

Unlike the defects of all the other *mp* alleles characterized here, the defects of *mp-14* appeared more or less severe depending on the phenotype feature used to assess strength: as weak alleles in other backgrounds (Berleth and Jurgens, 1993), *mp-14* seedlings occasionally form a short hypocotyl with a central vein; by contrast, cotyledon separation defects of *mp-14* are similar to those of *mp-13*, the strongest Col allele; and vein pattern defects of *mp-14* are intermediate between those of *mp-13* and those of *mp-11*, the weakest allele described here. *mp-14* has an insertion at the beginning of the sequence encoding for MP's CTD, which mediates interaction with ARF proteins or AUX/IAA repressors (Guilfoyle and Hagen, 2012). The unusual behavior of *mp-14* might thus reflect the uneven contribution of these interactions to different developmental processes. This conclusion is consistent with the finding that *mp^{S319}/arf5-2*, which has an insertion only a few nucleotides downstream of the location of the *mp-14* insertion, has completely penetrant defects only in some of the developmental processes that depend on MP (Cole et al., 2009; Donner et al., 2009; Schlereth et al., 2010); it is also consistent with the finding that an MP protein lacking the entire CTD supplies semidominant functions only in a subset of MP-dependent developmental processes (Krogan et al., 2012).

In conclusion, by characterizing six mutant alleles of MP in the Col background—including four new alleles, among which the first low-expression allele and the strongest Col allele—we have provided the research community with new genetic resources to understand the role of MP-dependent auxin signalling in plant development.

3.3 Materials and methods

3.3.1 Plants

Origin of lines is in Table 3.1. Unless otherwise stated, seeds were sterilized and germinated as in the work by (Sawchuk et al., 2008). Genotyping strategies are in Table 3.2. Oligonucleotide sequences are in Table 3.3.

3.3.2 Vectorette PCR

About 500 ng of *mp^{G12}* DNA were digested with *Csp6I* for two hours and ligated to a vectorette unit generated by annealing the “V-PCR FORWARD” and “V-PCR rev” oligonucleotides (Table 3.3). The sequences flanking the ligated vectorette unit were amplified with Phusion High-Fidelity DNA Polymerase (Thermo Fisher Scientific inc., Waltham, MA) and the “V3” and “MP pro1 forw”, or the “V3” and “MP vec1 Rev”, oligonucleotides (Table 3.3). The resulting product was amplified with the “V4” and “MP pro3 forw”, or the “V4” and “MP vec2 Rev”, oligonucleotides (Table 3.3), and sequenced

3.3.3 RT-PCR

Total RNA was extracted as in the work by (Chomczynski and Sacchi, 1987) from 4-day-old seedlings grown in half-strength Murashige and Skoog salts (Caisson Laboratories, North Logan, UT), 15 g l⁻¹ sucrose (BioShop Canada Inc., Burlington, Canada), 0.5 g l⁻¹ MES (BioShop Canada Inc.), pH 5.7, at 25°C under continuous light (~65 μmol m⁻² sec⁻¹) on a rotary shaker at 50 rpm. RT-PCR was performed on 100 ng of total RNA with the “MP 1993 geno” and “WiscDsLoxHs148_12G/149_11H RP” oligonucleotides (Table 3.3), and with the “ROC1 F” and “ROC1 R” oligonucleotides (Beeckman et al., 2002) (Table 3.3), using the Access RT-PCR System (Promega, Fitchburg, WI).

3.3.4 Imaging

Three-day-old seedlings were fixed, cleared, and mounted as in (Scarpella et al., 2004). Images were acquired with an Olympus SZ61TR (Olympus Corporation, Shinjuku, Japan) or an AxioImager.M1 (Carl Zeiss AG, Oberkochen, Germany) microscope equipped with an AxioCam

Table 3.1. Origin of lines.

Name	Origin
<i>mp</i> ^{BS1354}	(Hardtke and Berleth, 1998)
<i>mp</i> ^{B4149}	(Weijers et al., 2005b)
SALK_144183	ARBC; (Alonso et al., 2003)
WiscDsLoxHs148_12G	ARBC (CS914207); (Nishal et al., 2005; Woody et al., 2007; Zhang et al., 2003)
WiscDsLox489-492C10	ARBC (CS858306); (Woody et al., 2007)
<i>mp</i> ^{G12}	(Hardtke and Berleth, 1998)
<i>arf5-1</i>	(Okushima et al., 2005)
<i>mp-11</i> /SAIL_1265_F06	ARBC (CS879048); (Geisler et al., 2002)
<i>mp-12</i> /SALK_149553	ARBC; (Alonso et al., 2003)
<i>mp-13</i>	ARBC (CS914200); (Nishal et al., 2005; Woody et al., 2007; Zhang et al., 2003)
/WiscDsLoxHs148_11H	Zhang et al., 2003)
<i>mp-14</i> /SALK_001058	ARBC; (Alonso et al., 2003)

Table 3.2. Genotyping strategies.

Name	Strategy
SALK_144183	<i>MP</i> : 'SALK_144183 LP' and 'SALK_144183 RP'; <i>mp</i> : 'SALK_144183 RP' and 'LBb1.3'
WiscDsLoxHs148_12G	<i>MP</i> : WiscDsLoxHs148_12G/148_11H LP ' and WiscDsLoxHs148_12G/149_11H RP '; <i>mp</i> : WiscDsLoxHs148_12G/149_11H RP ' and 'L4'
WiscDsLox489-492C10	<i>MP</i> : 'WiscDsLox489-492C10 LP' and 'WiscDsLox489- 492C10 RP'; <i>mp</i> : 'WiscDsLox489-492C10 RP' and 'p745'
<i>mp</i> ^{G12}	<i>MP</i> : 'BS1354-F' and 'BS1354-R'; <i>mp</i> : 'G12 inst 2 forw ' and 'MP vec2 Rev '
<i>arf5-1</i>	<i>MP</i> : 'SALK_023812 LP' and 'SALK_023812 RP' <i>mp</i> : ' MP2082-AS ' and 'LBb1.3';
<i>mp-11/SAIL_1265_F06</i>	<i>MP</i> : SAIL_1265_F06LP ' and ' SAIL_1265_F06RP '; <i>mp</i> : ' SAIL_1265_F06RP ' and 'LB3'
<i>mp-12/SALK_149553</i>	<i>MP</i> : 'SALK_149553 LP' and 'SALK_149553 RP'; <i>mp</i> : 'SALK_149553 RP' and 'LBb1.3'
<i>mp-13/WiscDsLoxHs148_11H</i>	<i>MP</i> : WiscDsLoxHs148_12G/148_11H LP ' and WiscDsLoxHs148_12G/149_11H RP '; <i>mp</i> : WiscDsLoxHs148_12G/149_11H RP ' and 'L4'
<i>mp-14/SALK_001058</i>	<i>MP</i> : 'SALK_001058 LP' and 'SALK_001058 RP'; <i>mp</i> 'SALK_001058 RP' and 'LBb1.3'

Table 3.3. Oligonucleotide sequences.

Name	Sequence (5' to 3')
SALK_144183 LP	AGAAACCTCCATGTGTGCTTG
SALK_144183 RP	AATTCCTCTGGTTTGTCTGG
LBb1.3	ATTTTGCCGATTTTCGGAAC
WiscDsLoxHs148_12G/148_11 H LP	TTTGTCTTTGAAAATGTGCC
WiscDsLoxHs148_12G/149_11 H RP	GTTAGCTTGTTTTGTGGCTGC
L4	TGATCCATGTAGATTTCCCGGACATGAAG
WiscDsLox489-492C10LP	GGCTCTTGCCTCTTCTCTTTT
WiscDsLox489-492C10RP	TTGGAAAGGAAAAGAACACCC
p745	AACGTCGCAATGTGTTATTAAGTTGTC
BS1354-F	GAGATGGCCTGGTTCTAAGTGGC
BS1354-R	GCCAGTTCAACATCTCGGTTATCG
G12 inst 2 forw	GGATAAAGGTTTGATGCCAAGCGTG
MP vec2 Rev	CAAGAGACTGGAAGGAAGAGACTTGTG
SALK_023812 LP	GAGAGGAAGTAAGCACCCGAC
SALK_023812 RP	TCATTACATCCAGGCTCATCC
MP2082-AS	ATGGATGGAGCTGACGTTTGAGTTCGGACTCAA CGTCAGCTCCATCCA
SAIL_1265_F06LP	GCTTCATCTCTTCAAGCAAGG
SAIL_1265_F06RP	TCCCAAAGTCTCACCCTCAC
LB3	TAGCATCTGAATTTCATAACCAATCTCGATACAC
SALK_149553 LP	AATTCCTCTGGTTTGTCTGG-
SALK_149553 RP	AGAAACCTCCATGTGTGCTTG
SALK_001058 LP	ATGGACTTGAGCAGTCAATGG
SALK_001058 RP	CCTTCTTCACTCATCTGCTGG
CIW11 Primer 1	CCCCGAGTTGAGGTATT
CIW11 Primer 2	GAAGAAATTCCTAAAGCATTC
CIW20 Primer 1	CATCGGCCTGAGTCAACT
CIW20 Primer 2	CACCATAGCTTCTTCCTTTCTT
NGA151 Primer 1	CAGTCTAAAAGCGAGAGTATGATG
NGA151 Primer 2	GTTTTGGGAAGTTTTGCTGG
NGA106 Primer 1	TGCCCCATTTTGTTCTTCTC
NGA106 Primer 2	GTTATGGAGTTTCTAGGGCACG
NGA249 Primer 1	GGATCCCTAACTGTAAAATCCC
NGA249 Primer 2	TACCGTCAATTTTCATCGCC

V-PCR FORWARD	TACAGGAGAGGACGCTGTCTGTCTCGAAGGTAAGGA ACGGACGAGAGAAGGGAGAG
V-PCR rev	CTCTCCCTTCTCGAATCGTAACCGTTCGTACGAGA ATCGCTGTCCTCTCCTG
V3	ATCGTAACCGTTCGTACGAGAATCGC
MP pro1 forw	GAGAGAGAAAGAGAAGAGGCAAGAGC
MP vec1 Rev	CATCTTGAGCAAAGCTAGTGTTGTTG
V4	ACCGTTCGTACGAGAATCGCTGTC
MP pro3 forw	GCTAAAGCCTAGTTAGTGTTGAGTGTGG
MP 1993 geno	TCGGGTCAGTCCATGGGATATCG
ROC1 F	CAAACCTCTTCTTCAGTCTGATAGAGA
ROC1 R	GAGTGCTCATTCTTATTTCTGGTAG

HR camera (Carl Zeiss AG, Oberkochen, Germany) or a Hamamatsu ORCA-AG camera (Hamamatsu Photonics K.K., Hamamatsu, Japan), respectively. Brightness and contrast were adjusted by linear stretching of the histogram with ImageJ (Rasband, 1997). Images were cropped with Adobe Photoshop 7.0 (Adobe Systems Inc., San Jose, CA) and assembled into figures with Canvas 8.0 (ACD Systems Inc., Victoria, Canada)

CHAPTER 4: CONTROL OF LEAF VASCULARIZATION BY CELL PROLIFERATION

4.1 Introduction

In most multicellular organisms, signals and nutrients are transported throughout the body by a vascular system. For normal development and optimal function, no area of the body should thus be devoid of vessels. Therefore, the growth of tissues and their vascularization must be tightly coordinated, and understanding the molecular basis of this coordination is a key question in biology.

In animals, signals from proliferating nonvascular tissues, mostly consisting of angiogenic mitogen factors such as the vascular endothelial growth factor A, promote their vascularization (Keck et al., 1989; Leung et al., 1989). In turn, vessels signal back to surrounding nonvascular tissues to control their growth and development [reviewed in (Cleaver and Dor, 2012)]. By contrast, in plant leaves, vascular and nonvascular tissues differentiate from the same precursor cells (Flot, 1905), and the relative timing of cessation of proliferation and onset of differentiation of these precursor cells controls the pattern of vascular and nonvascular tissues in the leaf: cell proliferation inhibits progression of precursor cells to nonvascular fate, thus permitting their recruitment into veins, and cessation of cell proliferation permits progression of precursor cells to nonvascular fate, thus preventing their recruitment into veins (Chapter 2). Therefore, despite the different development logics, in both plant and animal organs patterns of vascular and nonvascular tissues are controlled by the timing of cessation of cell proliferation.

As in animals, progression through the cell cycle in plants is promoted by complexes between transcriptional regulators members of the EARLY 2 FACTOR (E2F) and the DIMERIZATION PARTNER (DP) families [reviewed in (Dewitte and Murray, 2003; Inze and De Veylder, 2006)]. The activity of E2F/DP complexes is inhibited by the non-phosphorylated form of the RETINOBLASTOMA-RELATED (RBR) protein. Phosphorylation of RBR by complexes between cyclin-dependent kinases (CDKs) and their regulatory proteins, the cyclins, leads to RBR degradation and thus to activation of E2F/DP complexes. The activity of

CDK/cyclin complexes is inhibited by INTERACTORS OF CDC2 KINASE (ICKs)/KIP-RELATED PROTEINS (KRPs).

In both plants and animals, the timing of cessation of cell proliferation is controlled by antagonistic signals. On the one hand, transcription factors such as TCP4 (for TEOSINTE BRANCHED1/CYCLOIDEA/PROLIFERATING CELL FACTOR4) and SMAD4, for example, promote expression of CDK inhibitors and inhibit cell proliferation in plants and animals, respectively (Gomis et al., 2006a; Gomis et al., 2006b; Schommer et al., 2014; Seoane et al., 2004). On the other hand, signals that promote cell proliferation act antagonistically to those that inhibit cell proliferation. For example, in animals, the transcription factor ACTIVATING PROTEIN1 promotes *CYCLIN D1* (*CYCD1*) expression (Brown et al., 1998), promotes cell proliferation (Kovary and Bravo, 1991), and antagonizes SMAD function (Verrecchia et al., 2001). In plants, the transcription factor AINTEGUMENTA promotes *CYCD3;1* expression and cell proliferation (Mizukami and Fischer, 2000), but the effects of the loss of its function on vein networks are mild (Kang et al., 2007). By contrast, vein networks are most dramatically affected by loss of function of the transcription factor MONOPTEROS (MP) (Przemeck et al., 1996), which transduces the plant signal auxin [reviewed in (Chapman and Estelle, 2009; Guilfoyle and Hagen, 2007)]. The *mp* phenotype is suppressed by loss of *ALTERED MERISTEM PROGRAM1* (*AMPI*) function (Vidaurre et al., 2007), which is associated with higher expression of *CYCD3* (Nogue et al., 2000; Riou-Khamlichi et al., 1999). However, the mechanism by which *amp1* suppresses *mp* seems to be unrelated to the cell cycle defects (Li et al., 2013). Therefore, whether vein network defects of *mp* result from defects in leaf cell proliferation is unknown.

Here we tested the hypothesis that vein network defects of *mp* result from premature cessation of leaf cell proliferation. This hypothesis was suggested by two pieces of evidence: (1) premature cessation of precursor cell proliferation leads to the formation of vein networks resembling those of *mp* (Chapter 2) (Donner et al., 2009; Kang et al., 2007; Przemeck et al., 1996); (2) premature cessation of cell proliferation during embryo development leads to formation of seedlings that, as *mp* seedlings, lack roots (Berleth and Jurgens, 1993; Hemerly et al., 2000). By prolonging or prematurely ceasing leaf cell proliferation in WT or *mp* background, we show that vein network defects of *mp* result from premature cessation of leaf cell proliferation. Moreover, we show that the promoting effects of *MP* on leaf cell proliferation and vein network formation are antagonized by the functions of *CINCINNATA*-related *TCP* (*CIN-*

TCP) genes. Our results suggest a molecular mechanism by which timing of cessation of cell proliferation integrates tissue growth and vascularization in plants.

4.2 Results and Discussion

4.2.1 *MONOPTEROS* functions in Arabidopsis vein-network topology

The vein network geometry of mature first-leaves of Arabidopsis is defined by lateral veins that branch from a central midvein, and that connect apically to the midvein or to other lateral veins to form closed loops; and by minor veins that branch from midvein and loops, and that connect to other veins or terminate free of contact (Candela et al., 1999; Kinsman and Pyke, 1998; Mattsson et al., 1999; Nelson and Dengler, 1997; Sieburth, 1999; Steynen and Schultz, 2003; Telfer and Poethig, 1994) (Figure 4.1A). Whereas vein network geometry is reproducible from leaf to leaf (Candela et al., 1999; Kinsman and Pyke, 1998; Mattsson et al., 1999; Nelson and Dengler, 1997; Sieburth, 1999; Steynen and Schultz, 2003; Telfer and Poethig, 1994), topological features of the vein network, such as the number of veins in a leaf and whether a vein will connect to another vein at both ends or one end will terminate free of contact with other veins, are unpredictable (Candela et al., 1999; Kang and Dengler, 2004; Kinsman and Pyke, 1998; Sawchuk et al., 2007; Scarpella et al., 2004; Steynen and Schultz, 2003).

To quantify and compare effects of genes on vein network topology, we used the cardinality index—a proxy for the number of veins (Verna et al., 2015) (Chapter 2)—and the percentage of leaves in which lateral veins failed to contact apically other veins (i.e. percentage of leaves with open loops)—a measure of vein connectedness (Carland et al., 1999; Scarpella et al., 2004; Steynen and Schultz, 2003) (Chapter 2)—because these two descriptors can be compared statistically across genotypes and conditions to identify reproducible patterns and their controls (Carland et al., 1999; Scarpella et al., 2004; Steynen and Schultz, 2003; Verna et al., 2015) (Chapter 2).

To determine functions of the *MP* gene of Arabidopsis in vein network topology, we used the *mp-11* mutant allele because in this weak allele, unlike in stronger *mp* alleles, vascular differentiation is only mildly affected (Odat et al., 2014) (Chapter 3).

The cardinality index of vein networks of mature first leaves was lower in *mp* than in the control and the percentage of mature first leaves with open loops was higher in *mp* than in the control (Figure 4.1A,B,I,J), suggesting that *MP* promotes the formation of veins and their connection into networks.

4.2.2 Leaf cell proliferation and vein network topology

The hypothesis that *mp* defects in vein network topology result from premature cessation of leaf cell proliferation predicts that the effects on vein networks of premature cessation of leaf cell proliferation mimic those of *mp* mutation. To test this prediction, we used a variant of ICK2/KRP2 (KRP2 here after) in which the putative protein degradation signal (De Veylder et al., 2001; Torres Acosta et al., 2011) had been removed (KRP2^{Δ73-97}) (Chapter 2), and a dominant-negative variant of CDKA;1 (CDKA;1^{D146N}) (Hemerly et al., 1995) (Chapter 2); we expressed KRP2^{Δ73-97} and CDKA;1^{D146N} by the *RIBOSOMAL PROTEIN S5A (RPS5A)* promoter, which is active in all dividing cells (Weijers et al., 2001); and we calculated the cardinality index of vein networks of mature first leaves of RPS5A::KRP2^{Δ73-97} and RPS5A::CDKA;1^{D146N}, and the percentage of mature first leaves of RPS5A::KRP2^{Δ73-97} and RPS5A::CDKA;1^{D146N} with open loops, and compared them with those of control and *mp*.

The cardinality index of vein networks of RPS5A::KRP2^{Δ73-97} and RPS5A::CDKA;1^{D146N} was lower than that of the control, and the percentage of leaves of RPS5A::KRP2^{Δ73-97} and RPS5A::CDKA;1^{D146N} with open loops was higher than that of the control (Figure 4.1A,C,D,I,J), suggesting that premature cessation of leaf cell proliferation inhibits the formation of veins and their connection into networks, and thus that the effects on vein network topology of premature cessation of leaf cell proliferation mimic those of *mp* mutation.

4.2.3 Leaf cell proliferation and *MP*-dependent vein network topology

If *mp* defects in vein network topology resulted from premature cessation of leaf cell proliferation, such defects should be suppressed, at least partially, by prolonged leaf cell proliferation. To test this prediction, we used a hyperactive variant of CYCLIN D3;1 (CYCD3;1^{S343A}) (Menges et al., 2006) (Chapter 2), and a fusion between the activation domain of the Herpes simplex virus type 1 VIRION POLYPEPTIDE 16 (VP16) (Campbell et al., 1984) and E2Fa (E2Fa:VP16) (Chapter 2); we expressed CYCD3;1^{S343A} and E2Fa:VP16 by the *RPS5A*

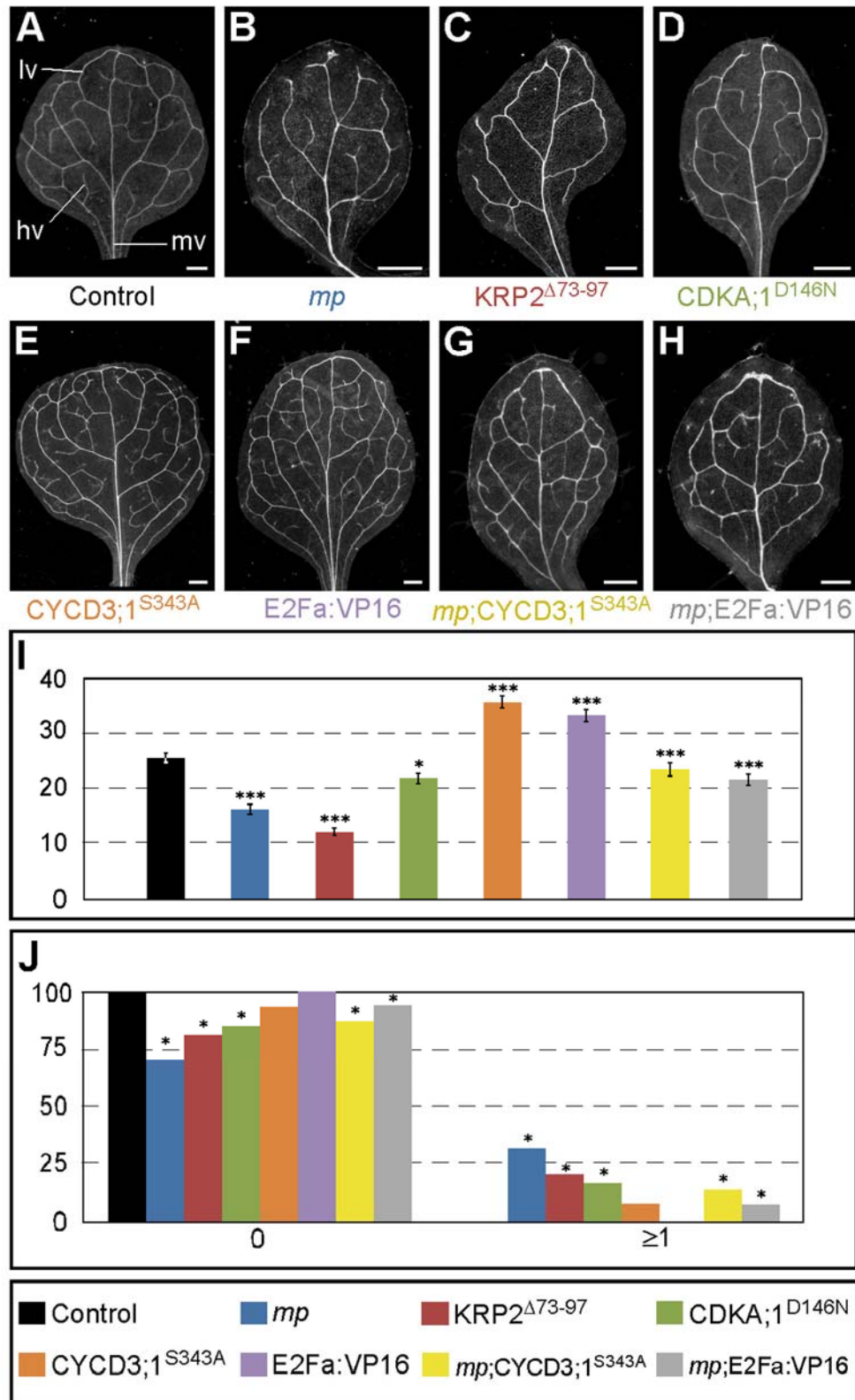


Figure 4.1. *MP*-dependent auxin signaling, cell proliferation and vein network formation in *Arabidopsis* leaves. (A-H) Dark-field illumination of mature first leaves of control (A), *mp-11*

(B), RPS5A::KRP2 Δ 73-97 (C), RPS5A::CDKA;1^{D146N} (D), RPS5A::CYCD3;1^{S343A} (E), RPS5A::E2Fa:VP16 (F), RPS5A::CYCD3;1^{S343A};mp-11 (G), and RPS5A::E2Fa:VP16;mp-11 (H). (I) Cardinality index of vein networks of mature first leaves expressed as mean \pm SEM. Difference between *mp-11* and control, between RPS5A::KRP2 Δ 73-97 and control, between RPS5A::CDKA;1^{D146N} and control, between RPS5A::CYCD3;1^{S343A} and control, between RPS5A::E2Fa:VP16 and control, between RPS5A::CYCD3;1^{S343A};mp-11 and *mp-11*, and between RPS5A::E2Fa:VP16;mp-11 and *mp-11* was significant at $P < 0.05$ (*), $P < 0.01$ (**) or $P < 0.001$ (***) by F-test and *t*-test with Bonferroni correction. (J) Percentage of mature first leaves with 0 or ≥ 1 open loops. Difference between *mp-11* and control, between RPS5A::KRP2 Δ 73-97 and control, between RPS5A::CDKA;1^{D146N} and control, between RPS5A::CYCD3;1^{S343A};mp-11 and *mp-11*, and between RPS5A::E2Fa:VP16;mp-11 and *mp-11* was significant at $P < 0.05$ (*) by Kruskal-Wallis and Mann-Whitney test with Bonferroni correction. Sample population sizes: control, 26; *mp-11*, 26; RPS5A::KRP2 Δ 73-97, 31; RPS5A::CDKA;1^{D146N}, 32; RPS5A::CYCD3;1^{S343A}, 30; RPS5A::E2Fa:VP16, 30; RPS5A::CYCD3;1^{S343A};mp-11, 23; RPS5A::E2Fa:VP16;mp-11, 31. Scale bars: 0.5 mm in A-F; 0.25 mm in G,H.

promoter in WT and *mp* backgrounds; and we compared the cardinality index of vein networks of mature first leaves, and the percentage of mature first leaves with open loops, of RPS5A::CYCD3;1^{S343A}, RPS5A::E2Fa:VP16, RPS5A::CYCD3;1^{S343A}; *mp*, RPS5A::E2Fa:VP16; *mp*, control and *mp*.

The cardinality index of vein networks of RPS5A::CYCD3;1^{S343A} and RPS5A::E2Fa:VP16 was higher than that of the control (Figure 4.1A,E,F,I), suggesting that prolonged leaf cell proliferation promotes the formation of veins. The cardinality index of vein networks of RPS5A::CYCD3;1^{S343A}; *mp* and RPS5A::E2Fa:VP16; *mp* was higher than that of *mp* (Figure 4.1B,G-I)—though not as high as those of the control (Figure 4.1A,I)—suggesting that *mp* defects in vein formation result, at least partially, from premature cessation of leaf cell proliferation. Further, the percentage of leaves with open loops of RPS5A::CYCD3;1^{S343A}; *mp* and RPS5A::E2Fa:VP16; *mp* was lower than that of *mp* (Figure 4.1J), suggesting that *mp* defects in vein connectedness result, at least partially, from premature cessation of leaf cell proliferation.

4.2.4 CIN-TCP-dependent repression of leaf cell proliferation and MP-dependent vein network topology

mp defects in vein network topology result, at least partially, from premature cessation of leaf cell proliferation; therefore, such defects should be suppressed, at least partially, by mutation in negative regulators of leaf cell proliferation. Available evidence suggest that CIN-TCP (for CINCINNATA-related TEOSINTE BRANCHED1/CYCLOIDEA/PROLIFERATING CELL FACTOR) transcription factors (Cubas et al., 1999) may be among such negative regulators: (1) CIN-TCP transcription factors promote expression of inhibitors of cell proliferation (Schommer et al., 2014); (2) mutation in *CIN-TCP* genes or overexpression of *microRNA319a* (*miR319a*), which targets five of the eight members of the *CIN-TCP* family (Palatnik et al., 2003), leads to prolonged leaf cell proliferation (Efroni et al., 2008; Nath et al., 2003); (3) gain of *CIN-TCP* function leads to premature cessation of cell proliferation (Sarvepalli and Nath, 2011); (4) defects in vein network topology induced by prolonged leaf cell proliferation mimic those induced by *miR319a* overexpression (Chapter 2; furthermore, compare Figure 4.1E,F with Figure 4.2C); (5) defects in vein network topology induced by *miR319a* overexpression are partially suppressed by mutation of *CYCD3;2* (Chapter 2). Therefore, we asked whether *mp* defects in vein network topology could be suppressed, at least partially, by reduction in *CIN-TCP* function.

To address this question, we overexpressed *miR319a* by the *UBIQUITIN10 (UBQ10)* promoter (Norris et al., 1993) in WT (Chapter 2) and *mp* backgrounds; and we compared the cardinality index of vein networks of mature first leaves, and the percentage of mature first leaves with open loops, of *UBQ10::miR319a*, *UBQ10::miR319a;mp*, WT and *mp*.

As previously reported (Chapter 2), the cardinality index of *UBQ10::miR319a* vein networks was higher than that of WT vein networks (Figure 4.2A,C,I), suggesting that *CIN-TCP*-dependent repression of leaf cell proliferation inhibits vein formation. The cardinality index of *UBQ10::miR319a;mp* vein networks was higher than those of *mp* vein networks (Figure 4.2B,C,I)—though not as high as that of WT vein networks (Figure 4.2A,I)—suggesting that *mp* defects in vein formation result, at least partially, from *CIN-TCP*-dependent repression of leaf cell proliferation. Further, the percentage of *UBQ10::miR319a;mp* leaves with open loops was lower than that of *mp* leaves with open loops (Figure 4.1K), suggesting that *mp* defects in vein connectedness result, at least partially, from *CIN-TCP*-dependent repression of leaf cell proliferation.

Because *miR319a* can target other genes in addition to *CIN-TCP* genes (Palatnik et al., 2003; Palatnik et al., 2007), we asked whether partial suppression of *mp* defects in vein network topology by *UBQ10::miR319a* resulted from reduction in *CIN-TCP* function. To address this question, we compared the cardinality index of vein networks of mature first leaves, and the percentage of mature fist leaves with open loops, of WT and *tcp4;tcp10 (tcp4;10 hereafter) cin-tcp* double-mutant grown in the absence or presence of the auxin antagonist auxinole, which competitively blocks binding of auxin to TRANSPORT INHIBITOR1 (TIR1)/AUXIN SIGNALING F-BOX (AFB) receptors and thus inhibits TIR1/AFB-mediated auxin responses, including ARF-dependent gene expression (Hayashi et al., 2012).

The cardinality index of *tcp4;10* vein networks was higher than that of WT vein networks (75.4 ± 2.5 , $n=26$ vs. 38.5 ± 1.9 , $n=26$; $P < 0.001$, F-test and *t*-test with Bonferroni correction) (Figure 4.2E,G), suggesting that *TCP4/TCP10*-dependent repression of leaf cell proliferation inhibits vein formation. The cardinality index of vein networks was lower, and the percentage of leaves with open loops was higher, in WT grown in the presence of auxinole than in WT grown in the absence of it (14.2 ± 0.9 , $n=27$ vs. 38.5 ± 1.9 , $n=26$; $P < 0.001$, F-test and *t*-test with Bonferroni correction) (Figure 4.2E,F,K), suggesting that TIR1/AFB-mediated auxin signaling promotes the formation of veins and their connection into networks. The cardinality index of

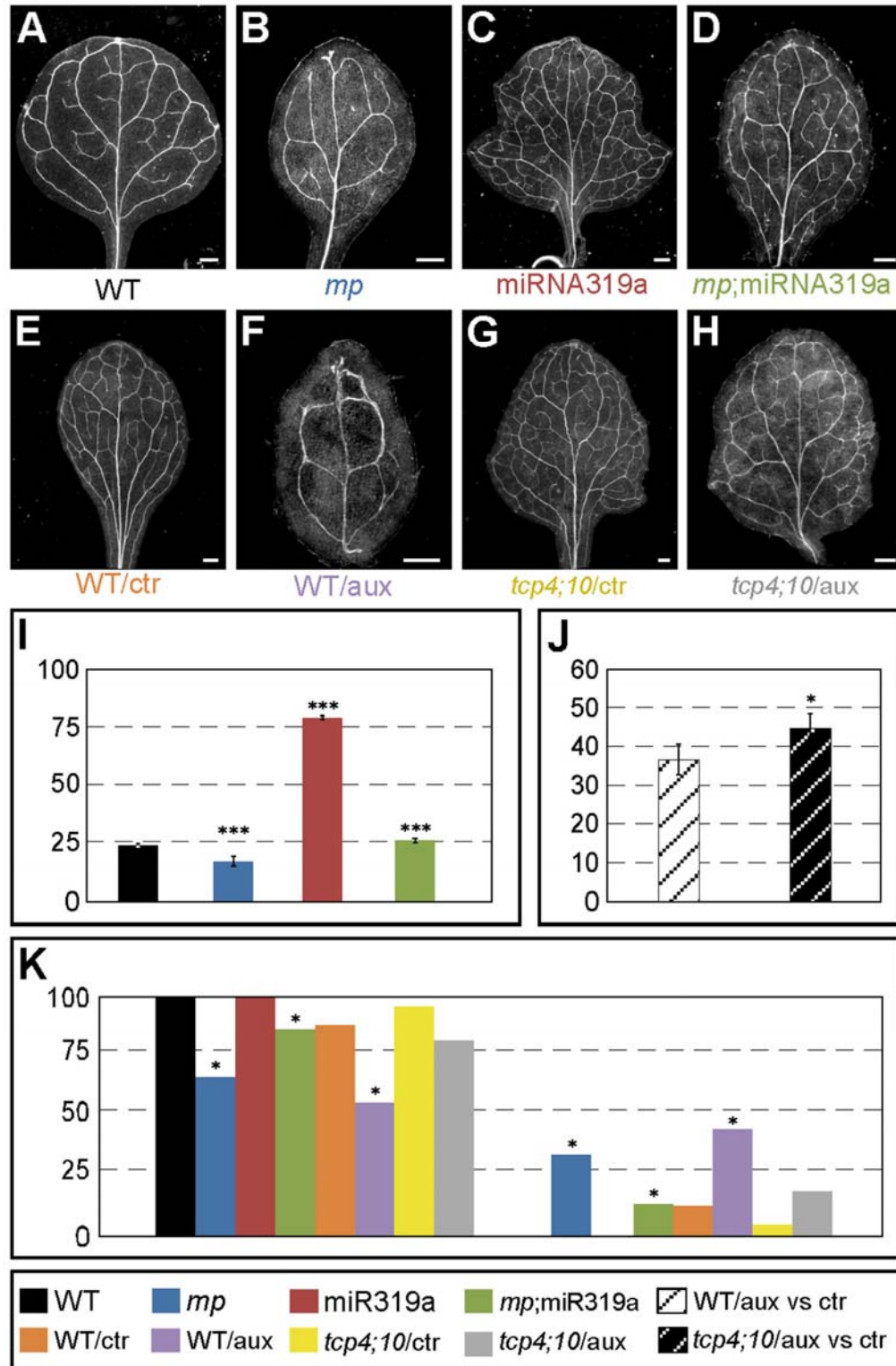


Figure 4.2. TIR1/AFB-mediated, *MP*-dependent auxin signaling, *CIN-TCP*-dependent inhibition of cell proliferation and vein network formation. (A-H) Dark-field illumination of mature first leaves of WT (A), *mp-11* (B), UBQ10::*miR319a* (C), UBQ10::*miR319a;mp-11* (D),

control-grown WT (E), auxinole-grown WT (F), control-grown *tcp4;tcp10* (G), and auxinole-grown *tcp4;tcp10* (H). (I) Cardinality index of vein networks of mature first leaves expressed as mean \pm SEM. Difference between *mp-11* and control, between UBQ10::miR319a and control, and between UBQ10::miR319a;*mp-11* and *mp-11* was significant at $P < 0.001$ (***) by F-test and *t*-test with Bonferroni correction. (J) Auxinole-induced reduction in cardinality index of vein networks of mature first leaves, expressed as percentage ratio \pm SEM of the mean cardinality index of vein networks of mature first leaves developed in the presence of auxinole to the mean cardinality index of vein networks of mature first leaves developed in the absence of auxinole. Difference between *tcp4;tcp10* and WT was significant at $P < 0.05$ (*) by F-test and *t*-test. (K) Percentage of mature first leaves with 0 or ≥ 1 open loops. Difference between *mp-11* and control, between UBQ10::miR319a and control, between UBQ10::miR319a;*mp-11* and *mp-11*, and between auxinole-grown WT and control-grown WT was significant at $P < 0.05$ (*) by Kruskal-Wallis and Mann-Whitney test with Bonferroni correction. Sample population sizes: WT, 31; *mp-11*, 27; UBQ10::miR319a, 28; UBQ10::miR319a;*mp-11*, 24; control-grown WT, 26; auxinole-grown WT, 27; control-grown *tcp4;tcp10*, 26; and auxinole-grown *tcp4;tcp10*, 22. Scale bars: 0.5 mm in A,C,E,G,H; 0.25 mm in B,D,F.

vein networks was also lower in *tcp4;10* grown in the presence of auxinole than in *tcp4;10* grown in the absence of it (34.1 ± 2.8 , $n=22$ vs. 75.4 ± 2.5 , $n=26$; $P < 0.001$, F -test and t -test with Bonferroni correction) (Figure 4.2G,H); however, it was proportionally less reduced than in WT (Figure 4.2J). Further, the percentage of *tcp4;10* leaves with open loops was unchanged by growth in the presence of auxinole (Figure 4.2K). We conclude that the defects in vein network topology induced by auxinole-mediated inhibition of TIR1/AFB-mediated auxin signaling result, at least partially, from *TCP4/TCP10*-dependent repression of leaf cell proliferation, and thus that partial suppression of *mp* defects in vein network topology by UBQ10::miR319a results from reduction in *CIN-TCP* function.

4.2.5 *MP*- and *CIN-TCP*-dependent expression of cell cycle regulators

Partial suppression of *mp* defects in vein network topology by reduction in *CIN-TCP*-dependent repression of leaf cell proliferation may reflect opposite effects of *mp* and UBQ10::miR319a on the expression of at least some cell cycle regulators. We tested this prediction by analyzing the expression of CDKA;1::CDKA;1:GUS (CDKA;1:GUS fusion protein expressed by the *CDKA;1* promoter) (Adachi et al., 2009), CYCD3;1::GUS (GUS reporter expressed by the *CYCD3;1* promoter) (Dewitte et al., 2007; Masubelele et al., 2005; Riou-Khamlichi et al., 1999), CYCD3;2::GFP:GUS (GFP:GUS fusion protein expressed by the *CYCD3;2* promoter) (Dewitte et al., 2007) and CYCD3;3::GFP:GUS (Dewitte et al., 2007) in first leaves of WT, *mp* and UBQ10::miR319a 4 days after germination. We focused on these cell cycle regulators because they are key integrators of developmental signals [reviewed in (Inze and De Veylder, 2006; Meijer and Murray, 2001; Nieuwland et al., 2009; Ramirez-Parra et al., 2005)].

Consistent with previous reports (Adachi et al., 2009), CDKA;1::CDKA;1:GUS was expressed ubiquitously in WT leaves, though more strongly in their basal parts (Figure 4.3A). CDKA;1::CDKA;1:GUS expression was extremely weak in *mp* and UBQ10::miR319a, but expression was weaker in *mp* and stronger in UBQ10::miR319a (Figure 4.3B,C).

In agreement with previous reports (Dewitte et al., 2007), CYCD3;1::GUS was expressed at the tip and lateral outgrowth of WT leaves (Figure 4.3D). No CYCD3;1::GUS expression was detected in *mp*, in UBQ10::miR319a CYCD3;1::GUS expression was stronger and additional, lateral foci of expression were detected (Figure 4.3E,F), consistent with the more-serrated leaves of this background (Figure 4.2A,C).

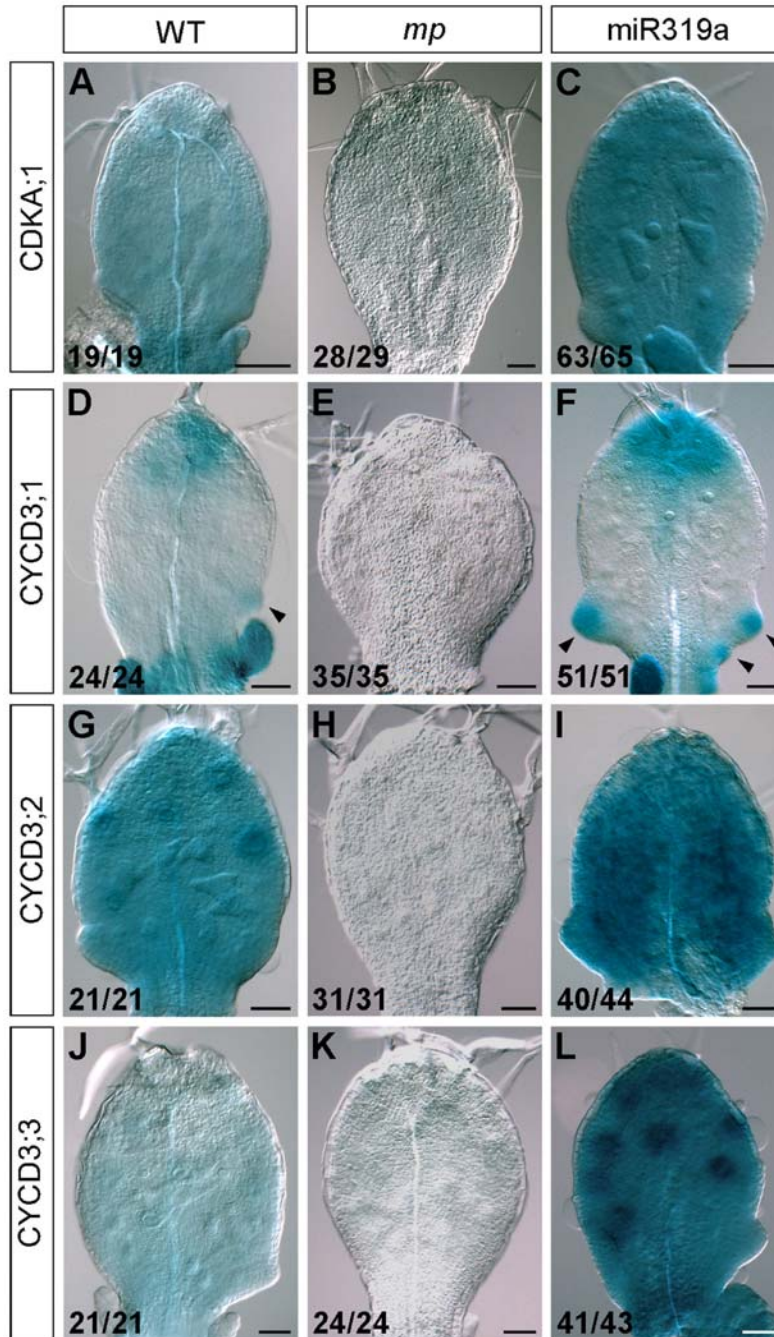


Figure 4.3. *MP*-dependent auxin signaling, *CIN-TCP*-dependent inhibition of cell proliferation and expression of cell cycle regulators. (A-L) Differential-Interference-Contrast illumination of first leaves 4 days after germination of WT (A,D,G,J), *mp-11* (B,E,H,K), and UBQ10::miR319a (C,F,I,L), expressing CDKA;1::CDKA;1:GUS (A-C), CYCD3;1::GUS (D-F), CYCD3;2::GFP:GUS (G-I), and CYCD3;3::GFP:GUS (J-L). Bottom left: reproducibility index. Scale bars: 50 μ m in A-L.

As previously reported (Dewitte et al., 2007), *CYCD3;2::GFP:GUS* and *CYCD3;3::GFP:GUS* were expressed ubiquitously in WT leaves, though expression of *CYCD3;2::GFP:GUS* was stronger than that of *CYCD3;3::GFP:GUS* (Figure 4.3G,J). Expression of both *CYCD3;2::GFP:GUS* and *CYCD3;3::GFP:GUS* was undetectable in *mp* and stronger in *UBQ10::miR319a* (Figure 4.3H,I,K,L).

In conclusion, the opposite effects of *mp* and *UBQ10::miR319a* on the expression of *CDKA;1*, *CYCD3;1*, *CYCD3;2* and *CYCD3;3* is consistent with the hypothesis that *mp* defects in vein network topology result from defective leaf cell proliferation and that such defects are suppressed, at least partially, by reduction in *CIN-TCP*-dependent inhibition of leaf cell proliferation.

4.2.6 Integration of tissue growth and vascularization by cell proliferation

How the growth of tissues and their vascularization are coordinated is a key, yet unanswered, question in biology. Our results suggest that in leaves these two processes are integrated by the activity of two pathways that antagonistically control the expression of *CDKA* and *CYCD3*, cell proliferation, and the formation of veins and their connection into networks (Figure 4.4): *CIN-TCP* genes inhibit these processes; *MP*-dependent auxin signaling promotes them.

How cell proliferation controls tissue growth is self-evident; how it instead controls tissue vascularization is unclear. Our results suggest that the patterning mechanism that controls vein formation requires fields of minimum cell numbers to generate a developmental outcome; such minimum cell numbers would only infrequently be achieved in *mp*, leading to vein formation defects. This may be similar to vascular strand formation during Arabidopsis embryogenesis, in which a single inner cell divides to give rise to a vascular cell and a ground cell (Gillmor et al., 2010; Mansfield and Briarty, 1991); in *mp*, failure of such inner cell to divide would invariably lead to failure in embryonic vascular-strand formation (Berleth and Jurgens, 1993; De Rybel et al., 2013; Ohashi-Ito et al., 2013). Likewise, it is possible that in *mp* leaves, cell proliferation defects lead to loss of the middle cell layer from which veins form (Foster, 1936; Stewart, 1978; Tilney-Bassett, 1986). Moreover, premature cessation of cell proliferation in *mp* would promote progression of precursor cells to mesophyll fate, thus preventing them to respond to vascular-fate-promoting auxin signals (Chapter 2).

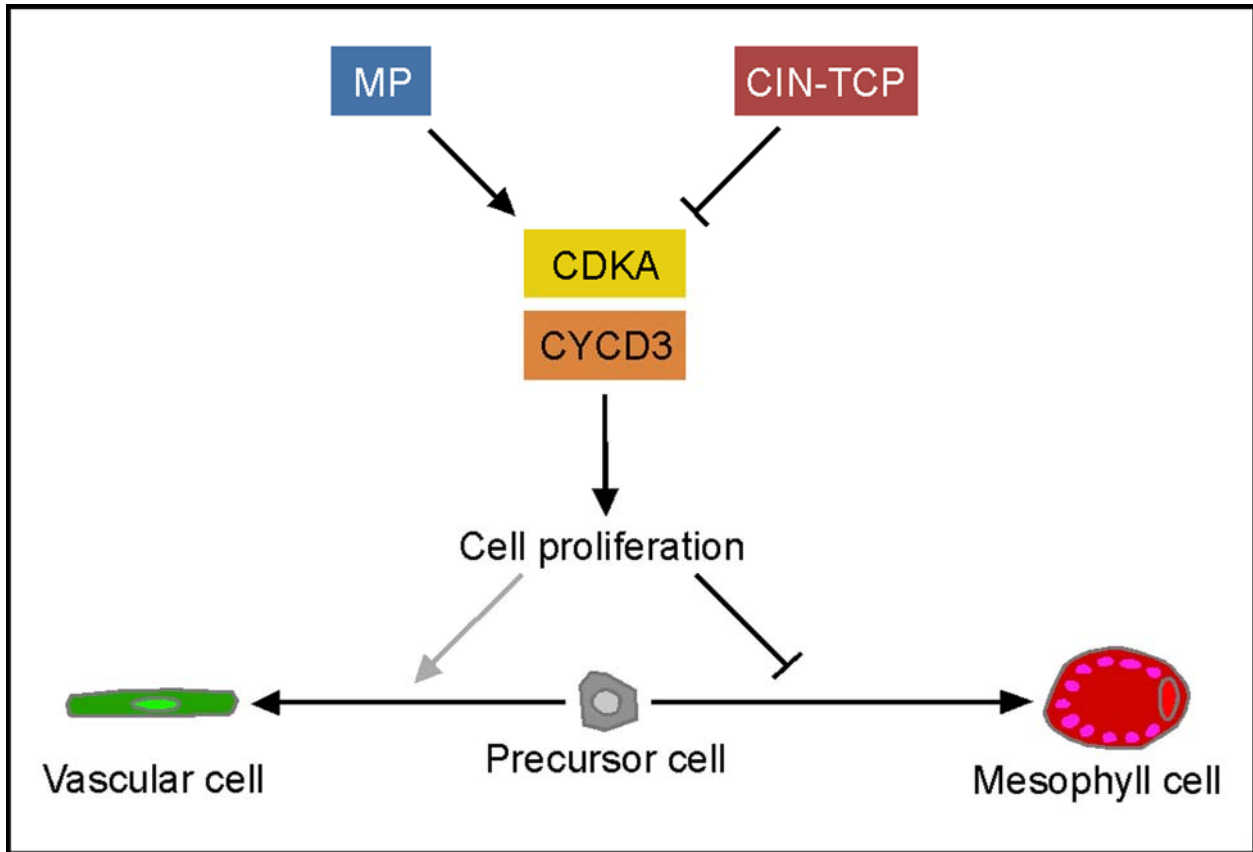


Figure 4.4. Summary and interpretation. During leaf development, *MP*-dependent auxin signaling promotes (black arrows), and *CIN-TCP* genes inhibit (black blunt-ended line), *CDKA*/*CYCD3*-mediated cell proliferation. Cell proliferation inhibits progression of ground cells to mesophyll fate, thus permitting their recruitment into veins; conversely, cessation of cell proliferation permits progression of ground cells to mesophyll fate, thus preventing their recruitment into veins. This account by no means excludes that cell proliferation might also directly promote progression of ground cells to vascular fate (grey arrow).

One other, non-mutually exclusive possibility is that *MP*-dependent cell proliferation permits files of precursor cells to progress to vascular fate, and that files of precursor cells that have progressed to vascular fate non-cell-autonomously inhibit progression of surrounding precursor cells to mesophyll fate (Chapter 2). The logic of this less-parsimonious account is similar to that underlying integration of tissue growth and vascularization in animals [e.g., (Cleaver and Melton, 2003)]; however, such logic is inconsistent with the apparent unresponsiveness of the timing of vascular fate specification to changes in leaf cell proliferation (Kang et al., 2007), and with the inability of vein-formation-inducing auxin signals to override progression of precursor cells to mesophyll fate (Scarpella et al., 2006). Our results thus suggest a molecular mechanism underlying the unique logic by which timing of cessation of cell proliferation integrates tissue growth and vascularization in plants.

4.3 Materials and methods

4.3.1 Plants

Origin and nature of lines, genotyping strategies and oligonucleotide sequences are in Tables 4.1–4.3. For all experiments, seeds were sterilized as in (Sawchuk et al., 2008). For auxinole-related experiments, seeds were germinated and seedlings grown in half-strength Murashige and Skoog salts (Caisson Laboratories Inc.), 15 g l⁻¹ sucrose (BioShop Canada Inc.), 0.5 g l⁻¹ MES (BioShop Canada Inc.), pH 5.7, at 25°C under continuous light (~80 μmol m⁻² s⁻¹) on a rotary shaker at 50 rpm. Auxinole (Hayashi et al., 2012) (a generous gift of Ken-ichiro Hayashi) was dissolved (50 mM) in dimethyl sulfoxide; dissolved auxinole was added to growth medium (50 μM) just before sowing and was replaced weekly. For all other experiments, seeds were germinated, seedlings and plants were grown (~80 μmol m⁻² s⁻¹), and plants were transformed as in (Sawchuk et al., 2008).

4.3.2 Imaging

Mature leaves were fixed, cleared and mounted as in Chapter 2. Mounted leaves were imaged as in (Odat et al., 2014). β-glucuronidase (GUS) activity in developing leaves was detected, and leaves were fixed, cleared and mounted as in (Scarpella et al., 2004) Marker-line-specific

Table 4.1. Origin and nature of lines

Line	Origin/Nature
<i>mp-11</i>	((Odat et al., 2014); Chapter 3)
RPS5A::KRP2 ^{Δ73-97}	Transcriptional fusion of <i>RPS5A</i> (AT3G11940; -2236 to -1; primers: ‘RPS5a XhoI Forw’ and ‘RPS5a Sall Rev’) to KRP2 ^{Δ73-97} (Chapter 2)
RPS5A::CDKA;1 ^{D146N}	Transcriptional fusion of <i>RPS5A</i> (AT3G11940; -2236 to -1; primers: ‘RPS5a XhoI Forw’ and ‘RPS5a Sall Rev’) to CDKA;1 ^{D146N} (Chapter 2)
RPS5A::CYCD3;1 ^{S343A}	Transcriptional fusion of <i>RPS5A</i> (AT3G11940; -2236 to -1; primers: ‘RPS5a XhoI Forw’ and ‘RPS5a Sall Rev’) to CYCD3;1 ^{S343A} (Chapter 2)
RPS5A::E2Fa:VP16	Transcriptional fusion of <i>RPS5A</i> (AT3G11940; -2236 to -1; primers: ‘RPS5a XhoI Forw’ and ‘RPS5a Sall Rev’) to E2Fa:VP16 (Chapter 2)
UBQ10::miR319a	(Chapter 2)
<i>tcp4-1</i>	(Schommer et al., 2008)
<i>tcp10-1</i>	(Koyama et al., 2010)
CDKA;1::CDKA;1:GUS	(Adachi et al., 2009)
CYCD3;1::GUS	(Masubelele et al., 2005; Riou-Khamlichi et al., 1999)
CYCD3;2::GUS:GFP	(Dewitte et al., 2007)
CYCD3;3::GUS:GFP	(Dewitte et al., 2007)

Table 4.2. Genotyping strategies

Line	Strategy
<i>mp-11</i>	<i>MP</i> : ‘SAIL_1265_F06LP’ and ‘SAIL_1265_F06RP’; <i>mp</i> : ‘SAIL_1265_F06RP’ and ‘LB3’
<i>tcp4-1</i>	<i>TCP4</i> : ‘tcp4 geno LP’ and ‘tcp4 geno RP’; <i>tcp4</i> : ‘tcp4 geno RP’ and ‘LBb1.3’
<i>tcp10-1</i>	<i>TCP10</i> : ‘tcp10 geno LP’ and ‘tcp 10 geno Rp’; <i>tcp10</i> : ‘tcp 10 geno Rp’ and ‘LBb1.3’

Table 4.3. Oligonucleotide sequences

Name	Sequence (5' to 3')
RPS5a XhoI Forw	ATACTCGAGAGCAGGAGATCTATCAGTGC
RPS5a Sall Rev	ATAGTCGACGGCTGTGGTGAGAGAAACAGAG
SAIL_1265_F06LP	GCTTCATCTCTTCAAGCAAGG
SAIL_1265_F06RP	TCCCAAAGTCTCACCCTCAC
LB3	TAGCATCTGAATTCATAACCAATCTCGATACAC
tcp4 geno LP	TTGGGACCAAAAAGATTACGTG
tcp4 geno RP	ACTATCATCATCAGCATCCGC
LBb1.3	ATTTTGCCGATTTTCGGAAC
tcp10 geno LP	AGCAGCTTTCAGGTAGCTGTG
tcp10 geno Rp	TGATGATCCCAAGAACGAAAC

Table 4.4. Marker-line-specific conditions of β -glucuronidase (GUS) detection

Line	Concentration of Fe ²⁺ /Fe ³⁺ salts	Incubation time
CDKA;1::CDKA;1:GUS	5 mM each	2 hours
CYCD3;1::GUS	1 mM each	16 hours
CYCD3;2::GUS:GFP	5 mM each	4 hours
CYCD3;3::GUS:GFP	2 mM each	2 hours

conditions of detection are in Table 4.4. Mounted leaves were imaged with an AxioImager.M1 microscope (Carl Zeiss AG), and a MicroPublisher 5.0 digital camera (QImaging). Image brightness and contrast were adjusted by linear stretching of the histogram with ImageJ (National Institutes of Health). Images were cropped with Photoshop (Adobe Systems Inc.), and assembled into figures with Canvas (ACD Systems International Inc.).

4.3.3 Vein network analysis

Vein networks were analyzed as in (Verna et al., 2015) and Chapter 2.

CHAPTER 5: CHARACTERIZATION OF GENETIC SUPPRESSORS OF THE *monopteros* PHENOTYPE

5.1 Introduction

Auxin is a key regulator of plant development: during embryogenesis, it controls the formation of embryo parts; during post-embryonic development, it controls the formation of shoot organs, lateral roots, and their tissues (De Smet and Jurgens, 2007). The auxin signal is transduced by multiple pathways, the best characterized of which ends with the activation or repression of transcription of auxin-responsive genes by transcription factors of the AUXIN RESPONSE FACTOR (ARF) family (Chapman and Estelle, 2009). Of the 22 ARFs in Arabidopsis (Guilfoyle and Hagen, 2007), only one—MONOPTEROS (MP)/ARF5 (Hardtke and Berleth, 1998)—seems to have nonredundant functions in plant development (Okushima et al., 2005). Therefore, to understand auxin's actions in plant development, varied approaches have been applied to the identification of direct targets of MP function (Cole et al., 2009; Donner et al., 2009; Konishi et al., 2015; Schlereth et al., 2010; Yamaguchi et al., 2013; Zhao et al., 2010). However, at least some of auxin's inputs in plant development result from the interaction of auxin signal transduction with other, nonoverlapping pathways [reviewed in (Kuppusamy et al., 2009)]. For example, vein network formation results, at least partially, from the interaction of two pathways that antagonistically control leaf cell proliferation: *MP*-dependent auxin signaling, which promotes leaf cell proliferation, and *CIN-TCP* (for *CINCINNATA*-related *TEOSINTE BRANCHEDI/CYCLOIDEA/PROLIFERATING CELL FACTOR*)-dependent transcriptional regulation, which inhibits it (Chapter 4).

In animals, many such interactions between pathways have been identified by screening for genetic suppressors [e.g., (Hodgkin, 2005; Huang and Sternberg, 2006)]. A suppressor mutation is defined as a second mutation that suppresses the phenotypic effects of a first mutation. To identify new nonoverlapping pathways—as well as additional components of the leaf cell-proliferation pathway—that interact with auxin signal transduction in vein network formation, it would thus be highly desirable to identify genetic suppressors of the *mp* phenotype.

Unfortunately, all *mp* alleles identified so far are sterile (Berleth and Jurgens, 1993; Cole et al.,

2009; Donner et al., 2009; Hardtke and Berleth, 1998; Odat et al., 2014; Okushima et al., 2005; Przemeck et al., 1996; Weijers et al., 2005a) (Chapter 3), precluding a suppressor screen in an *mp* background. However, *mp* defects can be bypassed by a fusion between the MP protein and the hormone-binding domain of the vertebrate glucocorticoid receptor (MP::MP:GR) (Krogan et al., 2014). In the absence of a ligand (e.g., dexamethasone, or DEX), fusions between transcription factors and GR such as MP:GR are sequestered in the cytoplasm by multiple proteins, including heat-shock proteins (Picard et al., 1988). In the presence of DEX, the MP:GR fusion protein is released from the cytoplasmic complexes and transferred to the nucleus, where it can activate the expression of MP targets.

Seeds of *mp* plants containing the MP::MP:GR transgene (MP::MP:GR;*mp*) were mutagenized with ethyl methanesulfonate, and sterility was bypassed in the resulting ~12,500 M1 plants by spraying them with DEX (E. Scarpella, unpublished). Most of the ~125,000 M2 plants—derived from the self-fertilization of the M1 plants—were sterile, but 276 M2 plants were fertile to varying extent and thus identified as putative suppressors of the *mp* phenotype; here I report their initial characterization.

5.2 Results and Discussion

276 M2 plants were identified in a screen for genetic suppressors of the *mp* phenotype that were, to varying extent, fertile; however, 14 of these 276 M2 plants failed to produce enough seeds and were thus no further analyzed (Figure 5.1). The remaining 262 M2 plants produced abundant seeds and might be WT contaminants, contain a mutation that suppresses the *mp* phenotype, or have residual nuclear expression of MP::MP:GR. To eliminate WT contaminants, I sowed M3 seeds progeny of these 262 M2 plants on medium containing glufosinate ammonium, to which the MP::MP:GR construct confers resistance.

The M3 progeny of 196 of these 262 M2 plants were sensitive to glufosinate ammonium, suggesting that they are WT contaminants. By contrast, the M3 progeny of the remaining 66 M2 plants were resistant to glufosinate ammonium, suggesting that they contain a mutation that

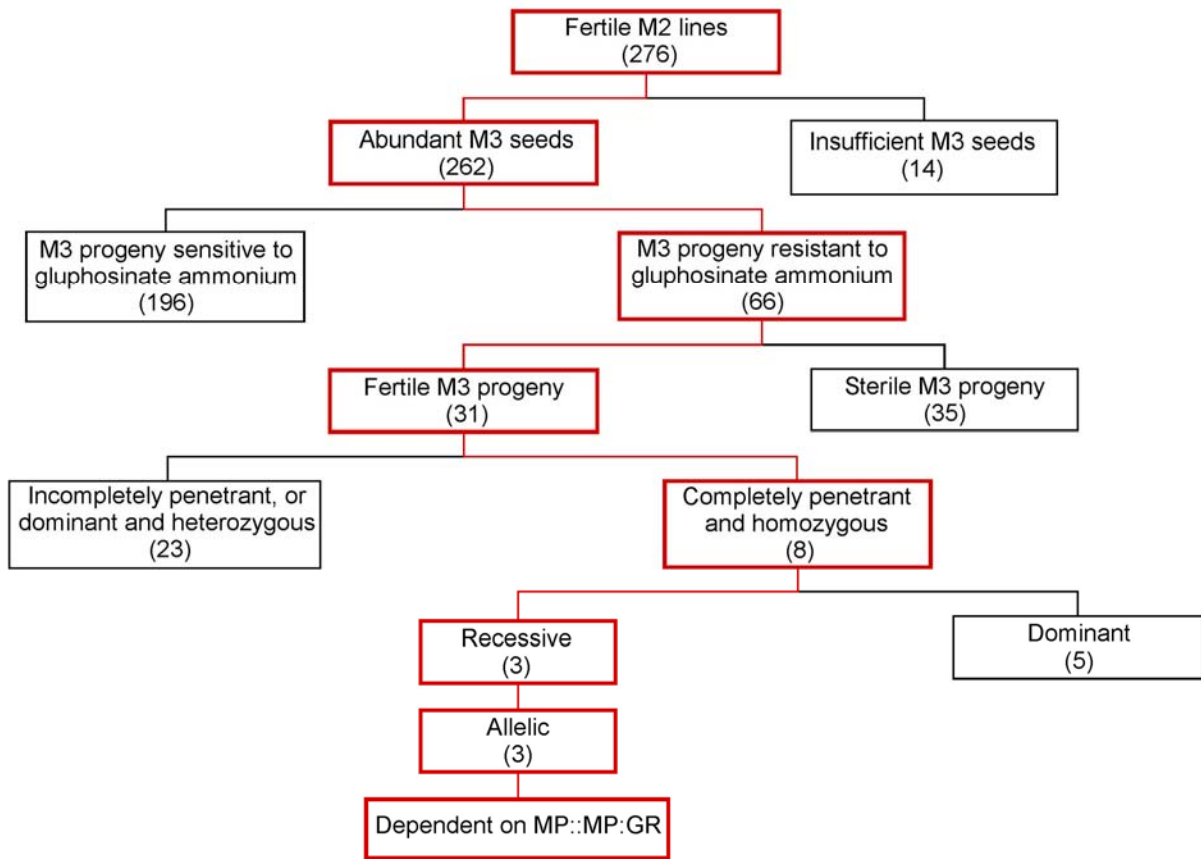


Figure 5.1. Overview of characterization of putative genetic suppressors of the *mp* phenotype. In red, experimental path followed.

suppresses the *mp* phenotype or have residual nuclear expression of MP::MP:GR. For each of these 66 M2 lines, I grew eight M3 plants to maturity.

The M3 progeny of 35 of these 66 M2 lines were sterile (Table 5.1), suggesting that suppression of the *mp* phenotype in these lines is not heritable (e.g., these lines had residual nuclear expression of MP::MP:GR). The M3 progeny of the remaining 31 M2 lines were fertile (Table 5.1)—though to varying extent—suggesting that these lines contain a mutation that suppresses the *mp* phenotype. To eliminate lines with incomplete penetrance of suppression of the *mp* phenotype, I sowed ~50 M3 seeds for each of these 31 M2 lines.

In the absence of dexamethasone, MP::MP:GR;*mp* seedlings are invariably rootless (Krogan et al., 2014). If in an M2 line the suppression of the *mp* phenotype were completely penetrant and the *mp* suppressor mutation were homozygous—irrespective of whether the *mp* suppressor mutation were recessive or dominant—all the M3 seedlings progeny of such M2 line should have a root. If, on the other hand, in an M2 line the suppression of the *mp* phenotype were incompletely penetrant and the *mp* suppressor mutation were homozygous—irrespective of whether the *mp* suppressor mutation were recessive or dominant—less than 100% of the M3 seedlings progeny of such M2 line should have a root.

If in an M2 line the suppression of the *mp* phenotype were completely penetrant and the *mp* suppressor mutation were recessive and heterozygous, 25% of the M3 seedlings progeny of such M2 line should have a root. If, on the other hand, in an M2 line the suppression of the *mp* phenotype were incompletely penetrant and the *mp* suppressor mutation were recessive and heterozygous, less than 25% of the M3 seedlings progeny of such M2 line should have a root.

If in an M2 line the suppression of *mp* phenotype were completely penetrant and the *mp* suppressor mutation were dominant and heterozygous, 75% of the M3 seedlings progeny of such M2 line should have a root. If, on the other hand, in an M2 line the suppression of the *mp* phenotype were incompletely penetrant and the *mp* suppressor mutation were dominant and heterozygous, less than 75% of the M3 seedlings progeny of such M2 line should have a root.

All the M3 seedlings progeny of eight of the 31 M2 lines had a root (Table 5.2), suggesting that these lines were homozygous for a completely penetrant suppressor of the *mp* phenotype. Between 68% and 97% of the M3 seedlings progeny of the remaining 23 M2 lines had a root (Table 5.2), suggesting that these lines contained: (i) an incompletely penetrant suppressor of the *mp* phenotype at the homozygous state; (ii) an incompletely penetrant, dominant suppressor of

Table 5.1. Fertility of M2 lines

M2 line	Fertility
1-4-1	+
2-3-1	+
2-9-1	+
3-9-1	-
3-9-3	+
4-1-1	+
4-3-1	-
4-3-2	+
5-2-12	+
5-10-1	+
6-7-1	+
6-7-3	+
6-7-4	+
8-5-1	+
9-2-3	+
9-4-1	+
9-4-2	+
9-7-1	+
9-7-3	+
9-7-5	+
9-7-6	+
10-9-1	-
16-5-1	+
18-9-1	+
18-10-1	+
18-10-2	+

18-10-3	+
21-1-1	-
21-2-1	-
21-3-1	-
21-4-1	-
21-5-1	-
21-6-1	-
21-7-1	-
21-8-1	-
21-9-1	-
21-10-1	-
21-11-1	-
21-12-1	-
22-1-1	-
22-2-1	-
22-3-1	-
22-4-1	-
22-5-1	-
22-6-1	-
22-7-1	-
22-8-1	-
22-9-1	-
22-10-1	-
22-12-1	-
23-1-1	-
23-2-1	-
23-3-1	+
23-4-1	+

24-11-4	+
24-11-7	+
25-3-1	+
25-3-2	+
25-3-3	+
25-9-1	-
26-4-1	-
26-5-1	-
26-6-1	-
26-8-1	-
26-9-1	-
26-12-1	-

Table 5.2. Penetrance of *mp* suppression in M2 lines

M2 line	No. of M3 seedlings with root	No. of rootless M3 seedlings	3:1 X ² value	Fails to exceed 3:1 X ² critical value (3.84)	1:3 X ² value	Fails to exceed 1:3 X ² critical value (3.84)
1-4-1	39	0	13.00	N	204.75	N
2-3-1	36	0	12.00	N	189.00	N
2-9-1	63	0	21.00	N	330.75	N
3-9-3	37	2	8.21	N	183.20	N
4-1-1	38	5	4.10	N	173.30	N
4-3-2	57	7	6.75	N	262.35	N
5-2-12	15	4	0.16	Y	59.47	N
5-10-1	42	7	3.00	Y	184.64	N
6-7-1	23	6	0.29	Y	91.74	N
6-7-3	23	4	1.49	Y	100.35	N
6-7-4	39	8	1.60	Y	164.74	N
8-5-1	46	8	2.99	Y	200.70	N
9-2-3	23	4	1.49	Y	100.35	N
9-4-1	18	5	0.13	Y	70.56	N
9-4-2	49	16	0.01	Y	182.75	N
9-7-1	38	11	0.17	Y	147.19	N
9-7-5	28	5	1.71	Y	121.58	N
9-7-6	34	1	9.15	N	172.87	N
10-9-1	20	4	0.89	Y	84.93	N
16-5-1	41	8	1.97	Y	174.998	N
18-9-1	38	0	12.67	N	199.50	N
18-10-1	27	6	0.82	Y	112.06	N
18-10-2	34	16	1.307	Y	109.4898	N
18-10-3	43	4	6.82	N	204.24	N

23-3-1	33	0	11.00	N	173.25	N
23-4	79	28	0.08	Y	286.37	N
24-11-4	31	6	1.52	Y	132.53	N
24-11-7	37	0	12.33	N	194.25	N
25-3-1	31	0	10.33	N	162.75	N
25-3-2	52	0	17.33	N	273.00	N
25-3-3	26	6	0.67	Y	106.96	N

the *mp* phenotype at the heterozygous state; or (iii) a completely penetrant, dominant suppressor of the *mp* phenotype at the heterozygous state.

Because I wished to focus on completely penetrant, recessive suppressors of the *mp* phenotype, I determined the pattern of inheritance of the *mp* suppressor mutations in the eight M2 lines that were homozygous for a completely penetrant suppressor of the *mp* phenotype. To this aim, I crossed M3 plants progeny of each of these eight M2 lines to *MP/mp*.

Should an *mp* suppressor mutation be recessive, I would expect half of the seedlings in the F1 progeny of such crosses to be rootless. By contrast, should an *mp* suppressor mutation be dominant, I would expect all the seedlings in the F1 progeny of such crosses to have a root.

Based on these expectations and on the phenotype of the F1 progeny of the cross between *MP/mp* and M3 plants progeny of each of the eight M2 lines that were homozygous for a completely penetrant suppressor of the *mp* phenotype (Table 5.3), I conclude that the *mp* suppressor mutation is dominant in five of the eight M2 lines and recessive in the remaining three M2 lines (M2 lines 2-3-1, 25-3-1 and 25-3-2).

To determine the number of genes defined by the three recessive, completely penetrant *mp* suppressor mutations, I crossed M3 plants progeny of M2 lines 2-3-1, 25-3-1 and 25-3-2 with one another.

Should M3 plants progeny of two different M2 lines contain mutations in the same *mp* suppressor gene, I would expect all the seedlings in the F1 progeny of such crosses to have a root. By contrast, should two plants contain mutations in different *mp* suppressor genes, I would expect all the seedlings in the F1 progeny of such crosses to be rootless.

Based on these expectations and on the phenotype of the F1 progeny of the three possible pairwise crosses between M3 plants progeny of M2 lines 2-3-1, 25-3-1 and 25-3-2 (Table 5.4), I conclude that these M2 lines contain mutations in a single *mp* suppressor gene.

To determine whether suppression of the *mp* phenotype in M2 lines 2-3-1, 25-3-1 and 25-3-2 depended on the presence of the *MP::MP:GR* construct, I attempted to isolate a WT-looking *mp/mp* plant lacking the *MP::MP:GR* construct in the F2 progeny of a cross between an M3 plant progeny of M2 line 25-3-2 and *MP/mp*. I would expect to find, on average, one WT-looking *mp/mp* plant lacking the *MP::MP:GR* construct in 64 F2 plants of such a cross.

I genotyped 98 WT-looking F2 plants of a cross between an M3 plant progeny of M2 line

Table 5.3. Phenotype of F1 progeny of crosses between M2 lines and *MP/mp*

M2 line	No. of F1 seedlings with root	No. of rootless F1 seedlings	1:1 X^2 value	Fails to exceed 1:1 X^2 critical value (3.84)
1-4-1	47	10	24.02	N
2-3-1	21	17	0.42	Y
2-9-1	30	1	27.13	N
18-9-1	24	0	24.00	N
23-3-1	39	2	33.39	N
24-11-7	56	0	56.00	N
25-3-1	33	25	1.10	Y
25-3-2	38	26	2.25	Y

Table 5.4. Phenotype of F1 progeny of crosses between M2 lines

M2 lines crossed	No. of F1 seedlings with root	No. of rootless F1 seedlings	1:1 X^2 value critical value (3.84)	Fails to exceed 3:1 X^2 critical value (3.84)
2-3-1 and 25-3-1	24	0	24	N
2-3-1 and 25-3-2	59	0	59	N
25-3-1 and 25-3-2	64	0	64	N

25-3-2 and *MP/mp* for the presence of the *MP::MP:GR* construct, and found 29 plants lacking the *MP::MP:GR* construct. I genotyped these 29 plants for the presence of the *MP* and *mp* alleles, and found 17 *MP/mp* plants but no *mp/mp* plants.

This was somewhat unexpected because the probability of finding a WT-looking *mp/mp* plant lacking the *MP::MP:GR* construct among 98 WT-looking F2 plants of a cross between an M3 plant progeny of M2 line 25-3-2 plant and *MP/mp* is ~80%. In any case, the *mp* suppressor mutation should be present at the homozygous state in 25% of the 17 *MP/mp* F2 plants lacking the *MP::MP:GR* construct, and at the heterozygous state in half of them.

If the *mp* suppressor mutation were present at the homozygous state in an *MP/mp* F2 plant lacking the *MP::MP:GR* construct, all the F3 seedlings progeny of such F2 plant should have a root. If, on the other hand, the *mp* suppressor mutation were present at the heterozygous state in an *MP/mp* F2 plant lacking the *MP::MP:GR* construct, 3/16 of the F3 seedlings progeny of such F2 plant should be rootless.

For none of the 17 *MP/mp* F2 plants lacking the *MP::MP:GR* construct was the F3 progeny exclusively composed of seedlings with root; however, three *MP/mp* F2 plants lacking the *MP::MP:GR* construct segregated rootless seedlings in a 3:13 ratio in the F3 generation (Table 5.5), suggesting that the *mp* suppressor mutation was present at the heterozygous state in these three *MP/mp* F2 plants.

In a further attempt to isolate a WT-looking *mp/mp* plant lacking the *MP::MP:GR* construct, I grew F3 plants progeny of one of the three *MP/mp* F2 plants lacking the *MP::MP:GR* construct that was supposedly heterozygous for the *mp* suppressor mutation (plant no. 14). I would expect to find, on average, one WT-looking *mp/mp* plant lacking the *MP::MP:GR* construct in 16 such F3 plants.

I genotyped for the presence of the *MP* and *mp* alleles 58 WT-looking F3 plants progeny of plant no. 14—which lacked the *MP::MP:GR* construct, was heterozygous for *mp*, and was supposedly heterozygous for the *mp* suppressor mutation—but found no *mp/mp* plants.

This was unexpected because the probability of finding a WT-looking *mp/mp* plant among 58 WT-looking plants progeny of a plant (plant no. 14) that lacked the *MP::MP:GR* construct, was heterozygous for *mp*, and was supposedly heterozygous for the *mp* suppressor mutation is ~98%.

The inability to find a WT-looking *mp/mp* plant lacking the *MP::MP:GR* construct in the progeny of a cross between line 25-3-2 and *MP/mp* suggests that the *mp* suppressor effect of the

Table 5.5. Phenotype of F3 progeny of *MP/mp* F2 plants lacking *MP::MP:GR* derived from cross between M2 line 25-3-2 and *MP/mp*

F2 plant	No. of F3 seedlings with root	No. of rootless F3 seedlings	3:1 X ² value	Fails to exceed 3:1 X ² critical value (3.84)	13:3 X ² value	Fails to exceed 13:3 X ² critical value (3.84)
1	32	10	0.03	Y	0.71	Y
2	39	6	3.27	Y	0.87	Y
3	34	10	0.12	Y	0.46	Y
4	34	13	0.18	Y	2.45	Y
5	33	12	0.07	Y	1.85	Y
6	33	6	1.92	Y	0.29	Y
7	42	6	4.00	N	1.23	Y
8	33	12	0.07	Y	1.85	Y
9	28	17	3.92	N	10.69	N
10	44	3	8.69	N	4.72	N
11	32	3	5.04	N	2.38	Y
12	33	17	2.16	Y	7.63	N
13	39	13	0	Y	1.33	Y
14	125	27	4.25	N	0.1	Y
15	41	9	1.31	Y	0.02	Y
16	150	0	17.00	N	11.77	N
17	22	7	0.01	Y	0.55	Y

mutation in line 25-3-2 depends on the presence of the MP::MP:GR construct. One possibility to account for this behavior is that in the presence of such *mp* suppressor mutation the MP:GR fusion protein becomes constitutively active. For example, the mutation could reside in a gene encoding HEAT-SHOCK PROTEIN90 (HSP90), and prevent HSP90 from binding the MP:GR fusion protein. One other possibility is that the mutation resides in the GR domain of the MP:GR fusion protein, and prevent the MP:GR fusion protein from binding HSP90. In either case, in the absence of DEX the MP:GR fusion protein would no longer be sequestered in the cytoplasm by HSP90 but constitutively translocated to the nucleus.

Future research will determine whether the *mp* suppressor effects of the mutations in the dominant suppressors or in the incompletely penetrant suppressors (Tables 5.2 and 5.3) depend on the presence of the MP::MP:GR construct.

5.3 Materials and methods

Seeds were sterilized and germinated, and plants were grown as described (Sawchuk et al., 2008). The *mp*^{G12} allele (Hardtke and Berleth, 1998), which lacks the region from nucleotide +288 to nucleotide +2748 of the *MP* gene (Odat et al., 2014) (Chapter 3), was used for all experiments. The origin of MP::MP:GR;*mp*^{G12} has been reported (Krogan et al., 2014). The *MP* and *mp*^{G12} alleles were genotyped as in (Odat et al., 2014) (Chapter 3). The MP::MP:GR construct was genotyped by primers ‘MP Seq 4750/2369’ (5’-ATGGCAGAAAATTGCGACACC-3’) and ‘GR BsrGI Rev’ (5’-ACGTGTACAGTCATTTTTGATGAAAC-3’).

CHAPTER 6: DISCUSSION

6.1 Conclusion summary

In most multicellular organisms, signals and nutrients are transported throughout the body by a vascular system. For normal development and optimal function, no area of the body should thus be devoid of vessels. Therefore, the growth of tissues and their vascularization must be tightly coordinated, and understanding the molecular basis of this coordination is a key question in biology. In animals, signals from proliferating nonvascular tissues promote their vascularization (Keck et al., 1989; Leung et al., 1989); in turn, vessels signal back to surrounding nonvascular tissues to control their growth and development [reviewed in (Cleaver and Dor, 2012)]. By contrast, in plant leaves, vascular and nonvascular tissues differentiate from the same precursor cells (Flot, 1905); yet it is possible that the logic that integrates the growth of tissues and their vascularization in plants is no different from that in animals. The scope of my PhD thesis was to investigate this possibility for *Arabidopsis* leaves, in which internal, ground cells proliferate and differentiate into either mesophyll or veins (Kang and Dengler, 2004; Scarpella et al., 2004).

My results suggest that cell proliferation inhibits progression of ground cells to mesophyll fate, thus permitting their recruitment into veins, and that cessation of cell proliferation permits progression of ground cells to mesophyll fate, thus preventing their recruitment into veins (Chapter 2). This logic resembles that of tissue patterning in animal appendages [e.g., (Lopez-Rios et al., 2012; Towers et al., 2008; Zhu et al., 2008)], but it is different from that which integrates tissue growth and vascularization in animal organs [e.g., (Cleaver and Melton, 2003)]. What molecular mechanisms control the integration of tissue growth and vascularization in plant organs?

My results suggest that leaf growth and vascularization are integrated by the activity of two pathways that antagonistically control cell proliferation and vein network formation: transcriptional input provided by the CINCINNATA-related TCP (for TEOSINTE BRANCHED1/CYCLOIDEA/PROLIFERATING CELL FACTOR) proteins (Cubas et al., 1999) inhibits these processes; transduction of the signaling molecule auxin mediated by the MONOPTEROS transcription factor (Hardtke and Berleth, 1998) promotes them (Chapters 3 and

4). My results thus suggest a molecular mechanism that controls the unique logic by which timing of cessation of cell proliferation integrates tissue growth and vascularization in plants.

In the Discussion section of the respective chapters, I provided an account of how I reached these conclusions from the experimental data, how these conclusions could be integrated with one another and with those of studies of others to advance our understanding of vein development and of how tissue growth and vascularization are controlled and integrated in plants. Here I instead wish to attempt to account for the mechanism by which the interaction between auxin signalling and cell proliferation results in vein network formation. The hypothesis I propose below should be understood as an attempt to develop a conceptual framework to guide future experimentation, rather than an exhaustive mechanistic account.

6.2 A model of vein formation by auxin-dependent cell proliferation

Five tissue layers can be distinguished in cross sections of mature leaves of dicotyledonous plants [reviewed in (Foster, 1936)] (Figure 6.1A): (1) upper epidermis; (2) palisade mesophyll; (3) middle layer; (4) lower spongy mesophyll; (5) lower epidermis. The middle layer comprises veins and upper spongy mesophyll, both of which typically differentiate from middle-layer ground cells [reviewed in (Stewart, 1978; Tilney-Bassett, 1986)]. Clonal analysis in dicotyledonous plants has shown that at early stages of leaf tissue development each of the three nonepidermal, inner tissue layers is composed of a single layer of cells; near the margin of the leaf, all the three single-cell layers derive from successive divisions of the L2 single-cell layer of the shoot apical meristem (SAM), whereas in central regions of the leaf the middle single-cell layer directly derives from the L3 single-cell layer of the SAM (Stewart, 1978; Tilney-Bassett, 1986) (Figure 6.1A). The three inner single-cell layers near the margin of developing *Arabidopsis* flowers seem to derive from cell divisions of the L2 layer of the SAM that are oriented parallel to the lateral axis of flower primordium outgrowth (Reddy et al., 2004). Though it is unknown whether and how the three inner single-cell layers derive from the L2 of the SAM during *Arabidopsis* leaf development, it seems that only upon formation of all the three inner single-cell layers does the middle one initiate expression of middle-layer-specific genes (Matsumoto and Okada, 2001; Nakata et al., 2012; Nakata and Okada, 2012; Shimizu et al., 2009).

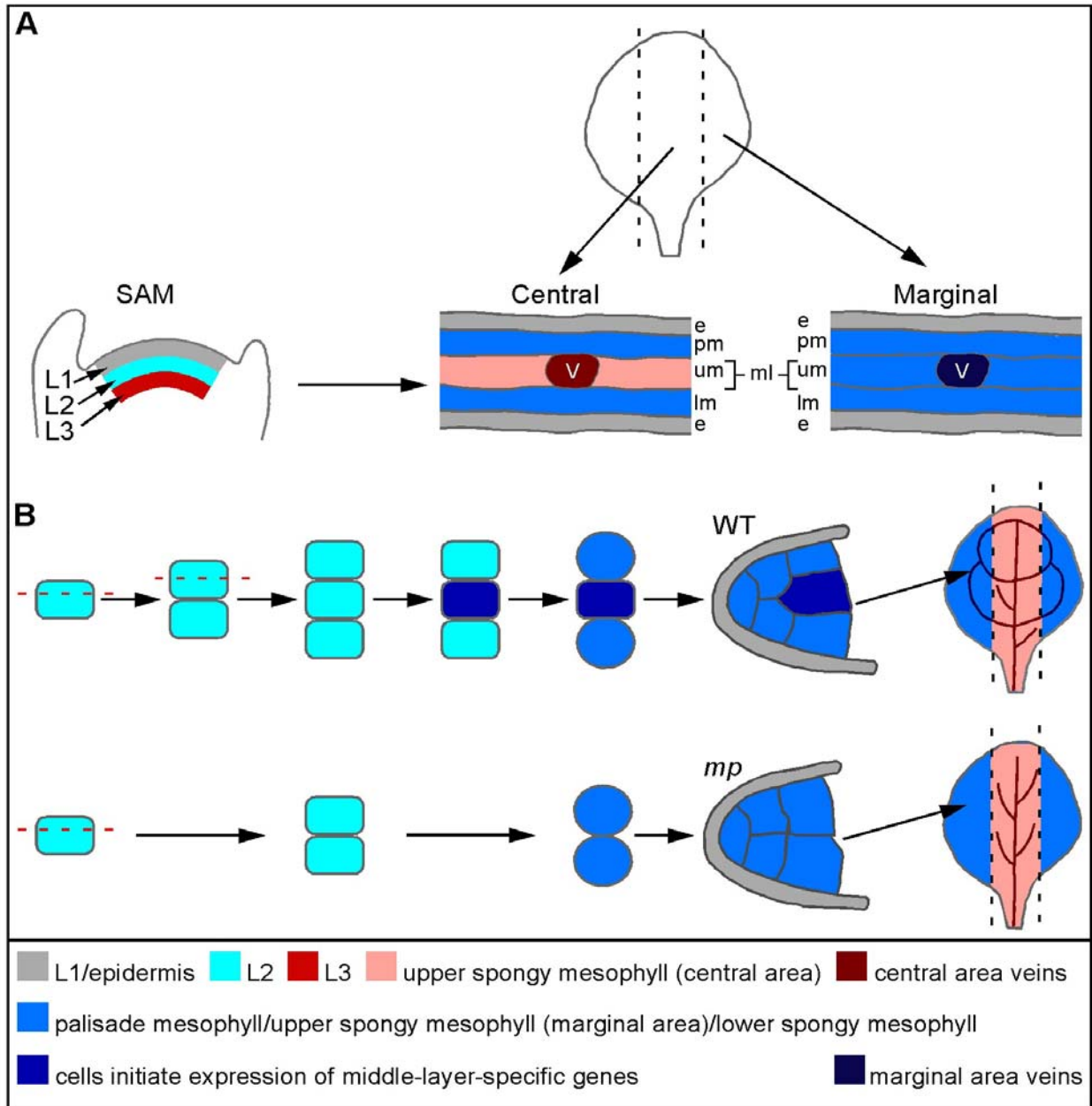


Figure 6.1. A model of vein formation by auxin-dependent cell proliferation. (A) Clonal analysis in dicotyledonous plants has shown that the L1 layer of the SAM will give rise to the leaf epidermis. In the central region of the leaf, the middle single-cell layer—which will give rise to the veins—is derived from the L3 single-cell layer of the SAM. In the marginal regions of the

leaf, all three inner single-cell layers derive from successive divisions of the L2 single-cell layer of the SAM. (B) I propose that the three inner single-cell layers near the margin of developing Arabidopsis leaves derive from cell divisions of the L2 layer of the SAM. In WT, the L2 cells will divide twice in order to form the three single-cell layers, the middle one of which will give rise to the veins. Because of premature cessation of cell proliferation in *mp* leaves, the L2 cells will occasionally fail to complete one of the two cell divisions which will prevent the formation of the three single-cell layers, and this will prevent vein formation.

I propose that as in *Arabidopsis* flower development, the three inner single-cell layers near the margin of developing *Arabidopsis* leaves derive from cell divisions of the L2 layer of the SAM that are oriented parallel to the lateral axis of leaf primordium outgrowth (Reddy et al., 2004) (Figure 6.1B). Because of premature cessation of cell proliferation in *mp* leaves (Chapter 4), I propose that in this background at least one of such formative cell divisions fails to occur (Figure 6.1B). Because it seems that only upon formation of all the three inner single-cell layers does the middle one initiate expression of middle-layer-specific genes (Matsumoto and Okada, 2001; Nakata et al., 2012; Nakata and Okada, 2012; Shimizu et al., 2009), because premature cessation of cell proliferation leads to premature progression to mesophyll fate (Chapter 2), and because cells that have progressed to mesophyll fate are insensitive to auxin-dependent vein-formation signals (Scarpella et al., 2006), failure to occur in *mp* of at least one of the cell divisions that I propose give rise to the three, inner single-cell layers of the developing leaf would lead to loss of the middle single-cell layer and of the veins that from it derive (Figure 6.1B). Likewise, defects in vein formation induced by premature cessation of leaf cell proliferation in a WT *MP* background—for example by interfering with cell cycle progression in the leaf (Chapters 2 and 4)—would be expected to result from loss of the middle single-cell layer because of failure to occur of at least one of the cell divisions that I propose give rise to the three, inner single-cell layers of the developing leaf. Conversely, delayed cessation of leaf cell proliferation—for example by reduction in *CIN-TCP* function (Chapters 2 and 4)—would be expected to prolong the leaf's ability to form at its margin a middle single-cell layer and thus the veins that from it derive. Finally, delaying cessation of cell proliferation in an *mp* background would restore, at least partially, the leaf's ability to form at its margin a middle single-cell layer and thus the veins that from it derive.

Not only can this hypothesis account for my results but it provides a mechanistic explanation for the observation that reduction or loss of *MP* function mainly leads to loss of vein formation near the margin of the leaf, where the formation of the middle single-cell layer would depend on divisions of the L2 layer of the SAM, whereas the formation of the veins in the central region of the leaf, where the middle single-cell layer would directly derive from the L3 single-cell layer of the SAM, is relatively unaffected (Berleth and Jurgens, 1993; Donner et al., 2009; Odat et al., 2014; Przemeck et al., 1996) (Chapter 3). Further, this hypothesis is consistent with vascular cell

formation during embryogenesis and the origin of the vascular defects in *mp* embryos. In fact, the first vascular cells of Arabidopsis form from the periclinal division of the lower tier of inner cells of the dermatogen-stage embryo (Gillmor et al., 2010; Mansfield and Briarty, 1991), and this division fails to occur in *mp* embryos, leading to loss of vascular cell formation in the embryo axis (Berleth and Jurgens, 1993; De Rybel et al., 2013; Ohashi-Ito et al., 2013).

Finally, the hypothesis I proposed is predictive, and many of the predictions it generates are immediately testable. For example, the hypothesis predicts defects in middle-layer formation in *mp* leaves, which could be tested by analyzing the expression of middle-layer-specific genes such as the *WUSCHEL-RELATED HOMEBOX1 (WOX1)* and *PRESSED FLOWER/WOX3* for which reporters are available (Nakata and Okada, 2012; Shimizu et al., 2009). Further, the hypothesis predicts premature progression of ground cells to mesophyll fate in *mp* leaves, which could be tested by analyzing the expression of the mesophyll specification marker *LHCB2.3::nYFP* (Sawchuk et al., 2008) (Chapter 2).

6.3 Unresolved questions and future approaches

Even though future experimental tests, including those suggested above, were to support the hypothesis I proposed, many questions would remain to be addressed. For example, the hypothesis relies on cell divisions in the L2 of the SAM that are oriented parallel to the lateral direction of leaf primordium outgrowth. What would control such orientation?

The available data seem to be equally consistent with both an *MP*-dependent and an *MP*-independent control of orientation of cell division. As it is sufficient to increase cell proliferation in an *mp* background to restore vein formation, the mechanism that controls the orientation of cell division would seem to be independent of *MP* function and would fail to operate in *mp* simply because of lack of substrate: cells dividing in the correct positions. On the other hand, the mechanism that controls the orientation of cell division could still depend on *MP* function but could simply be less sensitive to reductions in *MP* function than the *MP*-dependent control of cell proliferation.

Though it remains unclear whether *MP*-dependent auxin signalling controls the orientation of cell division, at least some evidence exists that the orientation of cell division is controlled by

auxin transport (Petrasek et al., 2002). Because of the interdependency of auxin transport, auxin signalling and vein formation (reviewed in Chapter 1), it will thus be difficult—if not altogether impossible—to evaluate intuitively the results of experimental tests designed to discriminate between *MP*-dependent and *MP*-independent control of orientation of cell division; a more precise formulation—a mathematical one, one that can be simulated computationally—may be necessary. Computer simulation could predict experimental conditions at which the hypotheses of *MP*-dependent and *MP*-independent control of orientation of cell division behave divergently, thereby providing with informative experimental tests to differentiate the ability of these hypotheses to describe plausibly vein formation and thus moving us one step closer to understanding how the growth of tissues and their vascularization are coordinated in plants—a key question to address if we are to understand how multicellular organisms develop and function.

LITERATURE CITED

- Adachi, S., Nobusawa, T., Umeda, M.**, 2009. Quantitative and cell type-specific transcriptional regulation of A-type cyclin-dependent kinase in *Arabidopsis thaliana*. *Dev Biol* 329, 306-314.
- Aloni, R.**, 1987. Differentiation of Vascular Tissues. *Ann. Rev. Plant Physiol.* 38, 179-204.
- Alonso-Peral, M.M., Candela, H., del Pozo, J.C., Martinez-Laborda, A., Ponce, M.R., Micol, J.L.**, 2006. The HVE/CAND1 gene is required for the early patterning of leaf venation in *Arabidopsis*. *Development* 133, 3755-3766.
- Alonso, J.M., Stepanova, A.N., Leisse, T.J., Kim, C.J., Chen, H., Shinn, P., Stevenson, D.K., Zimmerman, J., Barajas, P., Cheuk, R., Gadrinab, C., Heller, C., Jeske, A., Koesema, E., Meyers, C.C., Parker, H., Prednis, L., Ansari, Y., Choy, N., Deen, H., Geralt, M., Hazari, N., Hom, E., Karnes, M., Mulholland, C., Ndubaku, R., Schmidt, I., Guzman, P., Aguilar-Henonin, L., Schmid, M., Weigel, D., Carter, D.E., Marchand, T., Risseuw, E., Brogden, D., Zeko, A., Crosby, W.L., Berry, C.C., Ecker, J.R.**, 2003. Genome-wide insertional mutagenesis of *Arabidopsis thaliana*. *Science* 301, 653-657.
- Baima, S., Nobili, F., Sessa, G., Lucchetti, S., Ruberti, I., Morelli, G.**, 1995. The expression of the *Athb-8* homeobox gene is restricted to provascular cells in *Arabidopsis thaliana*. *Development* 121, 4171-4182.
- Beeckman, T., Przemeck, G.K., Stamatiou, G., Lau, R., Terry, N., De Rycke, R., Inze, D., Berleth, T.**, 2002. Genetic complexity of cellulose synthase a gene function in *Arabidopsis* embryogenesis. *Plant Physiol* 130, 1883-1893.
- Benazet, J.D., Pignatti, E., Nugent, A., Unal, E., Laurent, F., Zeller, R.**, 2012. *Smad4* is required to induce digit ray primordia and to initiate the aggregation and differentiation of chondrogenic progenitors in mouse limb buds. *Development* 139, 4250-4260.
- Berleth, T.**, 2000. Plant development: hidden networks. *Curr Biol* 10, R658-661.
- Berleth, T., Jurgens, G.**, 1993. The Role of the *Monopteros* Gene in Organizing the Basal Body Region of the *Arabidopsis* Embryo. *Development* 118, 575-587.
- Bezhani, S., Sherameti, I., Pfannschmidt, T., Oelmüller, R.**, 2001. A repressor with similarities to prokaryotic and eukaryotic DNA helicases controls the assembly of the CAAT box binding complex at a photosynthesis gene promoter. *J Biol Chem* 276, 23785-23789.
- Birkenbihl, R.P., Jach, G., Saedler, H., Huijser, P.**, 2005. Functional dissection of the plant-specific SBP-domain: overlap of the DNA-binding and nuclear localization domains. *J Mol Biol* 352, 585-596.
- Brown, J.R., Nigh, E., Lee, R.J., Ye, H., Thompson, M.A., Saudou, F., Pestell, R.G., Greenberg, M.E.**, 1998. Fos family members induce cell cycle entry by activating cyclin D1. *Mol Cell Biol* 18, 5609-5619.
- Campbell, M.E., Palfreyman, J.W., Preston, C.M.**, 1984. Identification of herpes simplex virus DNA sequences which encode a trans-acting polypeptide responsible for stimulation of immediate early transcription. *J Mol Biol* 180, 1-19.
- Candela, H., Martinez-Laborda, A., Micol, J.L.**, 1999. Venation pattern formation in *Arabidopsis thaliana* vegetative leaves. *Dev Biol* 205, 205-216.
- Cano-Delgado, A., Lee, J.Y., Demura, T.**, 2010. Regulatory mechanisms for specification and patterning of plant vascular tissues. *Annu Rev Cell Dev Biol* 26, 605-637.
- Capron, A., Chatfield, S., Provart, N., Berleth, T.**, 2009. Embryogenesis: pattern formation from a single cell. *Arabidopsis Book* 7, e0126.

Carland, F.M., Berg, B.L., FitzGerald, J.N., Jinamornphongs, S., Nelson, T., Keith, B., 1999. Genetic regulation of vascular tissue patterning in Arabidopsis. *Plant Cell* 11, 2123-2137.

Chapman, E.J., Estelle, M., 2009. Mechanism of auxin-regulated gene expression in plants. *Annu Rev Genet* 43, 265-285.

Chomczynski, P., Sacchi, N., 1987. Single-step method of RNA isolation by acid guanidinium thiocyanate-phenol-chloroform extraction. *Anal Biochem* 162, 156-159.

Cleaver, O., Dor, Y., 2012. Vascular instruction of pancreas development. *Development* 139, 2833-2843.

Cleaver, O., Melton, D.A., 2003. Endothelial signaling during development. *Nat Med* 9, 661-668.

Cole, M., Chandler, J., Weijers, D., Jacobs, B., Comelli, P., Werr, W., 2009. DORNROSCHE is a direct target of the auxin response factor MONOPTEROS in the Arabidopsis embryo. *Development* 136, 1643-1651.

Cubas, P., Lauter, N., Doebley, J., Coen, E., 1999. The TCP domain: a motif found in proteins regulating plant growth and development. *Plant J* 18, 215-222.

De Rybel, B., Moller, B., Yoshida, S., Grabowicz, I., Barbier de Reuille, P., Boeren, S., Smith, R.S., Borst, J.W., Weijers, D., 2013. A bHLH complex controls embryonic vascular tissue establishment and indeterminate growth in Arabidopsis. *Dev Cell* 24, 426-437.

De Smet, I., Jurgens, G., 2007. Patterning the axis in plants--auxin in control. *Curr Opin Genet Dev* 17, 337-343.

De Veylder, L., Beeckman, T., Beemster, G.T., Krols, L., Terras, F., Landrieu, I., van der Schueren, E., Maes, S., Naudts, M., Inze, D., 2001. Functional analysis of cyclin-dependent kinase inhibitors of Arabidopsis. *Plant Cell* 13, 1653-1668.

Demeulenaere, M., Beeckman, T., 2014. The interplay between auxin and the cell cycle during plant development, Auxin and its role in plant development. Springer.

Derynck, R., Gelbart, W.M., Harland, R.M., Heldin, C.H., Kern, S.E., Massague, J., Melton, D.A., Mlodzik, M., Padgett, R.W., Roberts, A.B., Smith, J., Thomsen, G.H., Vogelstein, B., Wang, X.F., 1996. Nomenclature: vertebrate mediators of TGFbeta family signals. *Cell* 87, 173.

Dewitte, W., Murray, J.A.H., 2003. The plant cell cycle. *Annual Review of Plant Biology* 54, 235-264.

Dewitte, W., Scofield, S., Alcasabas, A.A., Maughan, S.C., Menges, M., Braun, N., Collins, C., Nieuwland, J., Prinsen, E., Sundaresan, V., Murray, J.A., 2007. Arabidopsis CYCD3 D-type cyclins link cell proliferation and endocycles and are rate-limiting for cytokinin responses. *Proc Natl Acad Sci U S A* 104, 14537-14542.

Donnelly, P.M., Bonetta, D., Tsukaya, H., Dengler, R.E., Dengler, N.G., 1999. Cell cycling and cell enlargement in developing leaves of Arabidopsis. *Developmental Biology* 215, 407-419.

Donner, T.J., Scarpella, E., 2012. Transcriptional control of early vein expression of CYCA2;1 and CYCA2;4 in Arabidopsis leaves.

Donner, T.J., Scarpella, E., 2013. Transcriptional control of early vein expression of CYCA2;1 and CYCA2;4 in Arabidopsis leaves. *Mech Dev* 130, 14-24.

Donner, T.J., Sherr, I., Scarpella, E., 2009. Regulation of preprocambial cell state acquisition by auxin signaling in Arabidopsis leaves. *Development* 136, 3235-3246.

Efroni, I., Blum, E., Goldshmidt, A., Eshed, Y., 2008. A protracted and dynamic maturation schedule underlies Arabidopsis leaf development. *Plant Cell* 20, 2293-2306.

Esau, K., 1965. *Plant anatomy*, 2nd ed. ed. John Wiley, New York ; London.

Esteve-Bruna, D., Perez-Perez, J.M., Ponce, M.R., Micol, J.L., 2013. incurvata13, a novel allele of AUXIN RESISTANT6, reveals a specific role for auxin and the SCF complex in Arabidopsis embryogenesis, vascular specification, and leaf flatness. *Plant Physiol* 161, 1303-1320.

Flot, L., 1905. Recherches sur la naissance des feuilles et sur l'origine foliaire de la tige. *Revue générale de Botanique* 17, 449-472, 519-535.

Foster, A.S., 1936. Leaf differentiation in Angiosperms. *Bot Rev* 2, 349-372.

Foster, A.S., 1952. Foliar Venation in Angiosperms from an Ontogenetic Standpoint. *American Journal of Botany* 39, 752-766.

Fukuda, H., 2004. Signals that control plant vascular cell differentiation. *Nat Rev Mol Cell Biol* 5, 379-391.

Gardiner, J., Donner, T.J., Scarpella, E., 2011. Simultaneous activation of SHR and ATHB8 expression defines switch to preprocambial cell state in Arabidopsis leaf development. *Dev Dyn* 240, 261-270.

Geisler, M., Jablonska, B., Springer, P.S., 2002. Enhancer trap expression patterns provide a novel teaching resource. *Plant Physiol* 130, 1747-1753.

Gillmor, C.S., Park, M.Y., Smith, M.R., Pepitone, R., Kerstetter, R.A., Poethig, R.S., 2010. The MED12-MED13 module of Mediator regulates the timing of embryo patterning in Arabidopsis. *Development* 137, 113-122.

Gomis, R.R., Alarcon, C., He, W., Wang, Q., Seoane, J., Lash, A., Massague, J., 2006a. A FoxO-Smad synexpression group in human keratinocytes. *Proc Natl Acad Sci U S A* 103, 12747-12752.

Gomis, R.R., Alarcon, C., Nadal, C., Van Poznak, C., Massague, J., 2006b. C/EBPbeta at the core of the TGFbeta cytotostatic response and its evasion in metastatic breast cancer cells. *Cancer Cell* 10, 203-214.

Grosberg, R.K., Strathmann, R.R., 2007. The evolution of multicellularity: A minor major transition? *Annual Review of Ecology Evolution and Systematics* 38, 621-654.

Guilfoyle, T.J., Hagen, G., 2007. Auxin response factors. *Curr Opin Plant Biol* 10, 453-460.

Guilfoyle, T.J., Hagen, G., 2012. Getting a grasp on domain III/IV responsible for Auxin Response Factor-IAA protein interactions. *Plant Sci* 190, 82-88.

Gutierrez, C., 2009. The Arabidopsis cell division cycle. *Arabidopsis Book* 7, e0120.

Harashima, H., Dissmeyer, N., Schnittger, A., 2013. Cell cycle control across the eukaryotic kingdom. *Trends Cell Biol* 23, 345-356.

Hardtke, C.S., Berleth, T., 1998. The Arabidopsis gene MONOPTEROS encodes a transcription factor mediating embryo axis formation and vascular development. *Embo J* 17, 1405-1411.

Hardtke, C.S., Ckurshumova, W., Vidaurre, D.P., Singh, S.A., Stamatiou, G., Tiwari, S.B., Hagen, G., Guilfoyle, T.J., Berleth, T., 2004. Overlapping and non-redundant functions of the Arabidopsis auxin response factors MONOPTEROS and NONPHOTOTROPIC HYPOCOTYL 4. *Development* 131, 1089-1100.

Hatakeyama, J., Bessho, Y., Katoh, K., Ookawara, S., Fujioka, M., Guillemot, F., Kageyama, R., 2004. Hes genes regulate size, shape and histogenesis of the nervous system by control of the timing of neural stem cell differentiation. *Development* 131, 5539-5550.

Hayashi, K., Neve, J., Hirose, M., Kuboki, A., Shimada, Y., Kepinski, S., Nozaki, H., 2012. Rational design of an auxin antagonist of the SCF(TIR1) auxin receptor complex. *ACS Chem Biol* 7, 590-598.

Hemerly, A., Engler Jde, A., Bergounioux, C., Van Montagu, M., Engler, G., Inze, D., Ferreira, P., 1995. Dominant negative mutants of the Cdc2 kinase uncouple cell division from iterative plant development. *Embo J* 14, 3925-3936.

Hemerly, A.S., Ferreira, P.C., Van Montagu, M., Engler, G., Inze, D., 2000. Cell division events are essential for embryo patterning and morphogenesis: studies on dominant-negative *cdc2aAt* mutants of *Arabidopsis*. *Plant J* 23, 123-130.

Hodgkin, J., 2005. Genetic suppression. *WormBook*, 1-13.

Hosoda, K., Imamura, A., Katoh, E., Hatta, T., Tachiki, M., Yamada, H., Mizuno, T., Yamazaki, T., 2002. Molecular structure of the GARP family of plant Myb-related DNA binding motifs of the *Arabidopsis* response regulators. *Plant Cell* 14, 2015-2029.

Hu, Y., Xie, Q., Chua, N.H., 2003. The *Arabidopsis* auxin-inducible gene ARGOS controls lateral organ size. *Plant Cell* 15, 1951-1961.

Huang, L.S., Sternberg, P.W., 2006. Genetic dissection of developmental pathways. *WormBook*, 1-19.

Inze, D., De Veylder, L., 2006. Cell cycle regulation in plant development. *Annual Review of Genetics* 40, 77-105.

Jakoby, M., Weisshaar, B., Droge-Laser, W., Vicente-Carbajosa, J., Tiedemann, J., Kroj, T., Parcy, F., b, Z.I.P.R.G., 2002. bZIP transcription factors in *Arabidopsis*. *Trends Plant Sci* 7, 106-111.

Kalve, S., Fotschki, J., Beeckman, T., Vissenberg, K., Beemster, G.T., 2014. Three-dimensional patterns of cell division and expansion throughout the development of *Arabidopsis thaliana* leaves. *J Exp Bot* 65, 6385-6397.

Kang, J., Dengler, N., 2002. Cell cycling frequency and expression of the homeobox gene *ATHB-8* during leaf vein development in *Arabidopsis*. *Planta* 216, 212-219.

Kang, J., Dengler, N., 2004. Vein pattern development in adult leaves of *Arabidopsis thaliana*. *International Journal of Plant Sciences* 165, 231-242.

Kang, J., Mizukami, Y., Wang, H., Fowke, L., Dengler, N.G., 2007. Modification of cell proliferation patterns alters leaf vein architecture in *Arabidopsis thaliana*. *Planta* 226, 1207-1218.

Kazama, T., Ichihashi, Y., Murata, S., Tsukaya, H., 2010. The mechanism of cell cycle arrest front progression explained by a *KLUH/CYP78A5*-dependent mobile growth factor in developing leaves of *Arabidopsis thaliana*. *Plant Cell Physiol* 51, 1046-1054.

Keck, P.J., Hauser, S.D., Krivi, G., Sanzo, K., Warren, T., Feder, J., Connolly, D.T., 1989. Vascular permeability factor, an endothelial cell mitogen related to PDGF. *Science* 246, 1309-1312.

Kinsman, E.A., Pyke, K.A., 1998. Bundle sheath cells and cell-specific plastid development in *Arabidopsis* leaves. *Development* 125, 1815-1822.

Konishi, M., Donner, T.J., Scarpella, E., Yanagisawa, S., 2015. *MONOPTEROS* directly activates the auxin-inducible promoter of the *Dof5.8* transcription factor gene in *Arabidopsis thaliana* leaf provascular cells. *J Exp Bot* 66, 283-291.

Kosugi, S., Ohashi, Y., 2000. Cloning and DNA-binding properties of a tobacco Ethylene-Insensitive3 (*EIN3*) homolog. *Nucleic Acids Res* 28, 960-967.

Kovary, K., Bravo, R., 1991. The Jun and Fos Protein Families Are Both Required for Cell-Cycle Progression in Fibroblasts. *Molecular and Cellular Biology* 11, 4466-4472.

Koyama, T., Mitsuda, N., Seki, M., Shinozaki, K., Ohme-Takagi, M., 2010. TCP transcription factors regulate the activities of *ASYMMETRIC LEAVES1* and *miR164*, as well as the auxin response, during differentiation of leaves in *Arabidopsis*. *Plant Cell* 22, 3574-3588.

Krogan, N.T., Ckurshumova, W., Marcos, D., Caragea, A.E., Berleth, T., 2012. Deletion of MP/ARF5 domains III and IV reveals a requirement for Aux/IAA regulation in Arabidopsis leaf vascular patterning. *New Phytol.*

Krogan, N.T., Yin, X., Ckurshumova, W., Berleth, T., 2014. Distinct subclades of Aux/IAA genes are direct targets of ARF5/MP transcriptional regulation. *New Phytol* 204, 474-483.

Kuppusamy, K.T., Walcher, C.L., Nemhauser, J.L., 2009. Cross-regulatory mechanisms in hormone signaling. *Plant Mol Biol* 69, 375-381.

Lau, S., De Smet, I., Kolb, M., Meinhardt, H., Jurgens, G., 2011. Auxin triggers a genetic switch. *Nat Cell Biol* 13, 611-615.

Leung, D.W., Cachianes, G., Kuang, W.J., Goeddel, D.V., Ferrara, N., 1989. Vascular endothelial growth factor is a secreted angiogenic mitogen. *Science* 246, 1306-1309.

Leyser, O., 2010. The power of auxin in plants. *Plant Physiol* 154, 501-505.

Li, S.B., Liu, L., Zhuang, X.H., Yu, Y., Liu, X.G., Cui, X., Ji, L.J., Pan, Z.Q., Cao, X.F., Mo, B.X., Zhang, F.C., Raikhel, N., Jiang, L.W., Chen, X.M., 2013. MicroRNAs Inhibit the Translation of Target mRNAs on the Endoplasmic Reticulum in Arabidopsis. *Cell* 153, 562-574.

Lippuner, V., Chou, I.T., Scott, S.V., Ettinger, W.F., Theg, S.M., Gasser, C.S., 1994. Cloning and characterization of chloroplast and cytosolic forms of cyclophilin from Arabidopsis thaliana. *J Biol Chem* 269, 7863-7868.

Lopez-Rios, J., Speziale, D., Robay, D., Scotti, M., Osterwalder, M., Nusspaumer, G., Galli, A., Hollander, G.A., Kmita, M., Zeller, R., 2012. GLI3 constrains digit number by controlling both progenitor proliferation and BMP-dependent exit to chondrogenesis. *Dev Cell* 22, 837-848.

Mahonen, A.P., Bonke, M., Kauppinen, L., Riikonen, M., Benfey, P.N., Helariutta, Y., 2000. A novel two-component hybrid molecule regulates vascular morphogenesis of the Arabidopsis root. *Genes Dev* 14, 2938-2943.

Mansfield, S.G., Briarty, L.G., 1991. Early embryogenesis in Arabidopsis thaliana. II. The developing embryo. *Canadian Journal of Botany* 69, 461-476.

Masubelele, N.H., Dewitte, W., Menges, M., Maughan, S., Collins, C., Huntley, R., Nieuwland, J., Scofield, S., Murray, J.A., 2005. D-type cyclins activate division in the root apex to promote seed germination in Arabidopsis. *Proc Natl Acad Sci U S A* 102, 15694-15699.

Matsumoto, N., Okada, K., 2001. A homeobox gene, PRESSED FLOWER, regulates lateral axis-dependent development of Arabidopsis flowers. *Genes Dev* 15, 3355-3364.

Mattsson, J., Ckurshumova, W., Berleth, T., 2003. Auxin signaling in Arabidopsis leaf vascular development. *Plant Physiol* 131, 1327-1339.

Mattsson, J., Sung, Z.R., Berleth, T., 1999. Responses of plant vascular systems to auxin transport inhibition. *Development* 126, 2979-2991.

McKown, A.D., Dengler, N.G., 2009. Shifts in leaf vein density through accelerated vein formation in C(4) Flaveria (Asteraceae). *Annals of Botany* 104, 1085-1098.

Meijer, M., Murray, J.A., 2001. Cell cycle controls and the development of plant form. *Curr Opin Plant Biol* 4, 44-49.

Menges, M., Samland, A.K., Planchais, S., Murray, J.A., 2006. The D-type cyclin CYCD3;1 is limiting for the G1-to-S-phase transition in Arabidopsis. *Plant Cell* 18, 893-906.

Michniewicz, M., Brewer, P.B., Friml, J., 2007. Polar Auxin Transport and Asymmetric Auxin Distribution. *The Arabidopsis Book* 5, e0108. doi:0110.1199/tab.0108

Mizukami, Y., Fischer, R.L., 2000. Plant organ size control: AINTEGUMENTA regulates growth and cell numbers during organogenesis. *Proc Natl Acad Sci U S A* 97, 942-947.

Mockaitis, K., Estelle, M., 2008. Auxin receptors and plant development: a new signaling paradigm. *Annu Rev Cell Dev Biol* 24, 55-80.

Nakata, M., Matsumoto, N., Tsugeki, R., Rikirsch, E., Laux, T., Okada, K., 2012. Roles of the middle domain-specific WUSCHEL-RELATED HOMEODOMAIN genes in early development of leaves in *Arabidopsis*. *Plant Cell* 24, 519-535.

Nakata, M., Okada, K., 2012. The three-domain model: a new model for the early development of leaves in *Arabidopsis thaliana*. *Plant Signal Behav* 7, 1423-1427.

Nath, U., Crawford, B.C., Carpenter, R., Coen, E., 2003. Genetic control of surface curvature. *Science* 299, 1404-1407.

Nelson, T., Dengler, N., 1997. Leaf Vascular Pattern Formation. *Plant Cell* 9, 1121-1135.

Nieuwland, J., Scofield, S., Murray, J.A., 2009. Control of division and differentiation of plant stem cells and their derivatives. *Semin Cell Dev Biol* 20, 1134-1142.

Nishal, B., Tantikanjana, T., Sundaresan, V., 2005. An inducible targeted tagging system for localized saturation mutagenesis in *Arabidopsis*. *Plant Physiol* 137, 3-12.

Nogue, F., Grandjean, O., Craig, S., Dennis, S., Chaudhury, M., 2000. Higher levels of cell proliferation rate and cyclin CycD3 expression in the *Arabidopsis* amp1 mutant. *Plant Growth Regulation* 32, 275-283.

Normanly, J., 2010. Approaching cellular and molecular resolution of auxin biosynthesis and metabolism. *Cold Spring Harb Perspect Biol* 2, a001594.
doi:001510.001101/cshperspect.a001594

Norris, S.R., Meyer, S.E., Callis, J., 1993. The intron of *Arabidopsis thaliana* polyubiquitin genes is conserved in location and is a quantitative determinant of chimeric gene expression. *Plant Mol Biol* 21, 895-906.

Odat, O., Gardiner, J., Sawchuk, M.G., Verna, C., Donner, T.J., Scarpella, E., 2014. Characterization of an allelic series in the MONOPTEROS gene of *Arabidopsis*. *Genesis* 52, 127-133.

Ohashi-Ito, K., Oguchi, M., Kojima, M., Sakakibara, H., Fukuda, H., 2013. Auxin-associated initiation of vascular cell differentiation by LONESOME HIGHWAY. *Development* 140, 765-769.

Okushima, Y., Overvoorde, P.J., Arima, K., Alonso, J.M., Chan, A., Chang, C., Ecker, J.R., Hughes, B., Lui, A., Nguyen, D., Onodera, C., Quach, H., Smith, A., Yu, G., Theologis, A., 2005. Functional genomic analysis of the AUXIN RESPONSE FACTOR gene family members in *Arabidopsis thaliana*: unique and overlapping functions of ARF7 and ARF19. *Plant Cell* 17, 444-463.

Ori, N., Cohen, A.R., Etzioni, A., Brand, A., Yanai, O., Shleizer, S., Menda, N., Amsellem, Z., Efroni, I., Pekker, I., Alvarez, J.P., Blum, E., Zamir, D., Eshed, Y., 2007. Regulation of LANCEOLATE by miR319 is required for compound-leaf development in tomato. *Nat Genet* 39, 787-791.

Ossowski, S., Schwab, R., Weigel, D., 2008. Gene silencing in plants using artificial microRNAs and other small RNAs. *Plant J* 53, 674-690.

Palatnik, J.F., Allen, E., Wu, X., Schommer, C., Schwab, R., Carrington, J.C., Weigel, D., 2003. Control of leaf morphogenesis by microRNAs. *Nature* 425, 257-263.

Palatnik, J.F., Wollmann, H., Schommer, C., Schwab, R., Boisbouvier, J., Rodriguez, R., Warthmann, N., Allen, E., Dezulian, T., Huson, D., Carrington, J.C., Weigel, D., 2007. Sequence and expression differences underlie functional specialization of *Arabidopsis* microRNAs miR159 and miR319. *Dev Cell* 13, 115-125.

Perez-Perez, J.M., Candela, H., Robles, P., Lopez-Torrejon, G., del Pozo, J.C., Micol, J.L., 2010. A role for AUXIN RESISTANT3 in the coordination of leaf growth. *Plant Cell Physiol* 51, 1661-1673.

Petrasek, J., Elckner, M., Morris, D.A., Zazimalova, E., 2002. Auxin efflux carrier activity and auxin accumulation regulate cell division and polarity in tobacco cells. *Planta* 216, 302-308.

Petrasek, J., Friml, J., 2009. Auxin transport routes in plant development. *Development* 136, 2675-2688.

Picard, D., Salsler, S.J., Yamamoto, K.R., 1988. A movable and regulable inactivation function within the steroid binding domain of the glucocorticoid receptor. *Cell* 54, 1073-1080.

Pray, T.R., 1955. Foliar venation of Angiosperms. IV. Histogenesis of the venation of *Hosta*. *American Journal of Botany* 42, 698-706.

Prouse, M.B., Campbell, M.M., 2012. The interaction between MYB proteins and their target DNA binding sites. *Biochim Biophys Acta* 1819, 67-77.

Przemeck, G.K., Mattsson, J., Hardtke, C.S., Sung, Z.R., Berleth, T., 1996. Studies on the role of the Arabidopsis gene MONOPTEROS in vascular development and plant cell axialization. *Planta* 200, 229-237.

Ramirez-Parra, E., Desvoyes, B., Gutierrez, C., 2005. Balance between cell division and differentiation during plant development. *Int J Dev Biol* 49, 467-477.

Rasband, W.S., 1997. ImageJ. U.S. National Institutes of Health, Bethesda, Maryland, USA, <http://rsb.info.nih.gov/ij/>.

Raven, J.A., 1975. Transport of indole acetic acid in plant cells in relation to pH and electrical potential gradients, and its significance for polar IAA transport. *New Phytologist* 74, 163-172.

Reddy, G.V., Heisler, M.G., Ehrhardt, D.W., Meyerowitz, E.M., 2004. Real-time lineage analysis reveals oriented cell divisions associated with morphogenesis at the shoot apex of *Arabidopsis thaliana*. *Development* 131, 4225-4237.

Retting, K.N., Song, B., Yoon, B.S., Lyons, K.M., 2009. BMP canonical Smad signaling through Smad1 and Smad5 is required for endochondral bone formation. *Development* 136, 1093-1104.

Reyes, J.C., Muro-Pastor, M.I., Florencio, F.J., 2004. The GATA family of transcription factors in *Arabidopsis* and rice. *Plant Physiol* 134, 1718-1732.

Riou-Khamlichi, C., Huntley, R., Jacquard, A., Murray, J.A., 1999. Cytokinin activation of *Arabidopsis* cell division through a D-type cyclin. *Science* 283, 1541-1544.

Roeder, A.H., Cunha, A., Ohno, C.K., Meyerowitz, E.M., 2012. Cell cycle regulates cell type in the *Arabidopsis* sepal. *Development* 139, 4416-4427.

Rubery, P.H., Sheldrake, A.R., 1974. Carrier-Mediated Auxin Transport. *Planta* 118, 101-121.

Sachs, T., 1981. The control of the patterned differentiation of vascular tissues. *Advances in Botanical Research* 9, 151-262.

Sachs, T., 1989. The development of vascular networks during leaf development. *Current Topics in Plant Biochemistry and Physiology* 8, 168-183.

Sachs, T., 1991. Cell Polarity and Tissue Patterning in Plants. *Development Suppl* 1, 83-93.

Sarvepalli, K., Nath, U., 2011. Hyper-activation of the TCP4 transcription factor in *Arabidopsis thaliana* accelerates multiple aspects of plant maturation. *Plant J* 67, 595-607.

Satoh, R., Fujita, Y., Nakashima, K., Shinozaki, K., Yamaguchi-Shinozaki, K., 2004. A novel subgroup of bZIP proteins functions as transcriptional activators in hypoosmolarity-responsive expression of the ProDH gene in *Arabidopsis*. *Plant Cell Physiol* 45, 309-317.

- Sawchuk, M.G., Donner, T.J., Head, P., Scarpella, E., 2008.** Unique and overlapping expression patterns among members of photosynthesis-associated nuclear gene families in Arabidopsis. *Plant Physiol* 148, 1908-1924.
- Sawchuk, M.G., Edgar, A., Scarpella, E., 2013.** Patterning of Leaf Vein Networks by Convergent Auxin Transport Pathways. *PLoS Genet* 9, e1003294.
- Sawchuk, M.G., Head, P., Donner, T.J., Scarpella, E., 2007.** Time-lapse imaging of Arabidopsis leaf development shows dynamic patterns of procambium formation. *New Phytol* 176, 560-571.
- Scarpella, E., Francis, P., Berleth, T., 2004.** Stage-specific markers define early steps of procambium development in Arabidopsis leaves and correlate termination of vein formation with mesophyll differentiation. *Development* 131, 3445-3455.
- Scarpella, E., Marcos, D., Friml, J., Berleth, T., 2006.** Control of leaf vascular patterning by polar auxin transport. *Genes Dev* 20, 1015-1027.
- Schlereth, A., Moller, B., Liu, W., Kientz, M., Flipse, J., Rademacher, E.H., Schmid, M., Jurgens, G., Weijers, D., 2010.** MONOPTEROS controls embryonic root initiation by regulating a mobile transcription factor. *Nature* 464, 913-916.
- Schommer, C., Debernardi, J.M., Bresso, E.G., Rodriguez, R.E., Palatnik, J.F., 2014.** Repression of cell proliferation by miR319-regulated TCP4. *Mol Plant* 7, 1533-1544.
- Schommer, C., Palatnik, J.F., Aggarwal, P., Chetelat, A., Cubas, P., Farmer, E.E., Nath, U., Weigel, D., 2008.** Control of jasmonate biosynthesis and senescence by miR319 targets. *PLoS Biol* 6, e230.
- Schruff, M.C., Spielman, M., Tiwari, S., Adams, S., Fenby, N., Scott, R.J., 2005.** The AUXIN RESPONSE FACTOR 2 gene of Arabidopsis links auxin signalling, cell division, and the size of seeds and other organs. *Development* 133, 251-261.
- Schwab, R., Ossowski, S., Riester, M., Warthmann, N., Weigel, D., 2006.** Highly specific gene silencing by artificial microRNAs in Arabidopsis. *Plant Cell* 18, 1121-1133.
- Seki, M., Carninci, P., Nishiyama, Y., Hayashizaki, Y., Shinozaki, K., 1998.** High-efficiency cloning of Arabidopsis full-length cDNA by biotinylated CAP trapper. *Plant J* 15, 707-720.
- Seki, M., Narusaka, M., Kamiya, A., Ishida, J., Satou, M., Sakurai, T., Nakajima, M., Enju, A., Akiyama, K., Oono, Y., Muramatsu, M., Hayashizaki, Y., Kawai, J., Carninci, P., Itoh, M., Ishii, Y., Arakawa, T., Shibata, K., Shinagawa, A., Shinozaki, K., 2002.** Functional annotation of a full-length Arabidopsis cDNA collection. *Science* 296, 141-145.
- Seoane, J., Le, H.V., Shen, L., Anderson, S.A., Massague, J., 2004.** Integration of Smad and forkhead pathways in the control of neuroepithelial and glioblastoma cell proliferation. *Cell* 117, 211-223.
- Shimizu, R., Ji, J., Kelsey, E., Ohtsu, K., Schnable, P.S., Scanlon, M.J., 2009.** Tissue specificity and evolution of meristematic WOX3 function. *Plant Physiol* 149, 841-850.
- Sieburth, L.E., 1999.** Auxin is required for leaf vein pattern in Arabidopsis. *Plant Physiol* 121, 1179-1190.
- Stewart, R.N., 1978.** Ontogeny of the primary body in chimeral forms of higher plants, in: Sussex, I.M., Subtelny, S. (Eds.), *The clonal basis of development*. Academic Press, New York, pp. 131-160.
- Steynen, Q.J., Schultz, E.A., 2003.** The FORKED genes are essential for distal vein meeting in Arabidopsis. *Development* 130, 4695-4708.
- Strader, L.C., Monroe-Augustus, M., Rogers, K.C., Lin, G.L., Bartel, B., 2008.** Arabidopsis *iba* response5 suppressors separate responses to various hormones. *Genetics* 180, 2019-2031.

Swaminathan, K., Yang, Y., Grotz, N., Campisi, L., Jack, T., 2000. An enhancer trap line associated with a D-class cyclin gene in Arabidopsis. *Plant Physiol* 124, 1658-1667.

Taiz, L., Zeiger, E., 2006. *Plant physiology*, 4th ed. ed. W. H. Freeman ; Basingstoke : Palgrave [distributor], New York.

Telfer, A., Poethig, R.S., 1994. Leaf development in Arabidopsis, in: Meyerowitz, E.M., Somerville, C.R. (Eds.), *Arabidopsis*. Cold Spring Harbor Press, New York, pp. 379-401.

Tilney-Bassett, R.A.E., 1986. *Plant chimeras*. Edward Arnold, London.

Tiwari, S.B., Hagen, G., Guilfoyle, T., 2003. The roles of auxin response factor domains in auxin-responsive transcription. *Plant Cell* 15, 533-543.

Torres Acosta, J.A., Fowke, L.C., Wang, H., 2011. Analyses of phylogeny, evolution, conserved sequences and genome-wide expression of the ICK/KRP family of plant CDK inhibitors. *Ann Bot* 107, 1141-1157.

Towers, M., Mahood, R., Yin, Y., Tickle, C., 2008. Integration of growth and specification in chick wing digit-patterning. *Nature* 452, 882-886.

Ulmasov, T., Hagen, G., Guilfoyle, T.J., 1999a. Dimerization and DNA binding of auxin response factors. *Plant Journal* 19, 309-319.

Ulmasov, T., Hagen, G., Guilfoyle, T.J., 1999b. Activation and repression of transcription by auxin-response factors. *Proc Natl Acad Sci U S A* 96, 5844-5849.

Vanneste, S., Coppens, F., Lee, E., Donner, T.J., Xie, Z., Van Isterdael, G., Dhondt, S., De Winter, F., De Rybel, B., Vuylsteke, M., De Veylder, L., Friml, J., Inze, D., Grotewold, E., Scarpella, E., Sack, F., Beemster, G.T., Beeckman, T., 2011. Developmental regulation of CYCA2s contributes to tissue-specific proliferation in Arabidopsis. *EMBO J* 30, 3430-3441.

Vera-Sirera, F., Minguet, E.G., Singh, S.K., Ljung, K., Tuominen, H., Blazquez, M.A., Carbonell, J., 2010. Role of polyamines in plant vascular development. *Plant Physiol Biochem* 48, 534-539.

Verna, C., Sawchuk, M.G., Linh, N.M., Scarpella, E., 2015. Control of vein network topology by auxin transport. Submitted.

Verrecchia, F., Vindevoghel, L., Lechleider, R.J., Uitto, J., Roberts, A.B., Mauviel, A., 2001. Smad3/AP-1 interactions control transcriptional responses to TGF-beta in a promoter-specific manner. *Oncogene* 20, 3332-3340.

Vidaurre, D.P., Ploense, S., Krogan, N.T., Berleth, T., 2007. AMP1 and MP antagonistically regulate embryo and meristem development in Arabidopsis. *Development* 134, 2561-2567.

Weijers, D., Benkova, E., Jager, K.E., Schlereth, A., Hamann, T., Kientz, M., Wilmoth, J.C., Reed, J.W., Jurgens, G., 2005a. Developmental specificity of auxin response by pairs of ARF and Aux/IAA transcriptional regulators. *Embo J* 24, 1874-1885.

Weijers, D., Franke-van Dijk, M., Vencken, R.J., Quint, A., Hooykaas, P., Offringa, R., 2001. An Arabidopsis Minute-like phenotype caused by a semi-dominant mutation in a RIBOSOMAL PROTEIN S5 gene. *Development* 128, 4289-4299.

Weijers, D., Sauer, M., Meurette, O., Friml, J., Ljung, K., Sandberg, G., Hooykaas, P., Offringa, R., 2005b. Maintenance of embryonic auxin distribution for apical-basal patterning by PIN-FORMED-dependent auxin transport in Arabidopsis. *Plant Cell* 17, 2517-2526.

Wenzel, C.L., Marrison, J., Mattsson, J., Haseloff, J., Bougourd, S.M., 2012. Ectopic divisions in vascular and ground tissues of Arabidopsis thaliana result in distinct leaf venation defects. *J Exp Bot* 63, 5351-5364.

- Wenzel, C.L., Schuetz, M., Yu, Q., Mattsson, J., 2007.** Dynamics of MONOPTEROS and PIN-FORMED1 expression during leaf vein pattern formation in *Arabidopsis thaliana*. *Plant J* 49, 387-398.
- Wolpert, L., Tickle, C.A., Martinez, A., 2015.** Principles of Development Oxford University Press.
- Woody, S.T., Austin-Phillips, S., Amasino, R.M., Krysan, P.J., 2007.** The WiscDsLox T-DNA collection: an arabidopsis community resource generated by using an improved high-throughput T-DNA sequencing pipeline. *J Plant Res* 120, 157-165.
- Yamaguchi, N., Wu, M.F., Winter, C.M., Berns, M.C., Nole-Wilson, S., Yamaguchi, A., Coupland, G., Krizek, B.A., Wagner, D., 2013.** A molecular framework for auxin-mediated initiation of flower primordia. *Dev Cell* 24, 271-282.
- Yanagisawa, S., 2002.** The Dof family of plant transcription factors. *Trends Plant Sci* 7, 555-560.
- Zhang, S., Raina, S., Li, H., Li, J., Dec, E., Ma, H., Huang, H., Fedoroff, N.V., 2003.** Resources for targeted insertional and deletional mutagenesis in *Arabidopsis*. *Plant Mol Biol* 53, 133-150.
- Zhao, Y., 2010.** Auxin biosynthesis and its role in plant development. *Annu Rev Plant Biol* 61, 49-64.
- Zhao, Z., Andersen, S.U., Ljung, K., Dolezal, K., Miotk, A., Schultheiss, S.J., Lohmann, J.U., 2010.** Hormonal control of the shoot stem-cell niche. *Nature* 465, 1089-1092.
- Zhu, J., Nakamura, E., Nguyen, M.T., Bao, X., Akiyama, H., Mackem, S., 2008.** Uncoupling Sonic hedgehog control of pattern and expansion of the developing limb bud. *Dev Cell* 14, 624-632.